Chapter 5
Results and Discussion

CHAPTER 5
RESULTS & DISCUSSION

This chapter shows results and discussion under all the conditions of machining on duplex stainless steel. These are below;

5.1 Experimental Investigation Under Dry and Wet Conditions

The study focuses on a machinability investigation for drilling of DSS 2205 using TiAlN coated solid carbide drill under dry and wet conditions. The measured output was surface roughness, which was measured by a surface roughness tester. ANOVA is a mathematical method used to determine whether the means of two or more groups vary from one another statistically. It is used to judge the significant machining parameters influencing the evaluated parameters. Moreover, a regression model has been developed to generate a functional relationship among input and measured output/response parameters.

5.1.1 Experimental Results

Table 5.1 listed surface roughness (Ra) as evaluated parameters using TiAlN coated tool. As the drilling process has been employed instead of the drilling process, the key purpose is to identify the main contributing parameters that affected the studied response.

Table 5.1: Experimental Results for Ra under dry and wet conditions

S.No.	Machining Environment	Spindle speed (RPM)	Feed Rate (mm/rev.)	Surface roughness (micron)
1	Dry	600	00.03	00.857
2	Dry	600	00.05	00.912
3	Dry	900	00.03	00.796
4	Dry	900	00.05	00.869
5	Wet	600	00.03	00.802
6	Wet	600	00.05	00.849
7	Wet	900	00.03	00.748
8	Wet	900	00.05	00.785

5.1.2 Variation of Surface roughness with input variables

Table 5.1 gives the results obtained after the drilling of duplex stainless steel 2205 with TiAlN-coated solid carbide drill under dry and wet conditions. Also, figure 5.1 shows the main effect plot for the cutting parameters e.g. machining environment, spindle speed, feed rate, and their effect on surface roughness. After the DSS 2205 was machined, the surface roughness was measured using a surface roughness tester.

Fig. 5.1: Main effect Plot of Surface roughness (Ra)

It can be seen from the figure that within the scope of this investigation, as the spindle speed of the cutting tool increases, there isa decrease in surface roughness. For variation in the in-spindle speed of the cutting tool from 600 RPM to 900 RPM the average surface roughness varies from 0.748 to 0.912 microns. In the case of feed rate vs surface roughness, if the feed rate of the cutting tool increases, they're increasing in the surface roughness. For the variation in feed rate from 0.03 mm/rev to 0.05 mm/rev the average surface roughness was from 0.748 to 0.912 microns.

5.1.3 Interaction plot of Ra under dry, and wet conditions

Figure 5.2 shows the interaction effect plots of cutting parameters e.g. machining environment, spindle speed, and feed rate, and their effect on surface roughness as a response variable.

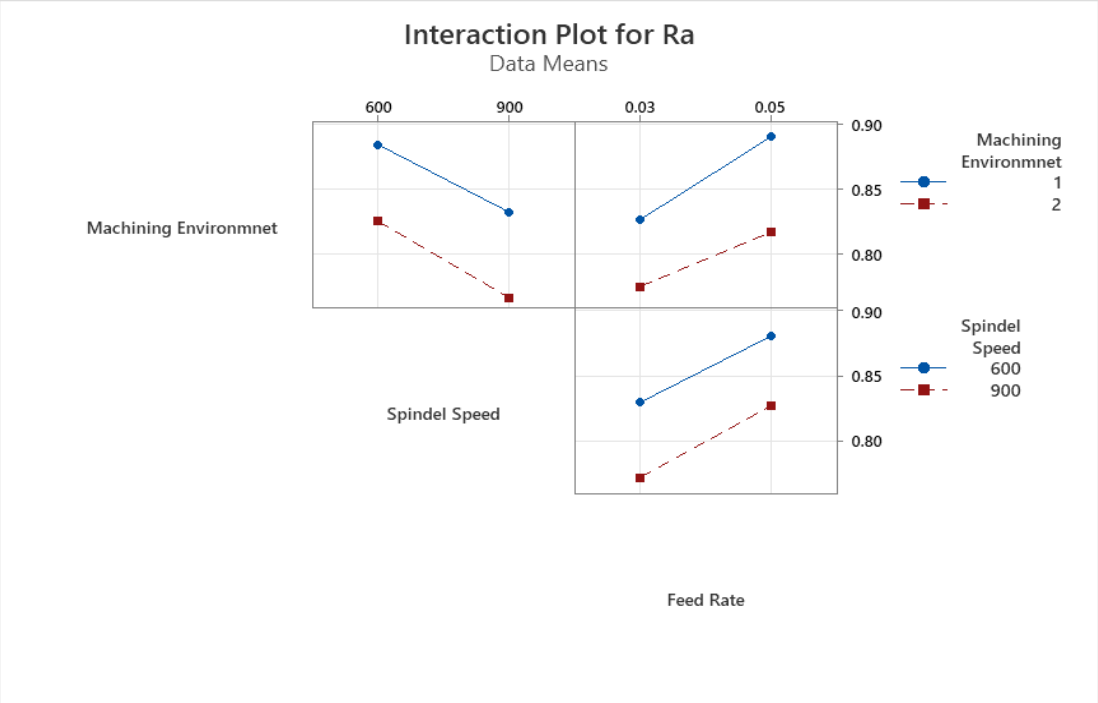

Fig. 5.2: Shows the interaction plot for Ra

Figure 5.2 gives the interaction effect of two factors on the surface roughness of duplex stainless steel 2205 with TiAlN-coated solid carbide drill variation under dry, and wet conditions. According to the interaction plot, it can be said that the interaction between the machining environment, spindle speed, and feed rate gives the minimum surface roughness values and better surface finish.

The figure 5.3 presented the lowest value of surface roughness and the best value of surface roughness. As per the figure, it was observed that the lowest value of surface roughness was 0.748 microns in a wet machining environment, high spindle speed of 900 RPM, and a minimum feed rate of 0.03 mm /rev.

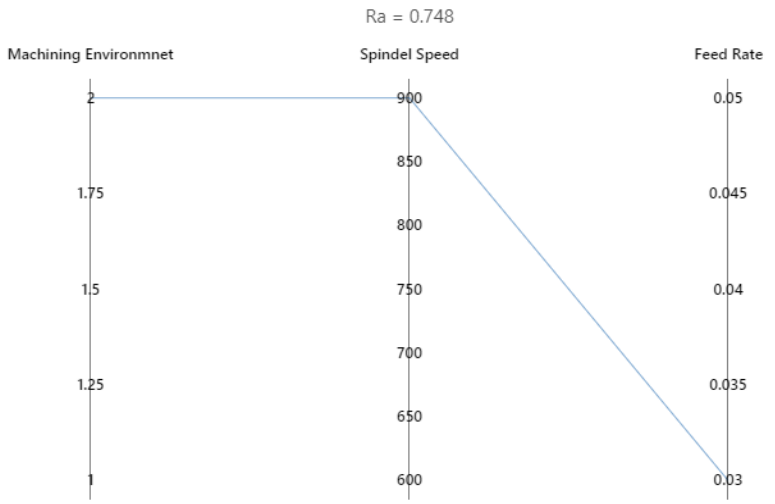

Fig. 5.3: Shows the best value of Ra

5.1.4 Response Table

The response table shows the range of the most effective process parameter. Table 5.2showsthe response table for Ra in term of the S/N ratio. The main effect of input variables e.g. Spindle speed, feed rate, and machining condition are 0.587, 0.554, and 0.665 respectively. After the analysis of the response table, it was observed that the most effective parameter is the machining condition compared to spindle speed and feed rate.

Table 5.2: Response Table

Level	Spindle Speed	Feed Rate	Machining Environment
1	1.3700	**1.9400**	1.3350
2	**1.9560**	1.3860	**1.9910**
Delta	0.5870	0.5540	0.6650
Rank	**2**	**3**	**1**

Figure 5.4 is a graphical representation of the delta value and rank of process parameters, which affect surface roughness (Ra). According to the figure, it was easily observed that the machining environment the is most effective process parameters on surface roughness compared to others e.g. spindle speed, and feed rate, respectively.

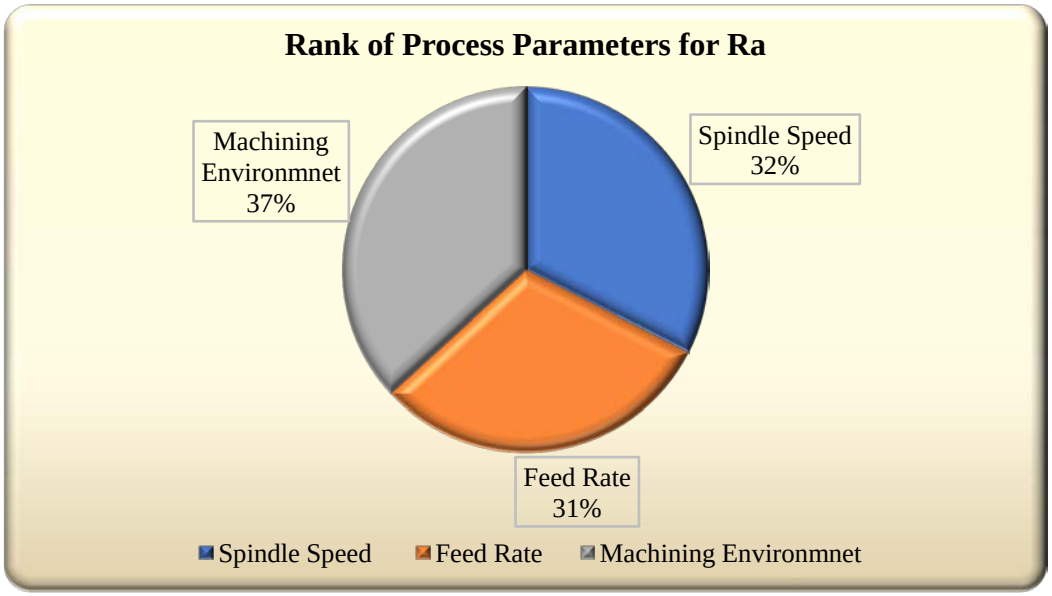

Fig. 5.4: Graphical representation of the response table

5.1.5 ANOVA Analysis

ANOVA is an analysis of variance, which means mostly affects process parameters on response and their contribution. Surface roughness (Ra) is largely determined by the machining, spindle speed, and feed rate, according to table 5.3. Machining environment, spindle speed, and feed rate all contribute 39.13%, 30.86 %, and 28.14% of the total, respectively for Ra. Figure 5.5 shows the graphical representation of the % of the contribution of cutting parameters on surface roughness (Ra). It can be seen that the machining environment, has the highest contribution on surface roughness in the drilling of DSS 2205 with TiAlN coated solid carbide drill under dry, and wet conditions followed by spindle speed, and feed rate.

Table 5.3: ANOVA analysis of Ra

Source	DF	Seq SS	Adj SS	Adj MS	F value	P value	Contribution
E	1	0.85877	0.85877	0.858773	88.25	0.001	39.13 %
SS	1	0.68859	0.68859	0.688594	70.76	0.001	30.86%
F	1	0.61408	0.61408	0.614077	63.10	0.002	28.14%
Error	4	0.03893	0.03893	0.009732			1.87%
Total	7	2.20037					100 %

Model Summary- S= 0.0097, R-Seq= 98.13%

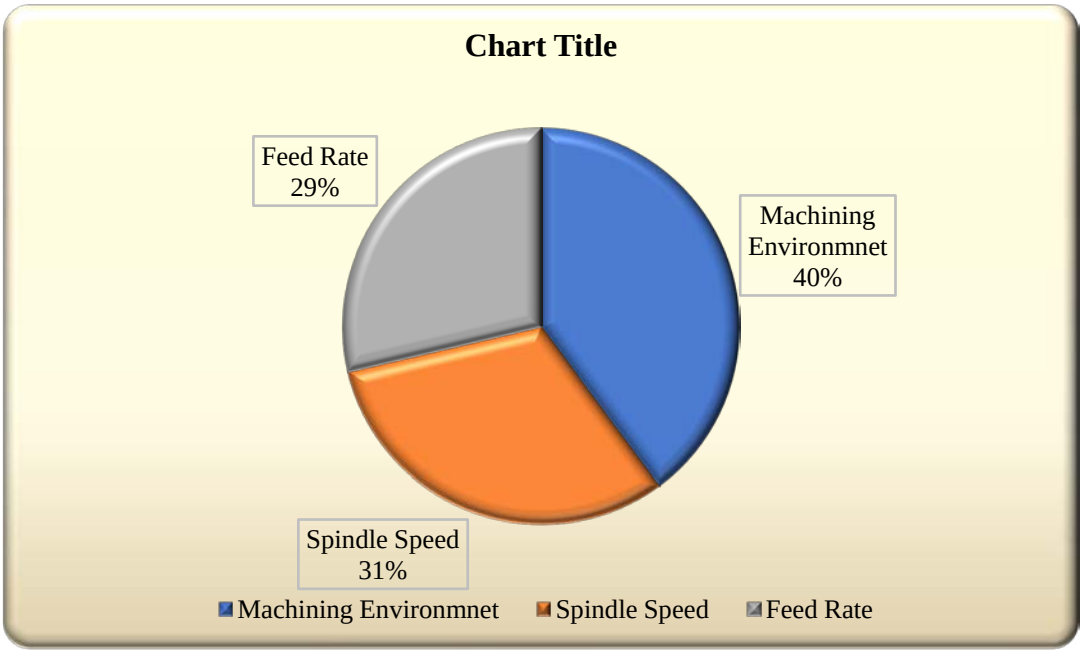

Fig. 5.5: Graphical representation of the contribution of process parameters

5.1.6 Regression Analysis

The dependent variables such as machining environment, spindle speed, and feed rate with one independent variable such as Ra was constructed using the Minitab 20.0 software tool. On each response, no modification has been applied. Eqn. (5.1), illustrates the prediction equations generated from the regression analysis for Ra.

Ra = 0.9538 - 0.06250 Environment - 0.000185 Spindle Speed + 2.650 Feed Rate +/-€.(5.1)

A coefficient of determination R^2 was used to test the capabilities of the created models. The coefficient of determination might be anything between zero and one. If it's close to one, the dependent and independent variables are likely to be well-matched. If R^2= 95 percent, it suggests that fresh observations were created with a 95 percent variability. The generated regression models for surface roughness (Ra) in this work had high R^2 values of 98.13%. The coefficients in the projected model were checked for significance using the residual plot. Residual analysis is the major diagnostic tool to check model adequacy [Vankanti et al., 2014]. Figure 5.6 show a normal probability plot for Ra, respectively. The residual plot shows the

normality of the assumption is satisfied as well as the points lying very close along a straight line. Residual lies close to a straight line indicating that errors are distributed normally. The predicted value and the experimental value are very close to each other.

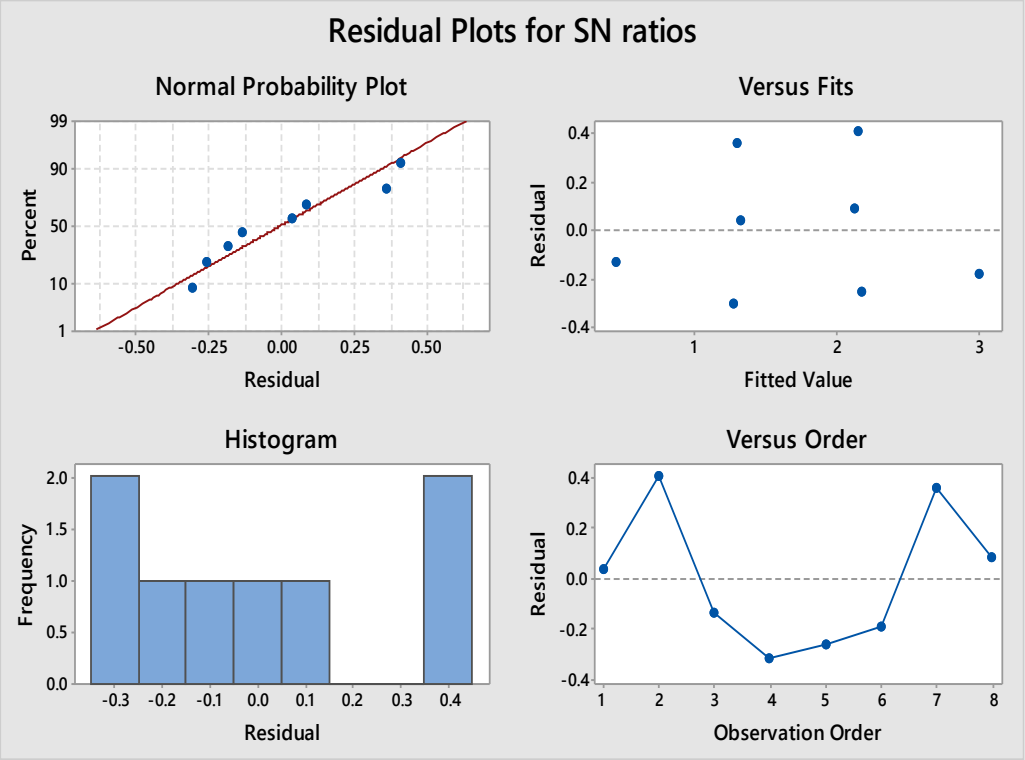

Fig. 5.6: Residual Plot for Ra

5.1.7 Contour plot for surface roughness (Ra)

A contour plot is a graphical representation of the input variable Vs response. Figure 5.7 shows a contour plot between spindle speed, feed rate, and machining environment Vs surface roughness.

The relationship between the response variable and two input variables is depicted in the contour plot graph. Figure 5.7 depicts the relationship between the input variable and the response variables of surface roughness (Ra). Figure 5.7 (a) shows a plot between input parameters e.g. machining environment, feed rate to surface roughness as a response variable. As per the counter plot, it can be said that if the value of the feed rate increases the Ra value also increases. In addition, wet machining provides the minimum value of surface roughness. Furthermore, the figure 5.7 (b) shows a plot between input parameters e.g. spindle speed and feed

rate, while surface roughness is as a response variable. After counter plot, It was found that the value of surface roughness reduces as spindle speed increases. Additionally, when feed rate increases, surface roughness value increases. Also, if the feed rate increases then the value of surface roughness increases. Similarly, the figure 5.7 (c) shows counter plot between input parameters e.g. machining environment and spindle speed whole surface roughness is as a response variable. After plot, it can be said that wet machining condition and high spindle speed provide better surface roughness.

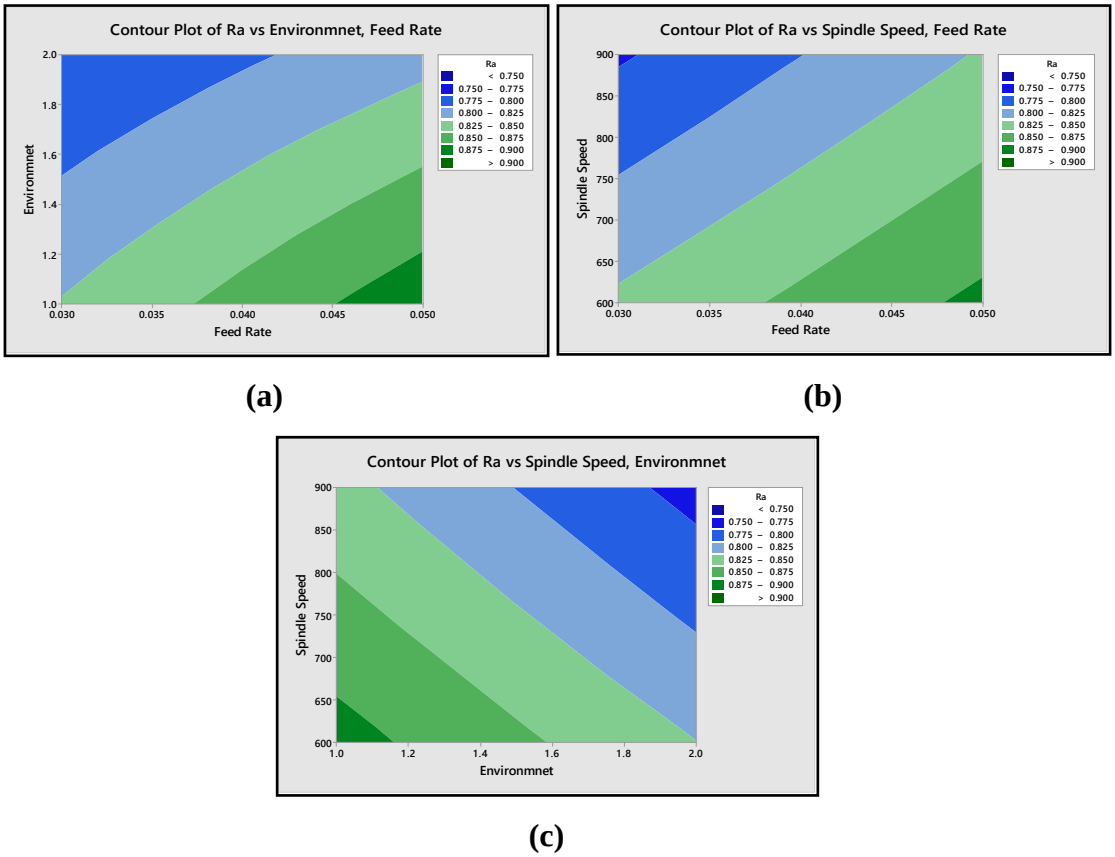

Fig. 5.7: (a, b, & c) Contour plot between input variable to the response

5.1.8 Confirmation test

For the validation of experimental results, a confirmation test is necessary. In this present study, the Taguchi result is validated as a predicated result by the regression model. The confirmation test was conducted under two set of experiment e.g. dry environment, 600 RPM, 0.03 mm/rev feed rate, and wet condition with 900 RPM, 0.05 mm/rev feed rate. Table 5.4 shows the confirmation test.

Table 5.4: Confirmation Test

Test (Level)	Experimental value	Predicated Value	% of error
1 (1-600-0.03)	0.857	0.8598	0.32 %
2 (2-900-0.05)	0.785	0.7973	1.56 %

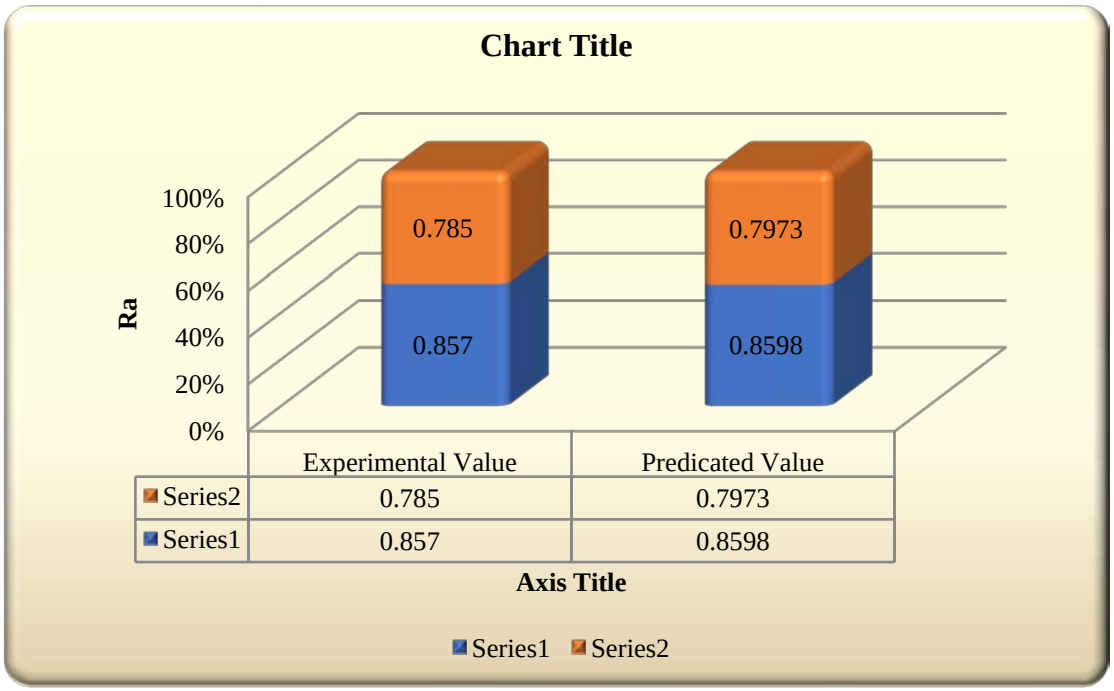

Fig. 5.8: Chart of the confirmation test

After analysis of the table 5.4 and figure 5.8, it was observed that the experimental value was nearest to predicated value with 0.32% to 1.56 % error. Figure 5.8 shows the error of experimental value and predicated value through the chart.

5.2 Experimental Investigation Under Dry, MQL, and LCO_2 Conditions

The study focuses on a machinability investigation for drilling of DSS 2205 using TiAlN coated solid carbide drill under dry, MQL, and LCO_2conditions. The measured output was surface roughness and hole deviation, which was measured by CMM and surface roughness tester. ANOVA is a mathematical method used to

determine whether the means of two or more groups vary from one another statistically. It is used to judge the significant machining parameters influencing the evaluated parameters. Moreover, a regression model has been developed to generate a functional relationship among input and measured output/response parameters. Furthermore, a confirmation test was carried out to compare the experimental results to predicated model results and also, to find out the % error between experimental results to predicted results. Furthermore, a genetic algorithm (GA) was implemented for the optimum value of process parameters and optimized value of responses, respectively.

5.2.1 Experimental Results

The surface roughness (Ra) and hole deviation were considered as evaluated parameters using TiAlN coated tool and are listed in the table 5.5. As the drilling process has been employed instead of the drilling process, the key purpose is to identify the main contributing parameters that affected the studied response.

Table 5.5: Experimental results for responses under dry, MQL, LCO_2 conditions

Exp. No.	Input Parameters			Output Parameters		S/N Ratio	
	Environment (E)	Spindle Speed (SS)	Feed rate (F)	Ra	Hole deviation	Ra	deviation
1	1	720	0.02	0.686	0.0754	3.27352	22.4526
2	1	720	0.04	0.618	0.0689	4.18023	23.2356
3	1	720	0.06	0.615	0.0723	4.22250	22.8172
4	2	920	0.04	0.585	0.0543	4.65688	25.3040
5	2	920	0.06	0.531	0.0489	5.49811	26.2138
6	2	920	0.02	0.471	0.0452	6.53958	26.8972
7	3	1120	0.06	0.573	0.0291	4.83691	30.7221
8	3	1120	0.02	0.426	0.0238	7.4118	32.4685
9	3	1120	0.04	0.390	0.0195	8.17871	34.1993

The Taguchi method is part of the design of the experiment (DOE) that is used to find the minimum number of experiments within the limitations of factor and level. The S/N ratio is utilized for apply the Taguchi approach, which presents the desired (mean) and unwanted (standard deviation) values for output variables. The S/N ratio is separated into three categories based on our study criteria: smaller is better, medium is better, and larger is better. Surface roughness (Ra) and hole deviation are two response variables in this article. As a result, equation 5.2 is used to calculate the S/N ratio, which is presented in Table 5.5. The influence of various input factors on response and analysis of variance is further illustrated in this article, which was done using Minitab 20 software.

S/N Ratio for smaller is better = $-10 \log 1/n \sum (R)^2$…….(5.2)

The various input parameters to output parameters are obtained by using the Taguchi method that is discussed below.

5.2.2 Variation of Surface roughness (Ra) With Input Parameters

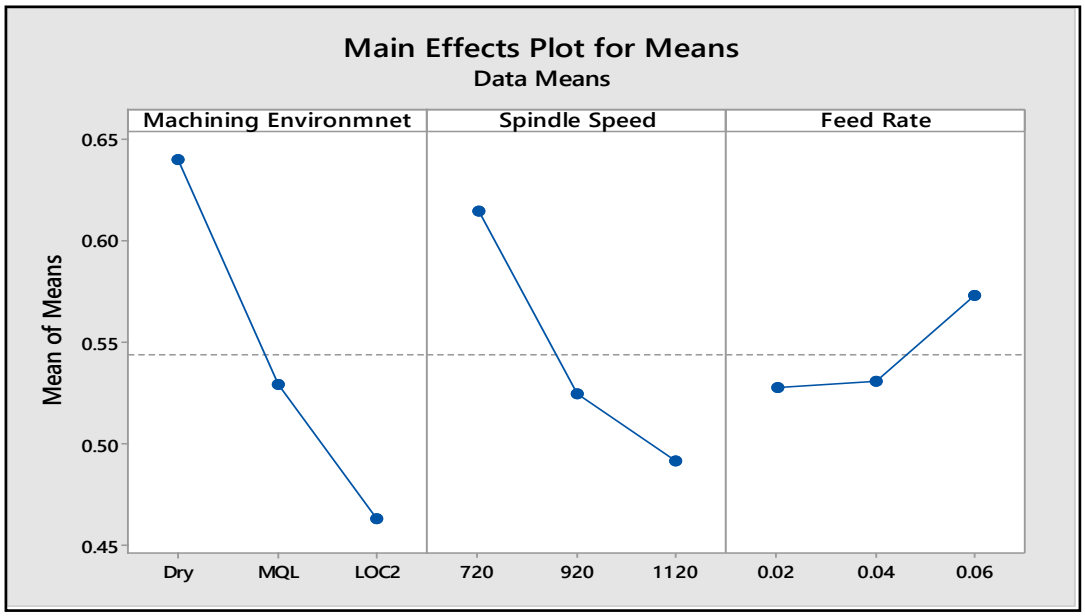

Fig. 5.9: Main effects plot for Means of Ra

The influence of various input factors on surface roughness is shown in Figure 5.9. Surface roughness (Ra) was found to be inversely related to spindle speed, as seen in the graph. Because if the spindle speed is increasing, then friction will cover more of the machining zone, which is why it is responsible for increasing

the machining temperature [Ankalagi et al., 2017]. Hence, the workpiece becomes soft due to thermal softening, so Ra is reduced. In addition, the feed rate was shown to be related to surface roughness. If the feed rate is increased, the value of surface roughness increases. The effect of spindle speed and feed rate on Ra value is similar to [Saravanakumar et al., 2016 &Sulaiman et al., 2014]. According to the graph and the literature review, the cooling environment has a considerable impact on machining. In the present study, cryogenic cooling techniques provide a minimum surface finish (0.39 microns) to MQL and dry machining, respectively for Ra.

5.2.3 Variation of hole deviation With Input Parameters

Figure 5.10 shows the influence of various input parameters on hole deviation. The hole deviation was found to be inversely related to the spindle speed, as seen in the graph. In terms of feed rate, it was observed that when the feed rate increased, hole deviation slightly decreased at 0.04 mm/rev but after the point hole deviation slightly increased. The effect of spindle speed and feed rate on hole deviation value is similar to [Vankanti et al., 2014].According to the graph and the literature review, the cooling environment has a considerable impact on machining. In this present study, cryogenic cooling techniques provide a minimum hole deviation error compared to MQL and dry machining, respectively for hole deviation.

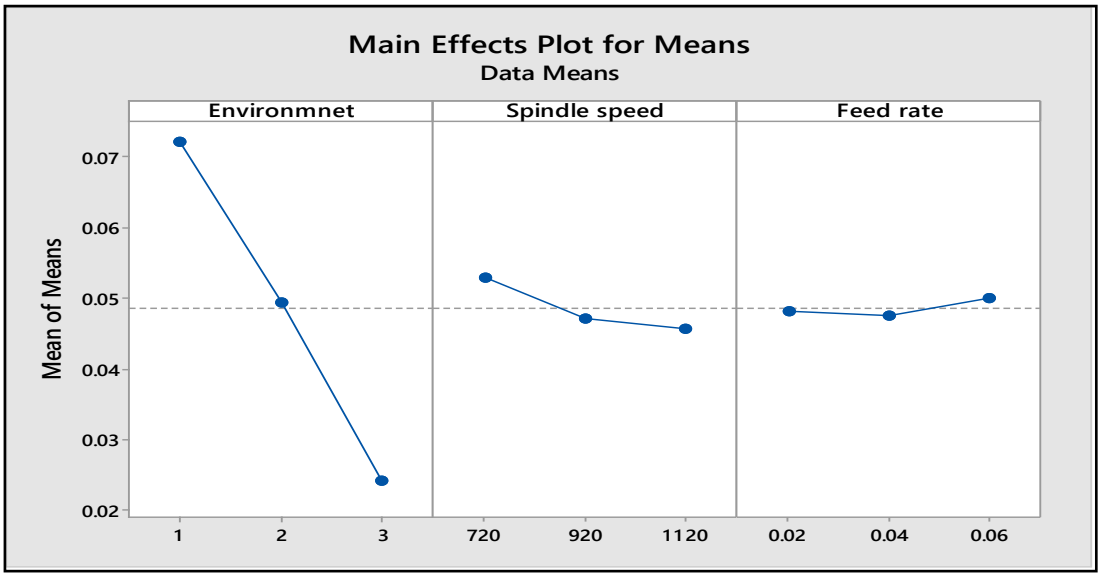

Fig. 5.10: Main effects plot for Means of hole deviation

5.2.4 Interaction Plot

5.2.4.1 Interaction plot of Ra

Figure shows the interaction effect plots of cutting parameters e.g. machining environment, spindle speed, and feed rate, and their effect on surface roughness as a response variable.

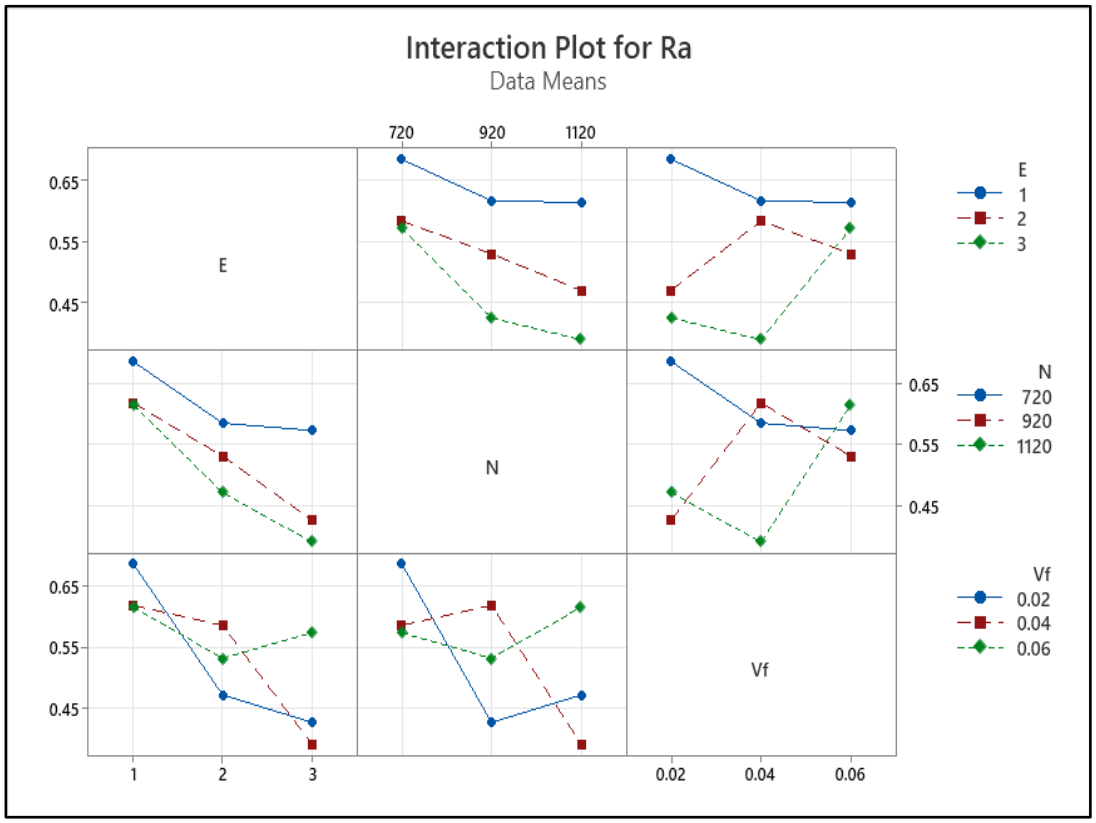

Fig. 5.11: Shows interaction plot for Ra

The figure 5.11 gives the interaction effect of two factors on the surface roughness of duplex stainless steel 2205 with TiAlN-coated solid carbide drill variation under dry, MQL, and LCO2conditions. According to the interaction plot, it can be said that the interaction between the machining environment, spindle speed, and feed rate gives the minimum surface roughness values and better surface finish. The figure 5.12 presented the lowest value of surface roughness and the best value of surface roughness. As per the figure, it was observed that the lowest value of surface roughness was 0.390 microns in a LCO_2 machining environment, high spindle speed of 1120 RPM, and a minimum feed rate of 0.03 mm /rev.

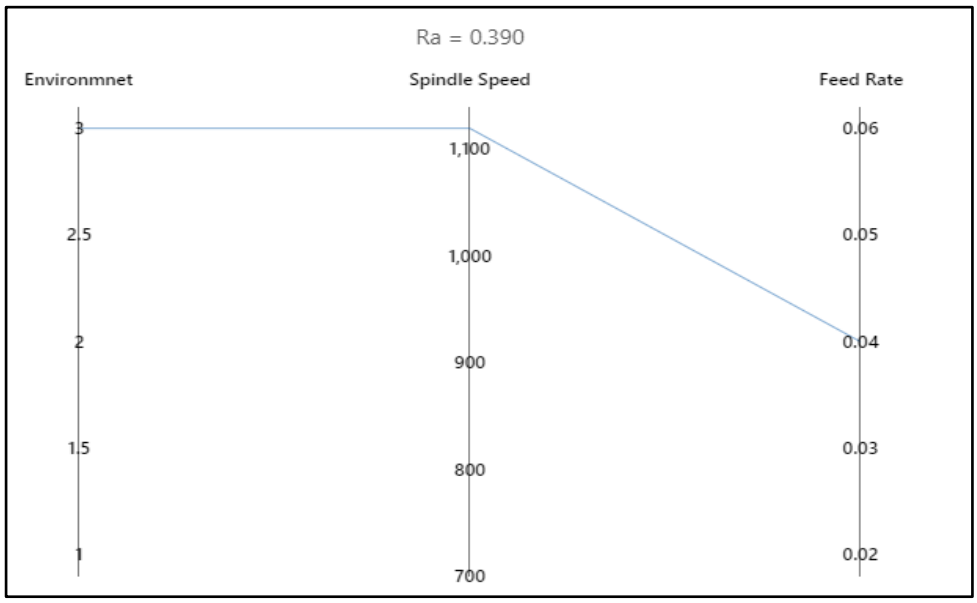

Fig. 5.12: the best value for Ra

5.2.4.2 Interaction plot of hole deviation

Figure 5.13 shows the interaction effect plots of cutting parameters e.g. machining environment, spindle speed, and feed rate, and their effect on hole deviation as a response variable.

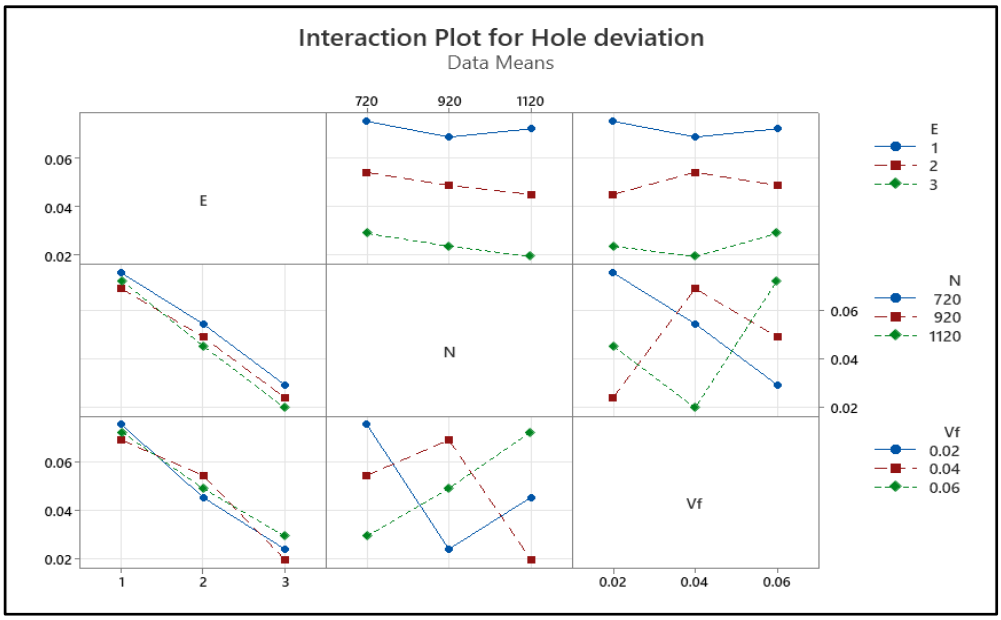

Fig. 5.13: Interaction plot for hole deviation

The figure gives the interaction effect of two factors on the hole deviation of duplex stainless steel 2205 with TiAlN-coated solid carbide drill variation under dry,

MQL, and LCO_2 conditions. According to the interaction plot, it can be said that the interaction between the machining environment, spindle speed, and feed rate gives the minimum value of hole deviation.

The figure 5.14 presented the lowest value of hole deviation and the best value of hole deviation. As per the figure, it was observed that the lowest value of hole deviation was 0.748 microns in a LCO_2 machining environment, high spindle speed of 1120 RPM, and a feed rate of 0.04 mm /rev.

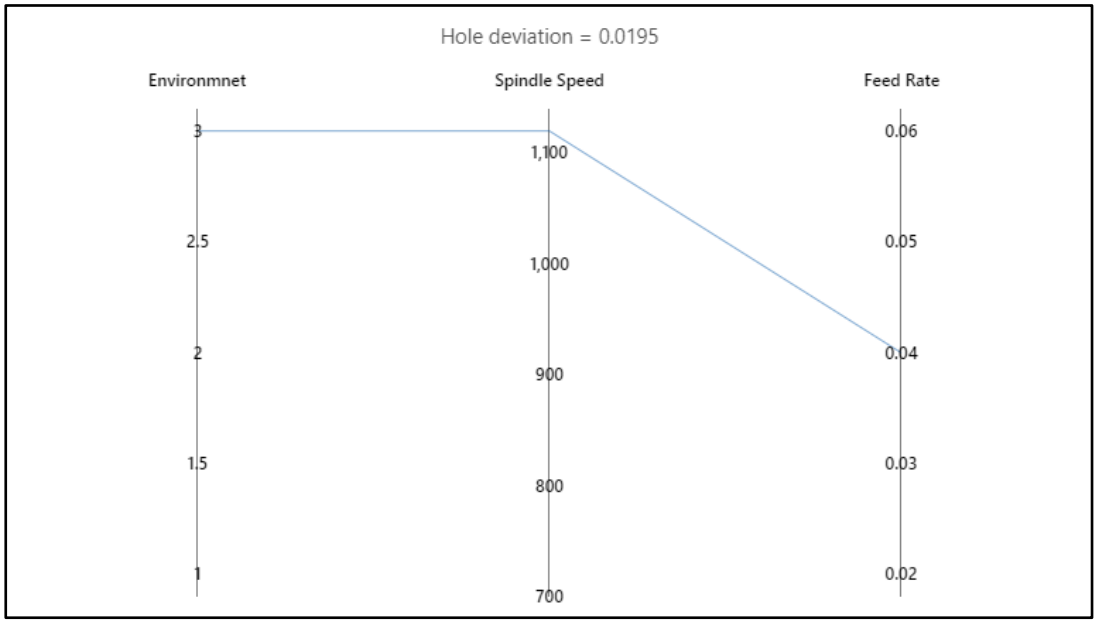

Fig. 5.14: The best value of hole deviation

5.2.5 Selection of optimum parameter condition in terms of Ra and hole deviation

5.2.5.1 Response Table for S/N Ratio of Ra

Table 5.6 shows the response table for surface roughness. As demonstrated in figure 5.15, the lowest means for Ra were obtained with a cryogenic cooling, spindle speed of 1120RPM, and feed rate of 0.02 mm/rev. According to Taguchi's analysis, the optimal process parameters for the lowest surface roughness are 1120 RPM spindle speed, 0.02 mm/rev feed rate, and cryogenic (LCO_2) cooling. The optimum combination of process parameters is LCO2-1120-0.02.

Table 5.6:Response Table for S/N ratio of Ra

Level	Machining Environment (E)	Spindle speed (SS)	Feed Rate (F)
1	3.892	4.256	**5.742**
2	5.565	5.697	5.672
3	**6.809**	**6.314**	4.853
Delta	2.917	2.058	0.889
Rank	1	2	3

The influence of machining input parameters e.g. machining environment, feed rate, and spindle speed 2.917, 0.889, 2.058 respectively on Ra. After the analysis of the response table, it was observed that the machining environment has an enormous effect on Ra compared to other input parameters.

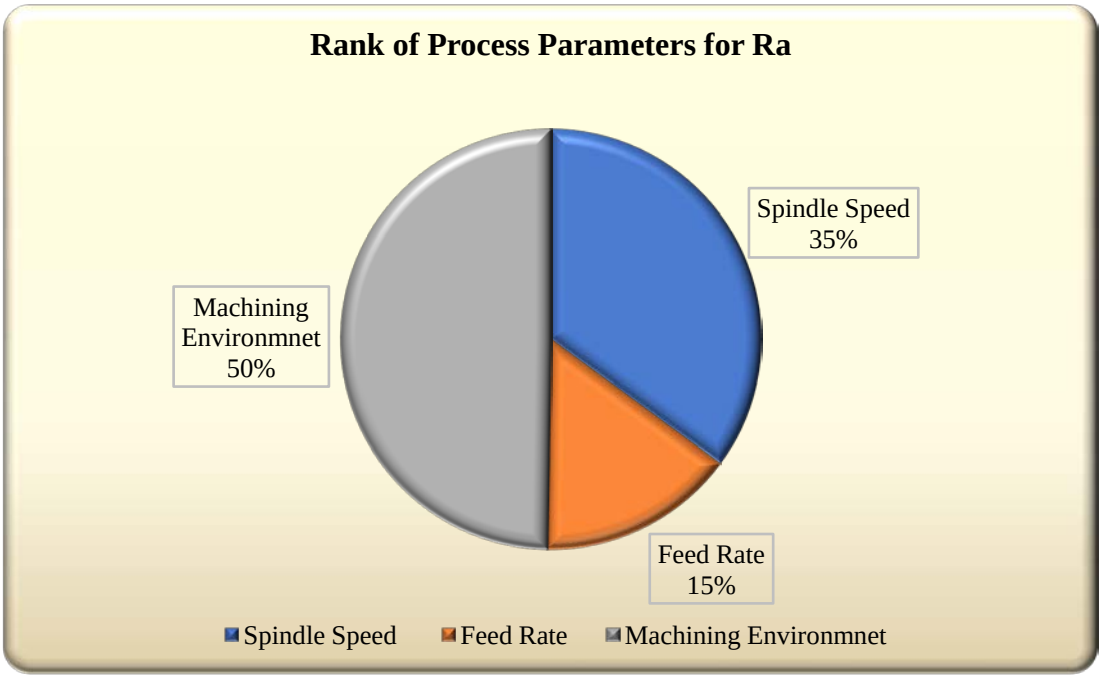

Fig. 5.15: Graphical representation of response for Ra

Figure 5.15 is a graphical representation of the delta value and rank of process parameters, which effect on surface roughness (Ra). According to the figure, it was easily observed that the machining environment the is most effective process

parameters on surface roughness compared to others e.g. spindle speed, and feed rate, respectively.

5.2.5.2 Response Table for S/N Ratio of hole deviation

Table 5.7 presents the hole deviation response table in the same way. The optimum process parameters for the lowest hole deviation are spindle speed at 1120 RPM, feed rate at 0.04, and cryogenic cooling technique, according to figure 5.16, and the predicated optimum process parameters for the lowest hole deviation are spindle speed at 1120 RPM, feed rate at 0.04, and cryogenic cooling technique, according to Taguchi analysis. The optimum combination of process parameters is LCO_2-1120-0.02.

Table 5.7:Response Table for S/N Ratio of hole deviation

Level	Machining Environment (E)	Spindle Speed (SS)	Feed rate (F)
1	22.84	26.16	27.27
2	26.14	27.31	**27.58**
3	**32.46**	**27.97**	26.58
Delta	9.63	1.81	1.00
Rank	1	2	3

The influence of machining input parameters e.g. machining environment, feed rate, and spindle speed 9.63, 1.00, 1.81 respectively on hole deviation. After the analysis of the response table, it was observed that the machining environment has an enormous effect on hole deviation compared to other input parameters.

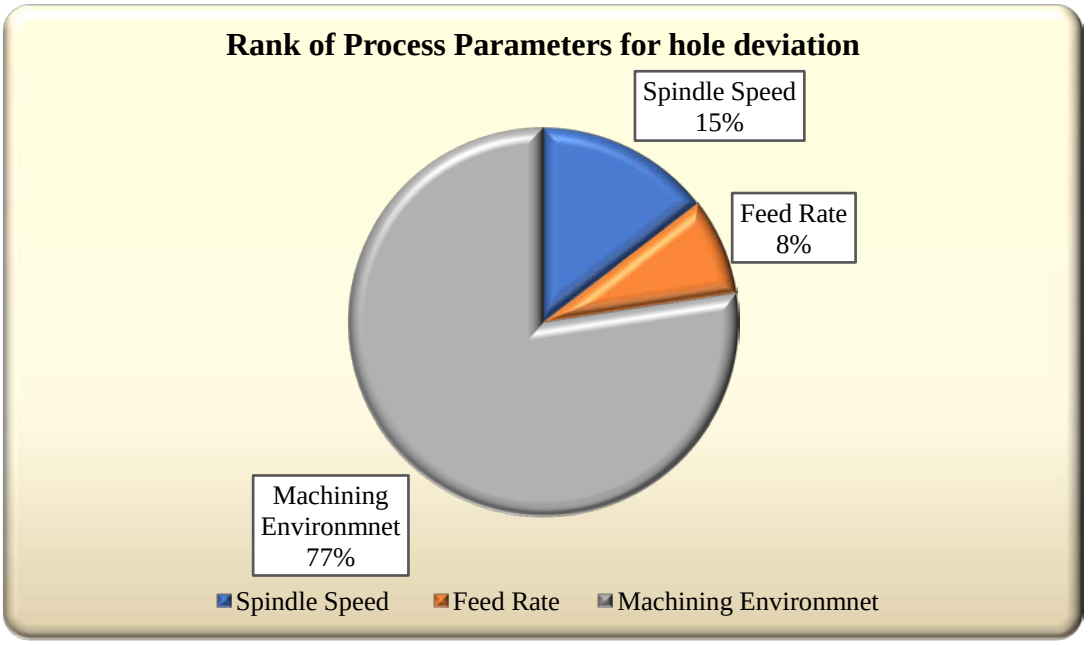

Fig. 5.16: Graphical representation of response for hole deviation

Figure 5.16 is a graphical representation of the delta value and rank of process parameters, which effect on hole deviation (Ra). According to the figure, it was easily observed that the machining environment the is most effective process parameters on surface roughness compared to others e.g. spindle speed, and feed rate, respectively.

5.2.6 ANOVA analysis for Ra and hole deviation

ANOVA is an analysis of variance, which means mostly affects process parameters on response and their contribution. Surface roughness (Ra) is largely determined by coolant type, spindle speed, and feed rate, according to table 5.8. Coolant, spindle speed, and feed rate all contribute 62.63 percent, 31.67 percent, and 5.02 percent of the total, respectively for Ra. Hole deviation is mostly impacted by coolant type, spindle speed, and feed rate, as shown in Table 5.9. The percentage contributions of coolant type, spindle speed, and feed rate, as indicated in the table, are 96.45 percent, 2.45 percent, and 0.30 percent, respectively for hole deviation. It was discovered that the coolant type impacted process parameters the most for Ra and hole deviation.

Table 5.8: ANOVA analysis for Ra

Source	DF	Seq SS	Adj SS	Adj MS	F value	P value	Contribution
E	2	0.047814	0.047814	0.023907	91.91	0.011	62.63 %
SS	2	0.024176	0.024176	0.012088	46.47	0.021	31.67 %
F	2	0.003830	0.003830	0.001915	7.36	0.120	5.02 %
Error	2	0.000520	0.000520	0.000260			0.68 %
Total	8	0.0763					100 %

S = 0.0161250, R-Seq = 99.32 %, R-Seq (Adj) = 97.27 %

Figure 5.17 shows the graphical representation of the % of the contribution of cutting parameters on surface roughness. It can be seen that the machining environment, has the highest contribution on surface roughness in the drilling of DSS 2205 with TiAlNcoated solid carbide drill under dry, MQL, and LCO_2 conditions followed by spindle speed and feed rate.

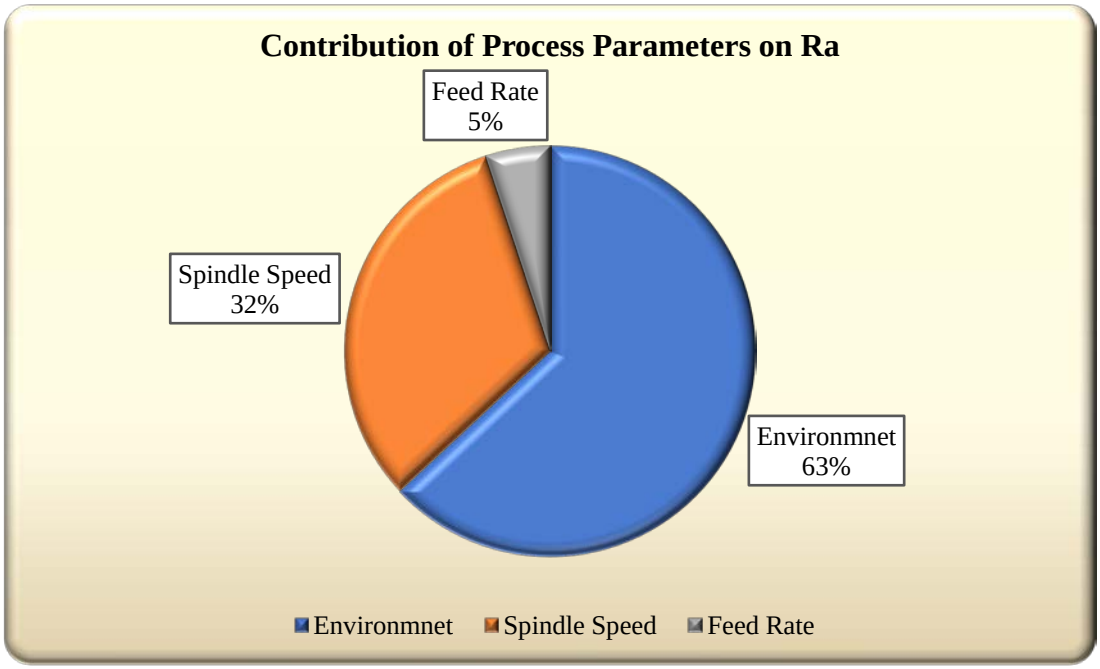

Fig. 5.17: Graphical representation of the contribution of input parameters on Ra

Table 5.9: ANOVA analysis for hole deviation

Source	DF	Seq SS	Adj SS	Adj MS	F Value	P Value	Contribution
E	2	0.003469	0.003469	0.001754	322.03	0.003	96.45 %
SS	2	0.000088	0.000088	0.000044	71.97	0.038	2.46 %
F	2	0.000011	0.000011	0.000005	1.00	0.501	0.30 %
Error	2	0.000011	0.000011	0.000005			0.30 %
Total	8	0.003578					100 %

S = 0.0023065, R-Seq = 99.70 %, R-Seq (Adj) = 98.81 %

Figure 5.18 shows the graphical representation of the % of contribution of cutting parameters on hole deviation. It can be seen that machining environment, has the highest contribution on surface roughness in drilling of DSS 2205 with TiAlN coated solid carbide drill under dry, and wet conditions followed by spindle speed and feed rate.

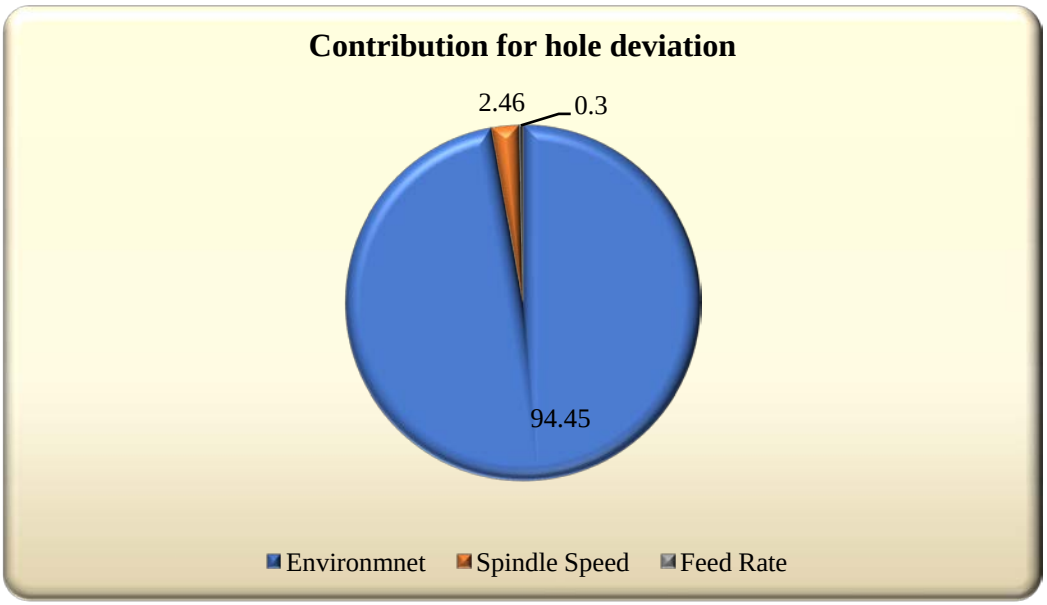

Fig. 5.18: Graphical representation of contribution of process parameters for hole deviation

5.2.7 Regression model analysis

The dependent variables such as coolant type, spindle speed, and feed rate with two independent variables such as Ra and hole deviation were constructed using the Minitab 20.0 software tool.On each response, no modification has been applied. Eqn. (5.3) and Eqn. (5.4), respectively, illustrate the prediction equations generated from the regression analysis for Ra and hole deviation.

Ra = 0.9574 – 0.0883 E – 0.000307 SS + 1.33 F (R-Seq = 99.32 %) +/-€..... (5.3)

Hole deviation = 0.11141 – 0.024033 E – 0.000018 SS + 0.0492 F +/-€
(R-Seq = 99.70%). (5.4)

A coefficient of determination R^2 was used to test the capabilities of the created models. The coefficient of determination might be anything between zero and one. If it's close to one, the dependent and independent variables are likely to be well-matched. If R^2= 95 percent, it suggests that fresh observations were created with a 95 percent variability. The generated regression models for surface roughness (Ra) and hole deviation in this work had high R^2 values of 99.32 % and 99.70% percent, respectively. The coefficients in the projected model were checked for significance using the residual plot. Residual analysis is the major diagnostic tool to check model adequacy [57]. Figures5.19 and 5.20 show a normal probability plot for Ra and hole deviation, respectively. The residual plot shows the normality of the assumption is satisfied as well as the points lying very close along a straight line. Residual lies close to a straight line indicating that errors are distributed normally. The predicted value and the experimental value are very close to each other.

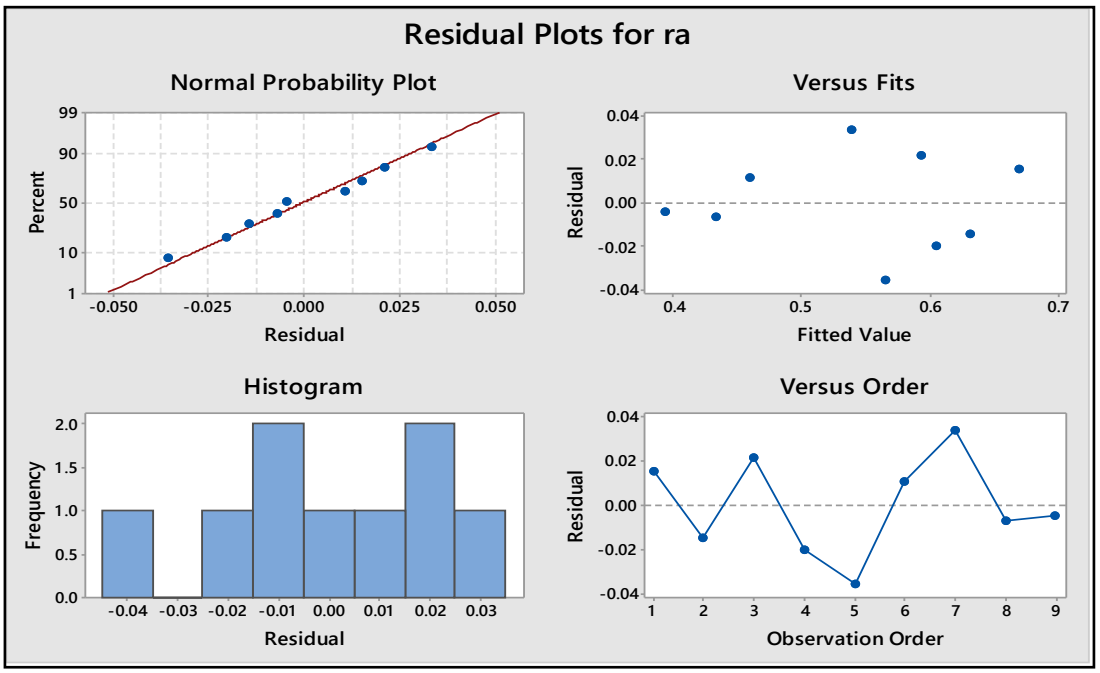

Fig. 5.19: Residual Plot for Ra

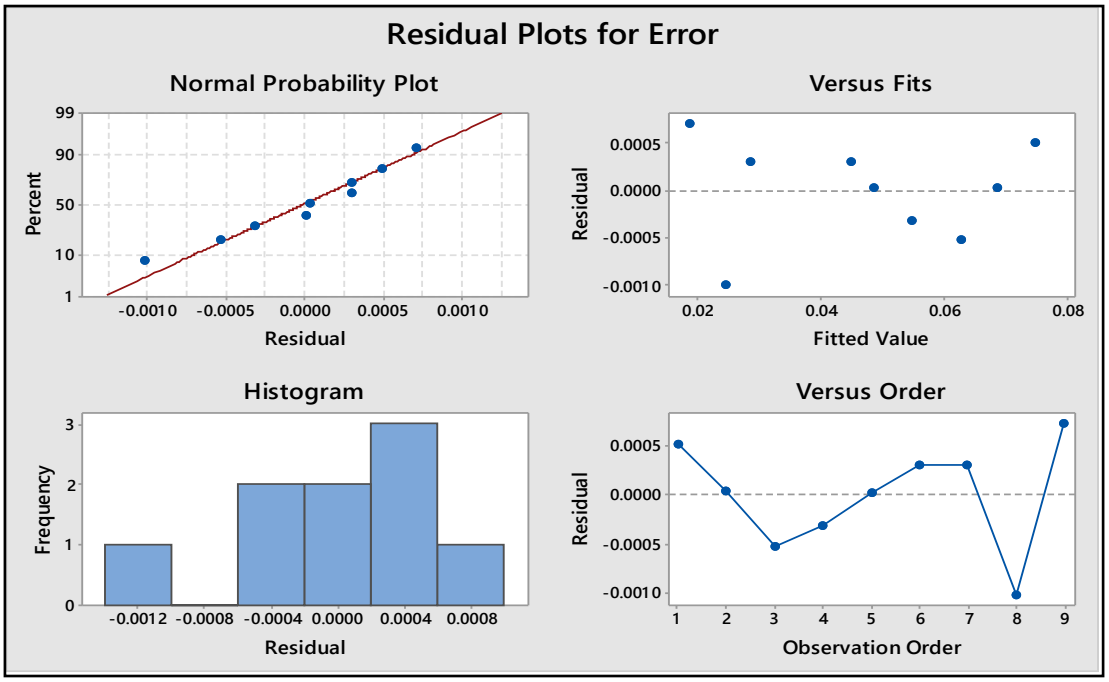

Fig.5.20: The Residual Plot for hole deviation

In this research, confirmation tests were done to validate the regression model and experimental results. These results are shown in Table5.5. The testing results were generated at random using the L9 orthogonal experimental design. As per the confirmation test, it was found that the built model results and experiments

result are in good agreement with each other with minimum % of error 1.68 & 0.13 for Ra and hole deviation, respectively.

The relationship between the response variable and two input variables is depicted in the contour plot graph. Figure 5.21 depicts the relationship between the input variable and the response variables of surface roughness (Ra) and hole diameter error/hole deviation. Figure 5.21 (a) shows the machining environment, spindle speed to surface roughness as the response variable. As per the contour plot, it can be said that the minimum surface roughness value was found at LCO_2 machining condition and the high spindle speed. Similarly, Figure5.21 (b) illustrates how a cryogenic coolant and a low feed rate improve surface roughness (Ra). High spindle speed and low feed rate also result in minimal surface roughness, as seen in Figure 5.21 (c). Figure 5.21 (d) plot between machining environment, and spindle speed while hole deviation as response variable. According to plot, it can be observed that optimal hole deviation was found LCO_2 machining environment and high spindle speed. Figure 5.21 (e) shows that cryogenic (LCO_2) coolant type and low feed rate improve the hole deviation. Furthermore, as shown in figure 5.21 (f), high spindle speed and low feed rate resulted in low hole deviation.

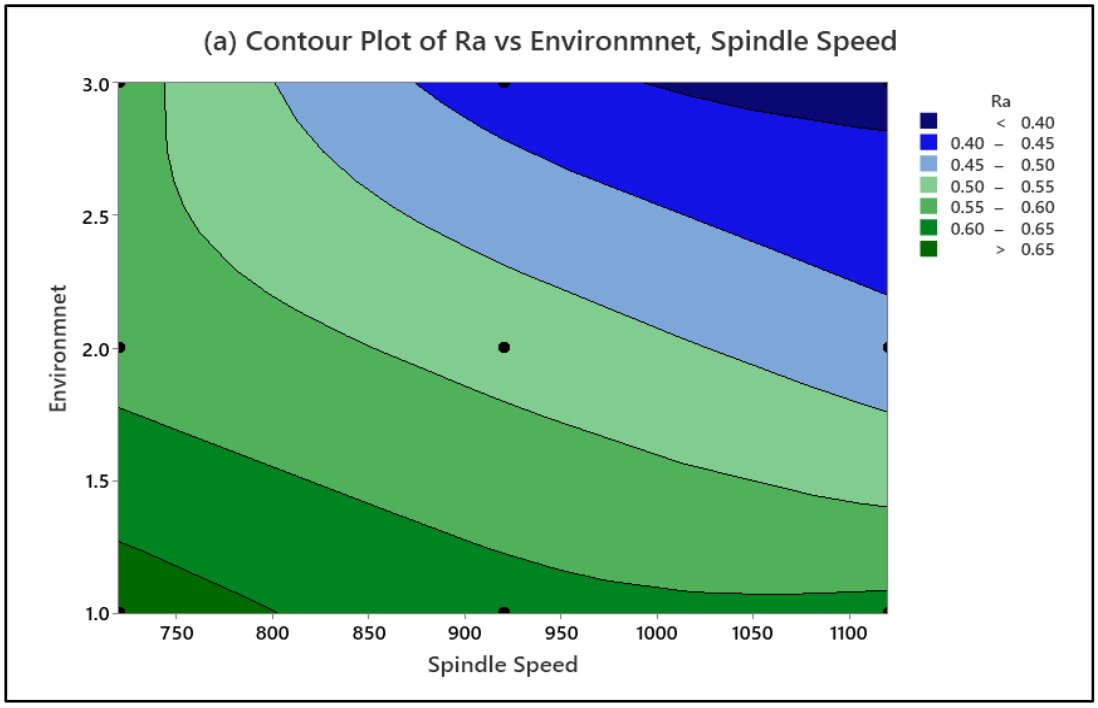

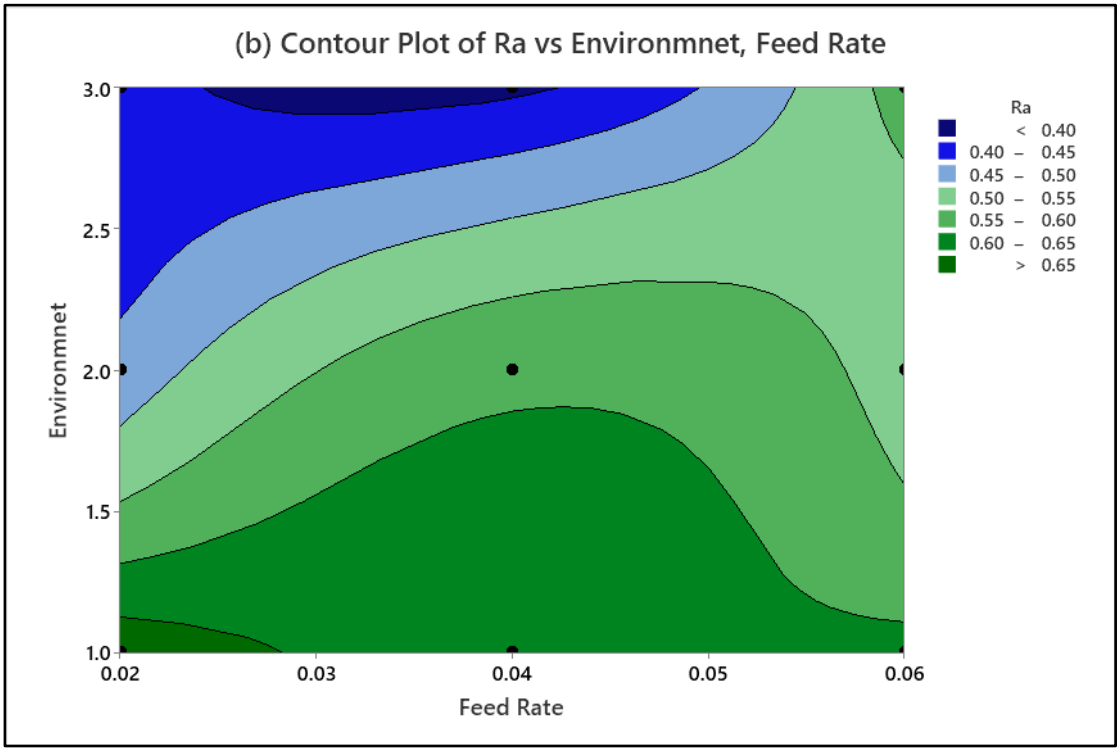
(b) Contour Plot of Ra vs Environmnet, Feed Rate
Environmnet
3.0
2.5
2.0
1.5
1.0
0.02
0.03
0.04
0.05
0.06
Feed Rate
Ra
< 0.40
0.40 – 0.45
0.45 – 0.50
0.50 – 0.55
0.55 – 0.60
0.60 – 0.65
> 0.65

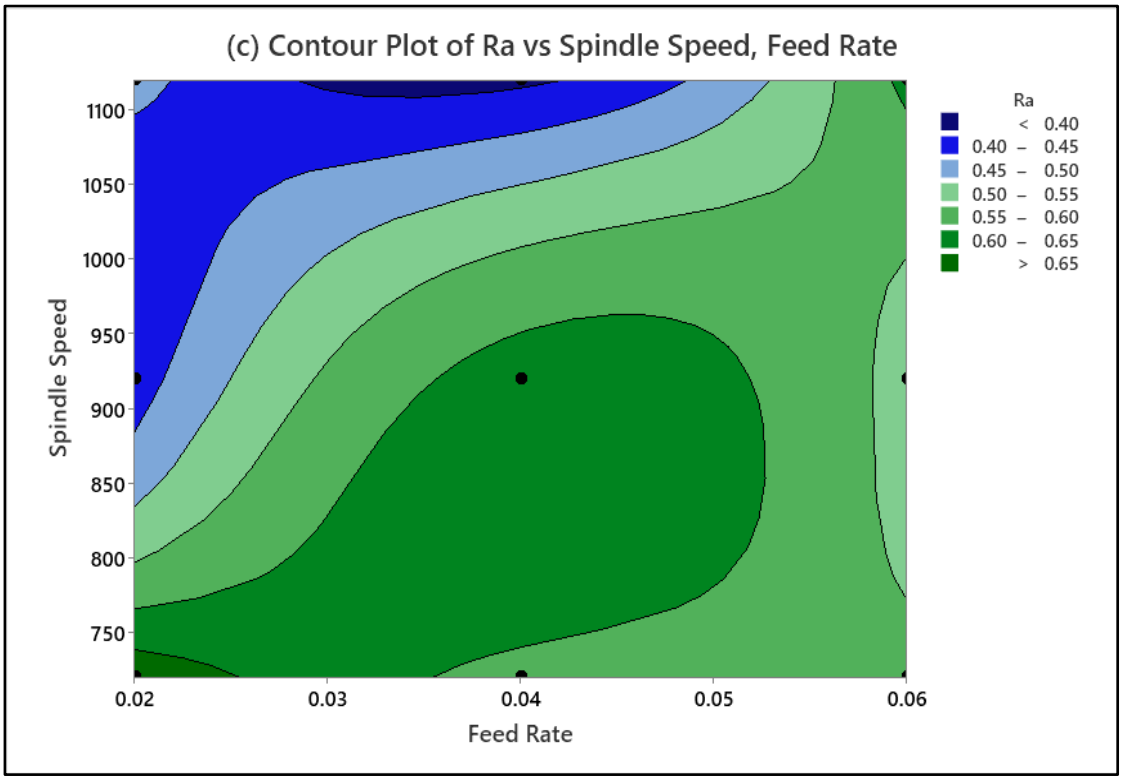
(c) Contour Plot of Ra vs Spindle Speed, Feed Rate
Spindle Speed
1100
1050
1000
950
900
850
800
750
0.02
0.03
0.04
0.05
0.06
Feed Rate
Ra
< 0.40
0.40 – 0.45
0.45 – 0.50
0.50 – 0.55
0.55 – 0.60
0.60 – 0.65
> 0.65

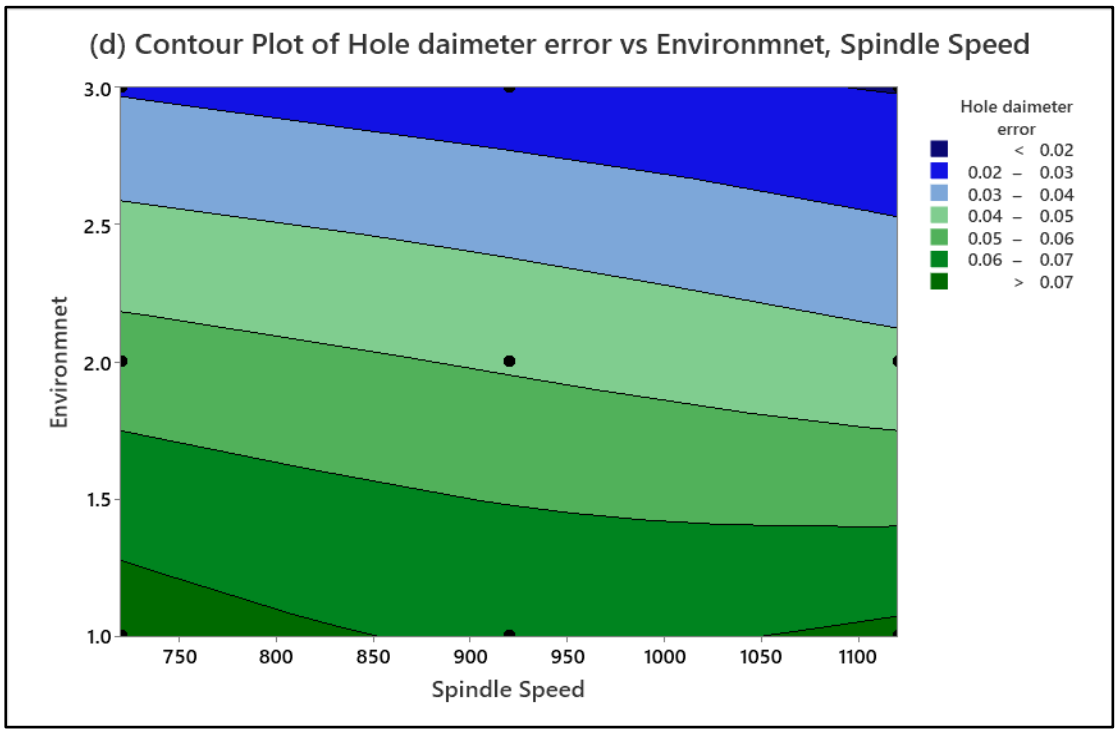
(d) Contour Plot of Hole daimeter error vs Environmnet, Spindle Speed
Environmnet
3.0
2.5
2.0
1.5
1.0
750
800
850
900
950
1000
1050
1100
Spindle Speed
Hole daimeter error
< 0.02
0.02 – 0.03
0.03 – 0.04
0.04 – 0.05
0.05 – 0.06
0.06 – 0.07
> 0.07

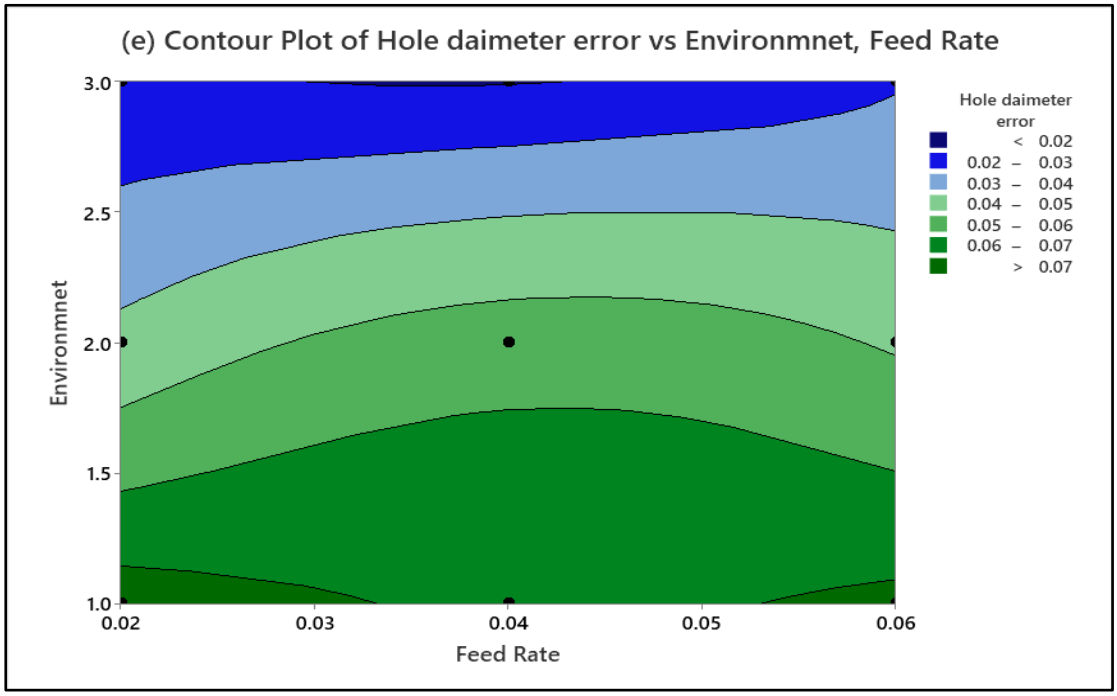
(e) Contour Plot of Hole daimeter error vs Environmnet, Feed Rate
Environmnet
3.0
2.5
2.0
1.5
1.0
0.02
0.03
0.04
0.05
0.06
Feed Rate
Hole daimeter error
< 0.02
0.02 – 0.03
0.03 – 0.04
0.04 – 0.05
0.05 – 0.06
0.06 – 0.07
> 0.07

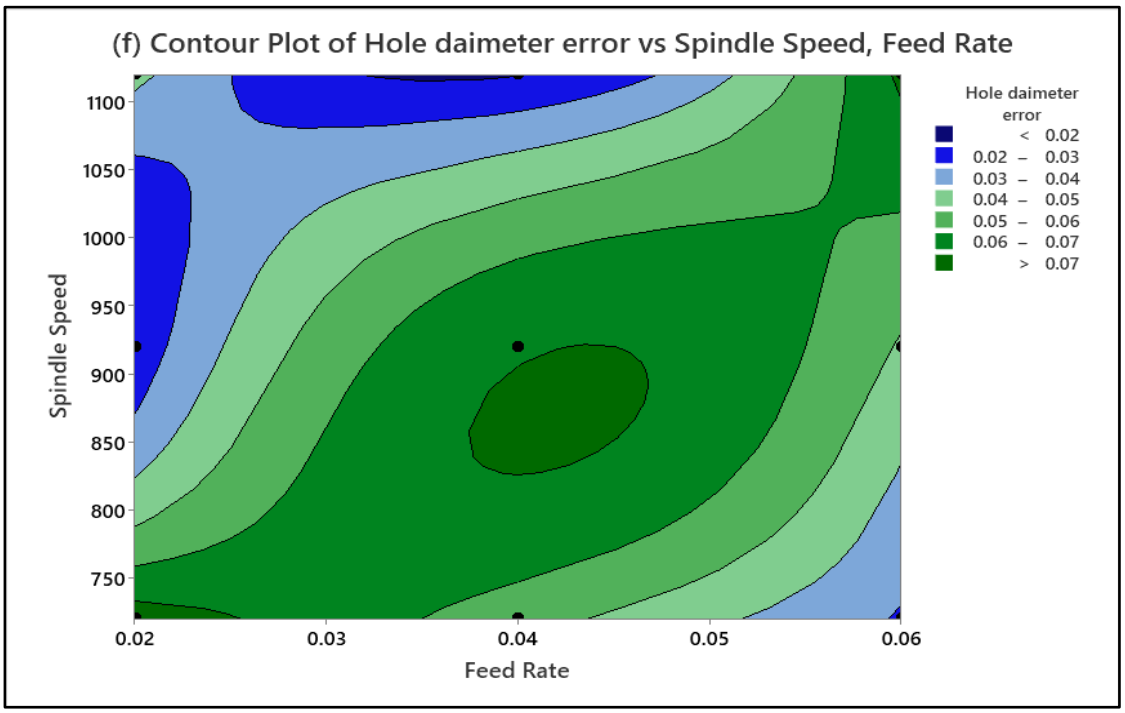

Fig.5.21: Contour plot for Ra and hole deviation with respect to the input variable

5.2.8 Confirmation test of Taguchi result

The experimental confirmation test is the final step to verify the results, which are drawn based on the Taguchi design approach. In the present study, a confirmation test was conducted through the levels of process parameters (E_1, N_1, V_{f1}) for responses shown in table 5.10. The purpose of the confirmation test was to validate the cutting conditions (E_1, N_1, V_{f1}) that were suggested by the experimental results, which corresponded with the predicted value for Ra and hole deviation. From table 5.11 it was observed that the predicted value is less than the experimental value. Also, the improvement of the S/N ratio is shown in table 5.12. Also, figure 5.22& 5.23 shows a comparison chart between predicted value to experimental value for responses, respectively.

Table 5.9:Level of process parameter for a confirmation test

Test	Environment (E)	Spindle Speed (SS)	Feed Rate (F)
1	1	720	0.02

Table 5.10: Comparison of experimental value and predicated model value

Test	Experimental Value		Predicated value through a regression equation		% of Error	
	Ra	Hole deviation	Ra	Hole deviation	Ra	Hole deviation
1	0.686	0.0754	0.67466	0.0753	1.68	0.13

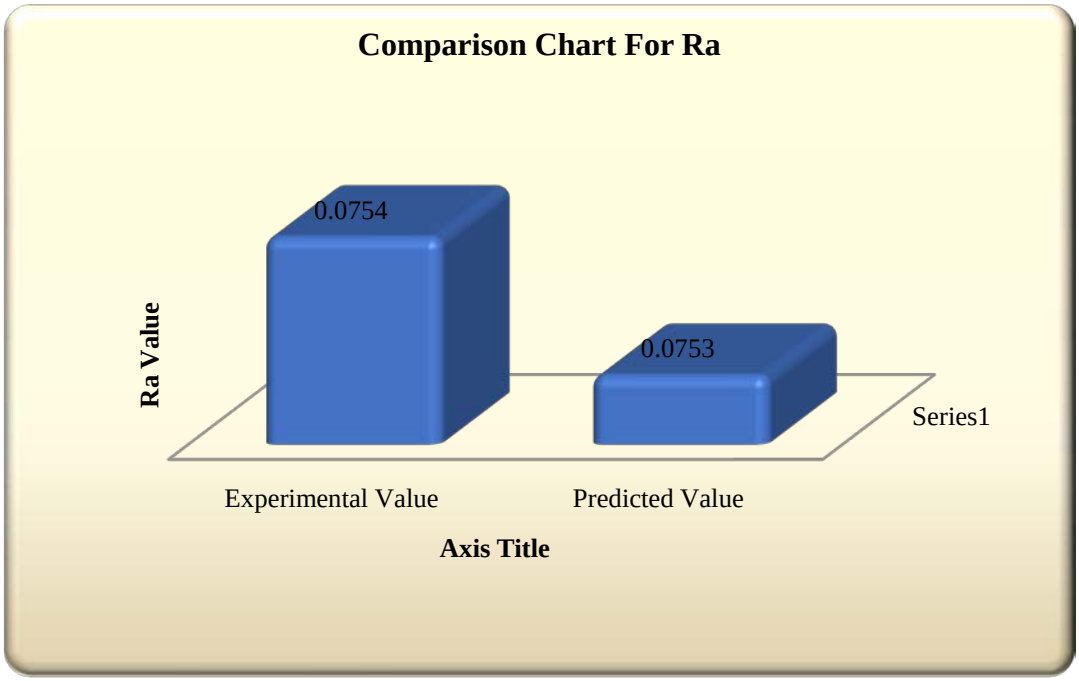

Fig. 5.22: Comparison chart for Ra

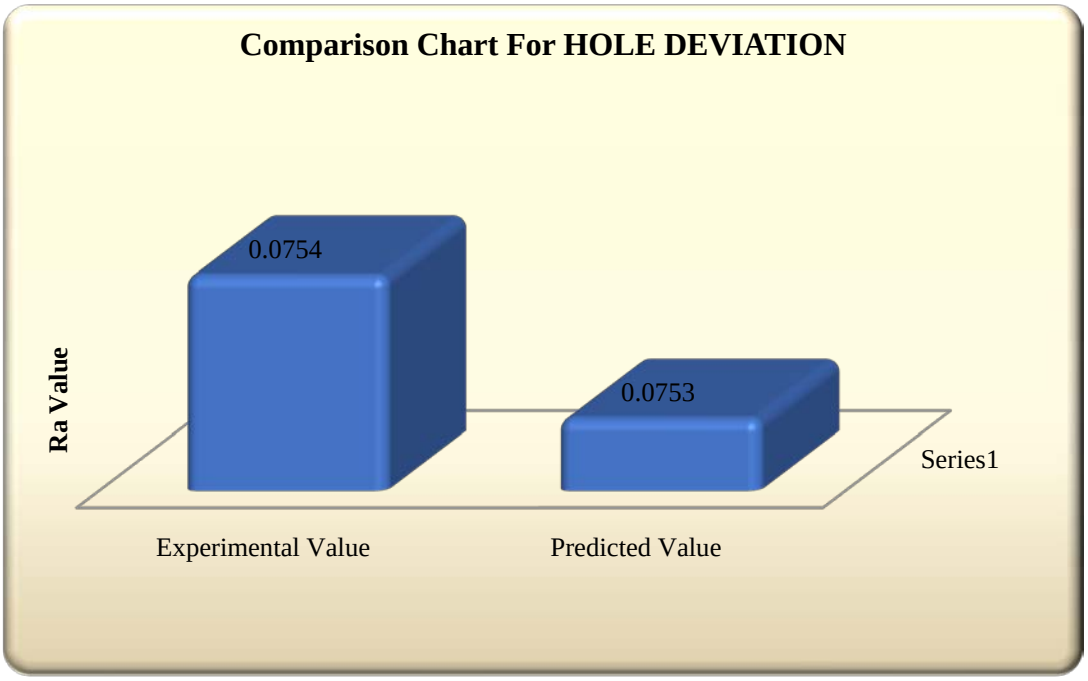

Fig.5.23: Comparison chart for hole deviation

Table 5.12: Confirmation test in terms of S/N ratio of Ra and hole deviation

	Surface Roughness (Ra)		**Hole deviation**	
Level	**E_1, SS_1, F_1**		**E_1, SS_1, F_1**	
	Experiment	**Predicated**	**Experiment**	**Predicated**
S/N Ratio	3.27352	3.04543	22.4526	21.9763

5.2.9 Implementation of Genetic Algorithm (GA)

The GA method is used on unconstrained and constrained optimization problems by using MATLAB software.

Genetic algorithms (GA) are computational models which are implemented by using evolution. These algorithms store a potential solution to a particular issue on a data structure resembling a chromosome. Even though genetic algorithms have been used to solve a wide variety of problems, they are often thought of as functional optimizers.

A population of chromosomes is often when a genetic algorithm is used first. When evaluating these kinds of structures and allocating reproduction opportunities, one should make sure that the chromosomes are given more opportunity to reproduce if they are thought to be a good solution to the goal issue. A solution's "goodness" is often assessed in relation to the present population.

The evolution process and natural genetics serve as the inspiration for the powerful, highly efficient optimization tool known as a genetic algorithm.

A genetic algorithm offers several benefits. It can swiftly find a sizable number of solutions. Bad ideas are readily abandoned; thus, they have little lasting impact on the outcome. The GA's nature implies that it doesn't need to be familiar with any laws and regulations because it operates on its own set of guidelines. This is really helpful for difficult issues.

5.2.9.1 Working Principle of GA

The most common applications for genetic algorithms include the solution of complicated problems, search, and problem-specific optimization. The biggest drawback of this strategy is that the algorithm consumes a lot of processing time.

The genetic algorithm starts with a set of solutions called the population.

- Replicating strategies from one population to produce a different one. The notion that the new population would be superior to the previous one strongly influences this.
- In order to create new, more appropriate solutions, solutions are chosen based on how well they work. They have a likelihood of having procreated.
- The process is continued until a certain condition is met. Follow these steps to create a genetic algorithm (GA). These are listed below.

5.2.9.2 Fitness function

A summary function called a fitness function is comparable to an objective function. To get the best results in terms of Ra and hole diameter inaccuracy, two different types of fitness functions are employed in this study. These are the following:

$Function_1$ = + 0.9574 – 0.0833 *E – 0.000307*SS + 1.33 *F (3);;

$Function_2$ = + 0.11141 – 0.024033* E – 0.000018* SS + 0.0492* F;;

5.2.9.3 Generation of the initial population

The vast population of chromosomes known as the initial populace is the basis of the Genetic Algorithm. The limits in this instance are the chromosomes that are created by the use of atypical abilities. In this method, continuous boundary obtains the required population. Every person in the two populations has their breaking point upsides of the choice variable selected from a provided legitimate reach.

5.2.9.4 Parameter Setting

No. of variable = 3,

Lower bound = [1, 720, 0.02],

Upper bound = [3, 920, 0.06].

5.2.9.5 Determine the optimal combination for Ra

The genetic algorithm was used to optimize the combined objective of response, namely surface roughness (Ra), for drilling on duplex stainless steel 2205, and the optimized value of process parameter and best value of Ra is illustrated in figure5.24.

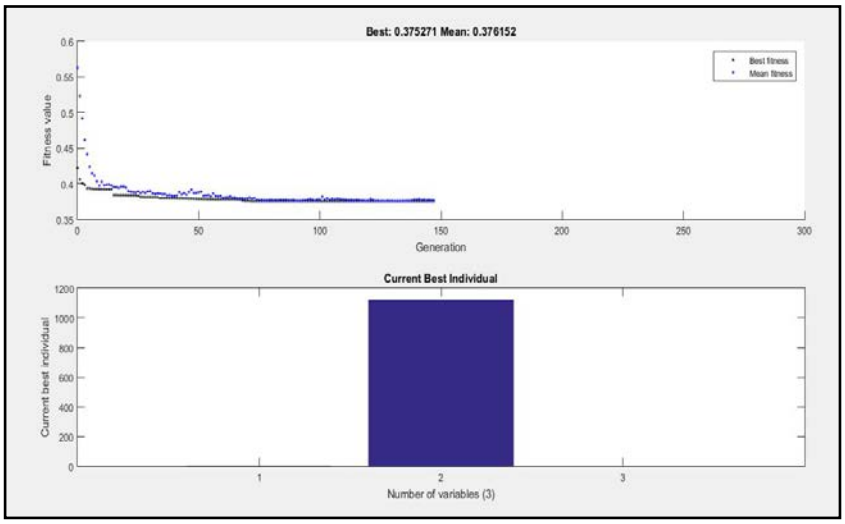

Fig.5.24: The optimized value of Ra

After implemented the genetic algorithm, it was discovered that the LCO2 environment has the best set of process parameters, with a spindle speed of 1120 and a feed rate of 0.02 for Ra as a response. And 0.3751 is the optimal value.

5.2.9.6 Determine the optimal combination for hole deviation

The genetic algorithm was used to optimize the combined objective of response, namely hole deviation, for drilling on duplex stainless steel 2205, and the optimized value of process parameter and best value of Ra is illustrated in figure 5.25.

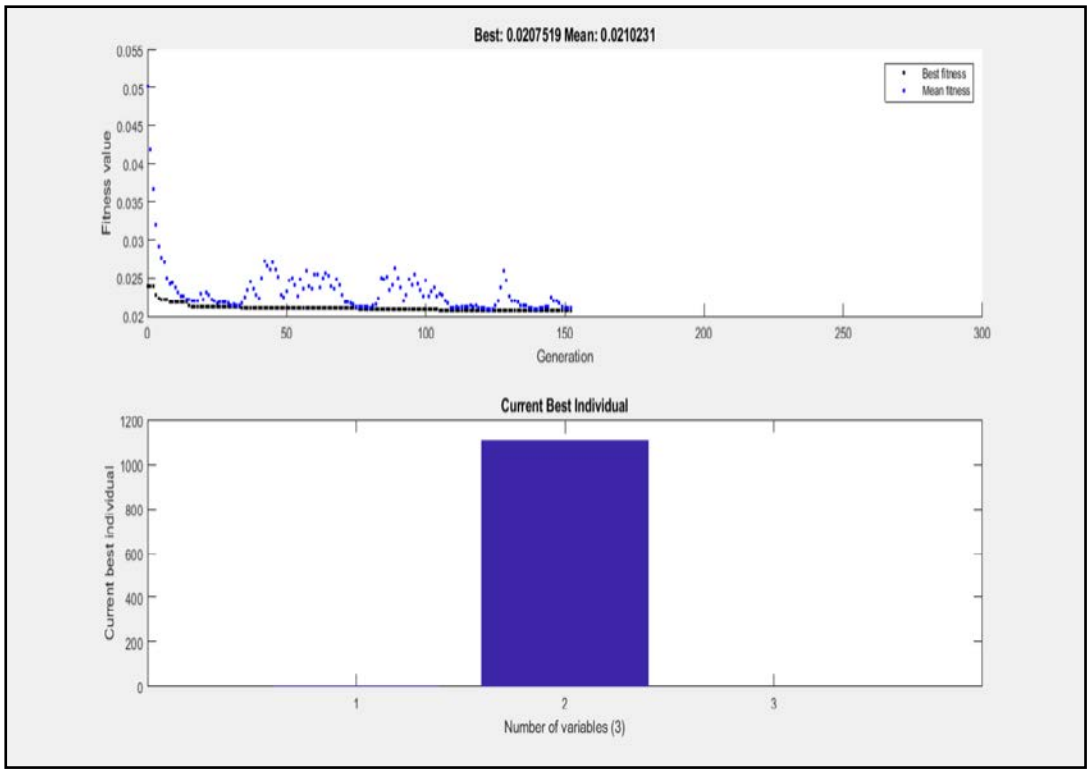

Fig. 5.25: The optimized value of hole deviation

After implementing the genetic algorithm, it was discovered that the LCO2 environment has the best set of process parameters, with a spindle speed of 1120 and a feed rate of 0.04 for Ra as a response. And 0.02075 is the optimal value.

5.2.10 Tool Wear Analysis

In this research, machining was carried out on duplex stainless steel 2205 under dry condition, MQL condition, and cryogenic machining with LCO2 with

TiAlN coated solid carbide. Machining was carried out with constant spindle speed (1100 RPM) and feed rate (0.020 mm /rev.).

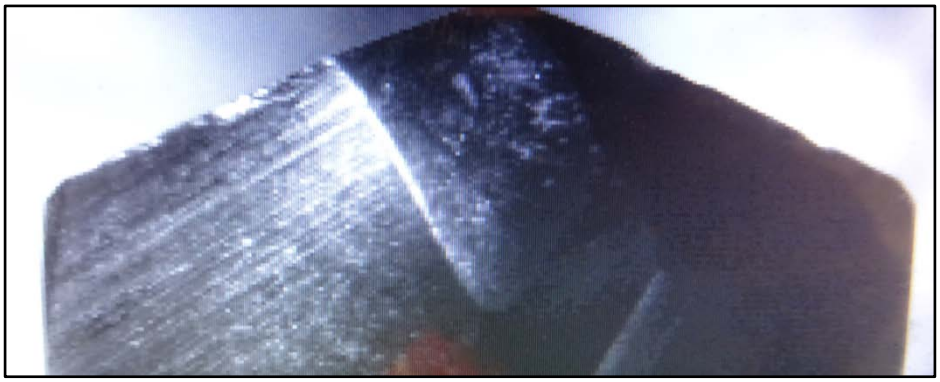

Dry Machining (a)

MQL Machining (b)

Cryogenic Machining (c)

Fig. 5.26: Tool wear analysis under dry, MQL, and LCO_2

After microscope analysis, it was observed that MQL machining gives minimum tool wear compared to cryogenic machining and dry machining. Because the MQL cooling system reduced cutting zone temperature, it reduced tool wear, as per figure 5.26.

5.3 Experimental Investigation Under Hybrid MQL-LCO_2 Condition

The study focuses on a machinability investigation for the drilling of DSS 2205 using a TiAlN-coated solid carbide drill in a hybrid MQL-LCO_2condition. The measured output was hole deviation, cylindricity error, and circularity error which was measured by CMM. The statistical difference between the means of two or more groups can be ascertained using the mathematical technique known as an ANOVA. It's employed to assess the important machining factors affecting the examined metrics. Furthermore, compare experimental results to predicated model results e.g. ANN, RSM, ANFIS, FLS. After that find, out % of error between experimental results to predicted results. Furthermore, TOPSIS techniques were implemented for finding the rank of the experiment.

5.3.1 Experimental Results

The hole deviation, cylindricity error, and circularity error were considered as evaluated parameters using TiAlN coated tool and are listed in the table 5.13. As the drilling process has been employed instead of the drilling process, the key purpose is to identify the main contributing parameters that affected the studied response.

Table 5.13: Experimental results under hybrid MQL-LCO_2 condition

Run order	Drill Diameter	Spindle Speed	Feed Rate	Experimental Value		
				Hole Deviation	Cylindricity	Circularity
1	-1	0	1	0.0292	0.0356	0.0061
2	0	-1	1	0.0305	0.0284	0.0063
3	1	1	0	0.0236	0.0320	0.0054
4	0	0	0	0.0273	0.0336	0.0056
5	-1	0	-1	0.0276	0.0310	0.0055
6	1	0	-1	0.0250	0.0295	0.00544
7	-1	-1	0	0.0282	0.0276	0.00567
8	0	0	0	0.0271	0.0287	0.0055

Run order	Drill Diameter	Spindle Speed	Feed Rate	Experimental Value		
				Hole Deviation	Cylindricity	Circularity
9	1	-1	0	0.0277	0.0230	0.00575
10	0	1	-1	0.0254	0.0306	0.0053
11	0	1	1	0.0270	0.0351	0.00589
12	1	0	1	0.02882	0.0312	0.00561
13	0	-1	-1	0.0290	0.0217	0.00602
14	-1	1	0	0.0279	0.0408	0.00597
15	0	0	0	0.0281	0.03259	0.00552

5.3.2 Variation of input parameters on responses

5.3.2.1 Variation of Hole deviation

Figure 5.27 shows the influence of various input parameters on hole deviation. In terms of drill diameter, the minimum value of hole deviation was found at a 6 mm drill diameter. The hole deviation was found to be inversely related to the spindle speed, as seen in the graph. In terms of feed rate, it was observed that when the feed rate increased, hole deviation continuously increases. According to the graph, it can be said that minimum hole deviation was found at 6 mm drill diameter, high spindle speed, and low feed rate.

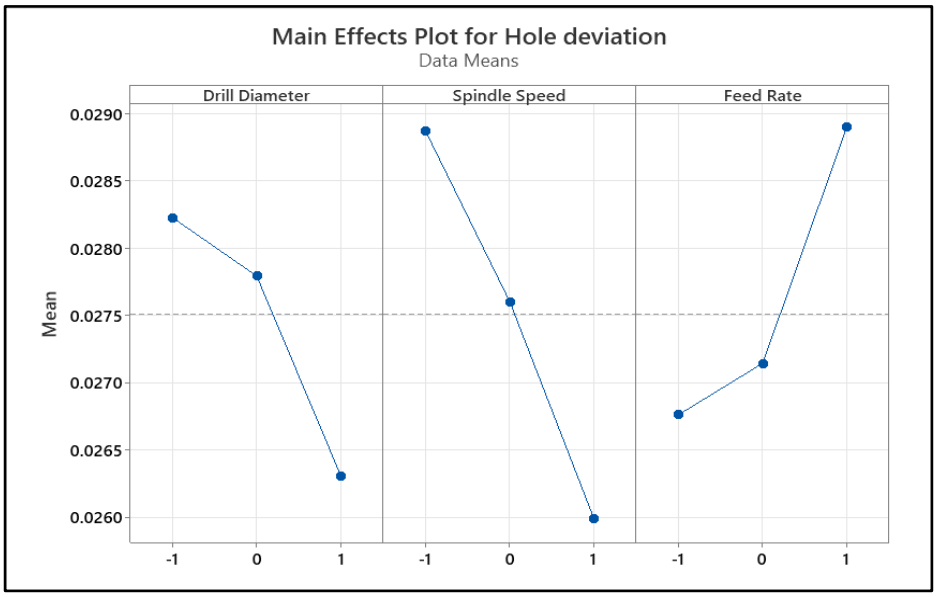

Fig. 5.27: Mean effect plot for hole deviation

5.3.2.2 Variation of cylindricity error

Figure 5.28 shows the influence of various input parameters on cylindricity error. In terms of drill diameter, the minimum value of cylindricity error was found at a 6 mm drill diameter. The cylindricity error was found to be proportionally related to the spindle speed, as seen in the graph. In terms of feed rate, it was observed that when the feed rate increased, cylindricity error continuously increases. According to the graph, it can be said that minimum cylindricity error was found at a 6 mm drill diameter, lowspindle speed, and low feed rate.

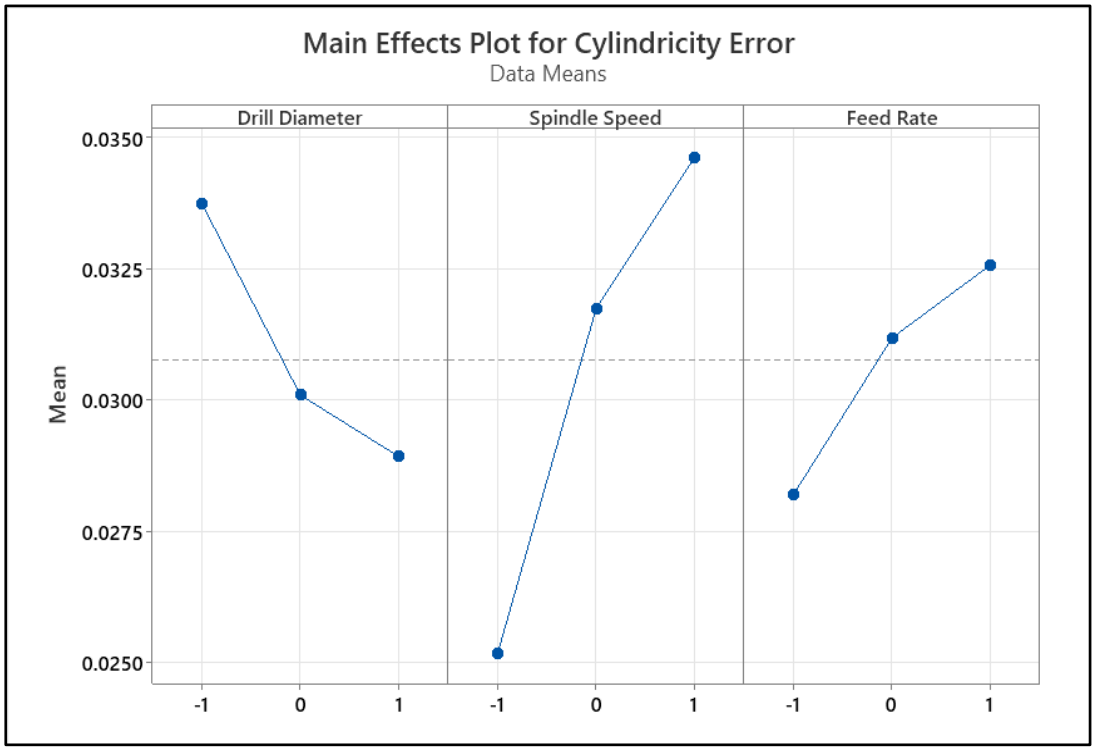

Fig. 5.28: Mean effect plot for cylindricity error

5.3.2.3 Variation of circularity error

Figure 5.29 shows the influence of various input parameters on circularity error. In terms of drill diameter, the minimum value of circularity error was found at a 6 mm drill diameter. The circularity error was found, when the spindle speed increases, the circularity error slightly decreases at 1300 RPM but after the point circularity error slightly increased. In terms of feed rate, it was observed that when the feed rate increased, circularity error continuously increases. According to the graph, it can be said that minimum circularity error was found at a 6 mm drill diameter, high spindle speed, and low feed rate.

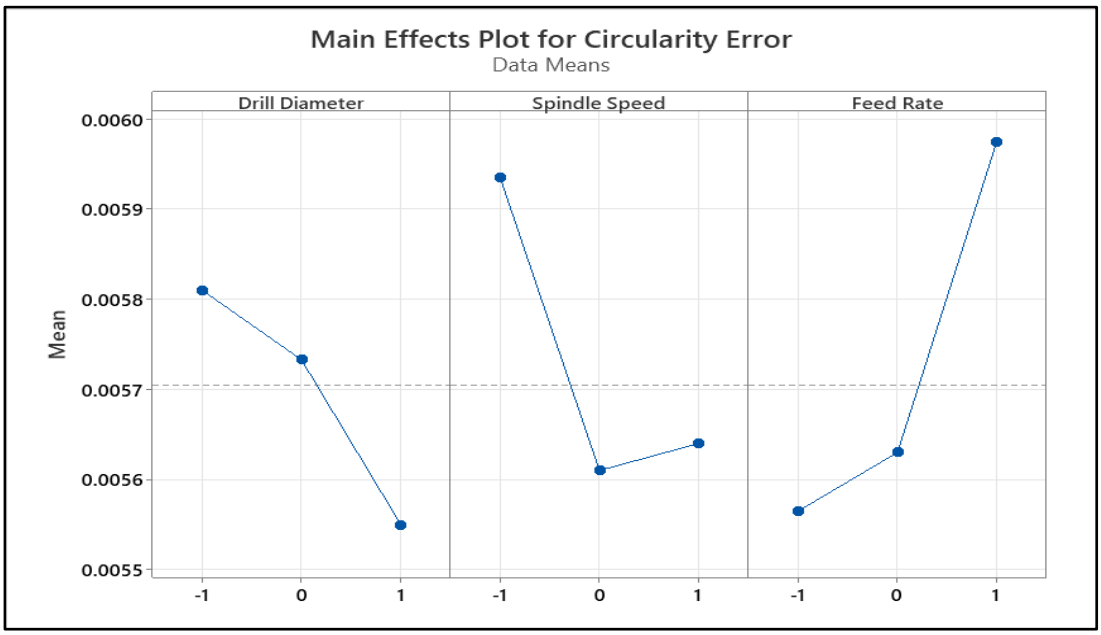

Fig. 5.29: Mean effect plot for circularity error

5.3.3 Interaction Plot

5.3.3.1 Interaction plot for hole deviation

Figure 5.30 shows the interaction effect plots of cutting parameters e.g. drill diameter, spindle speed, and feed rate, and their effect on hole deviation as a response variable.

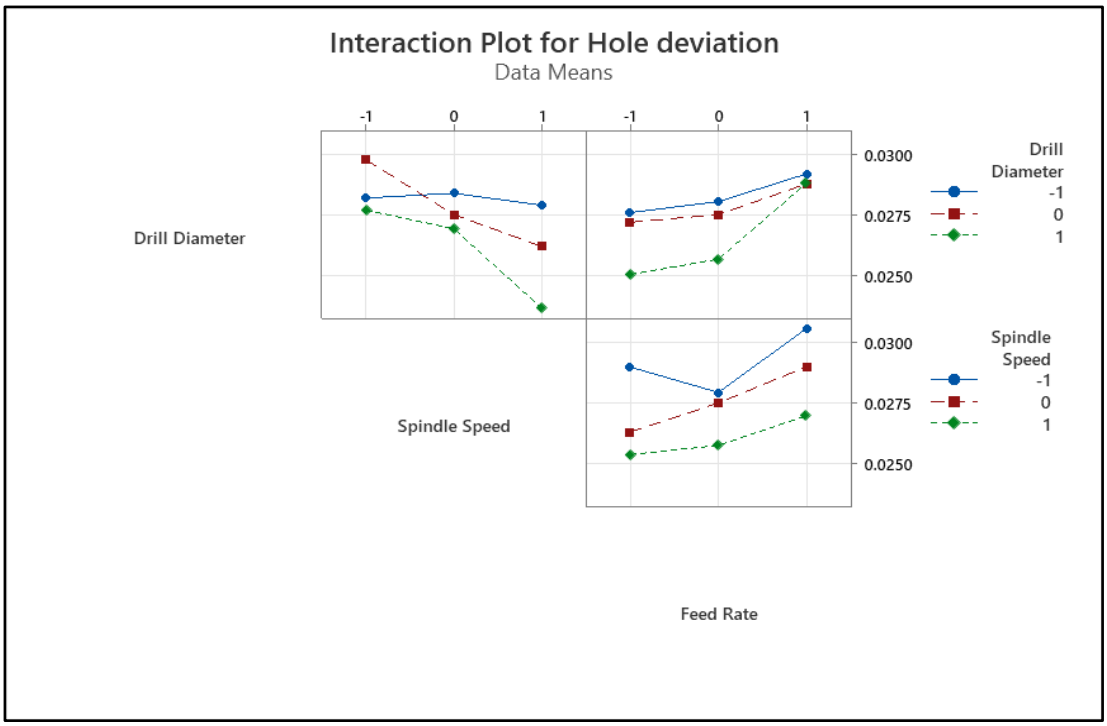

Fig. 5.30: Interaction plot for hole deviation

Figure 5.30 gives the interaction effect of two factors on the hole deviation of duplex stainless steel 2205 with TiAlN-coated solid carbide drill variation under hybrid MQL-LCO_2. According to the interaction plot, it can be said that the interaction between the drill diameter, spindle speed, and feed rate gives the minimum hole deviation values.

Figure 5.31 presented the lowest value of hole deviation and the best value of hole deviation. As per the figure, it was observed that the lowest value of hole deviation was 0.023 in a 6 mm drill diameter, high spindle speed of 1500 RPM, and a minimum feed rate of 0.01750 mm /rev.

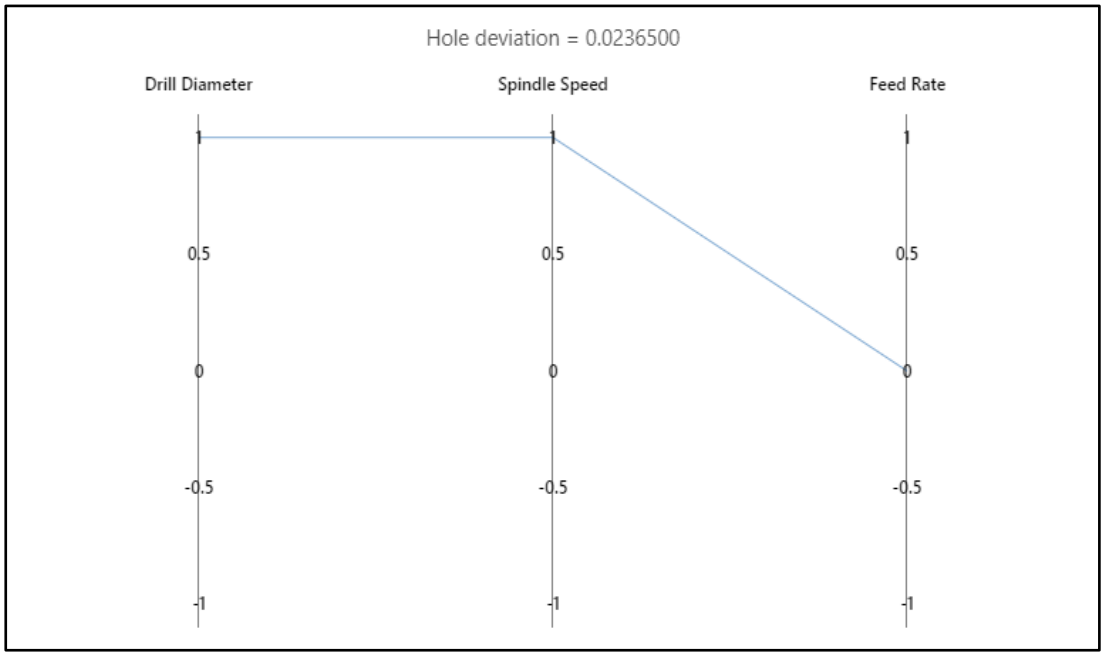

Fig. 5.31: The best value of hole deviation

5.3.3.2 Interaction plot for cylindricity error

Figure 5.32 shows the interaction effect plots of cutting parameters e.g. drill diameter, spindle speed, and feed rate, and their effect on cylindricity error as a response variable.

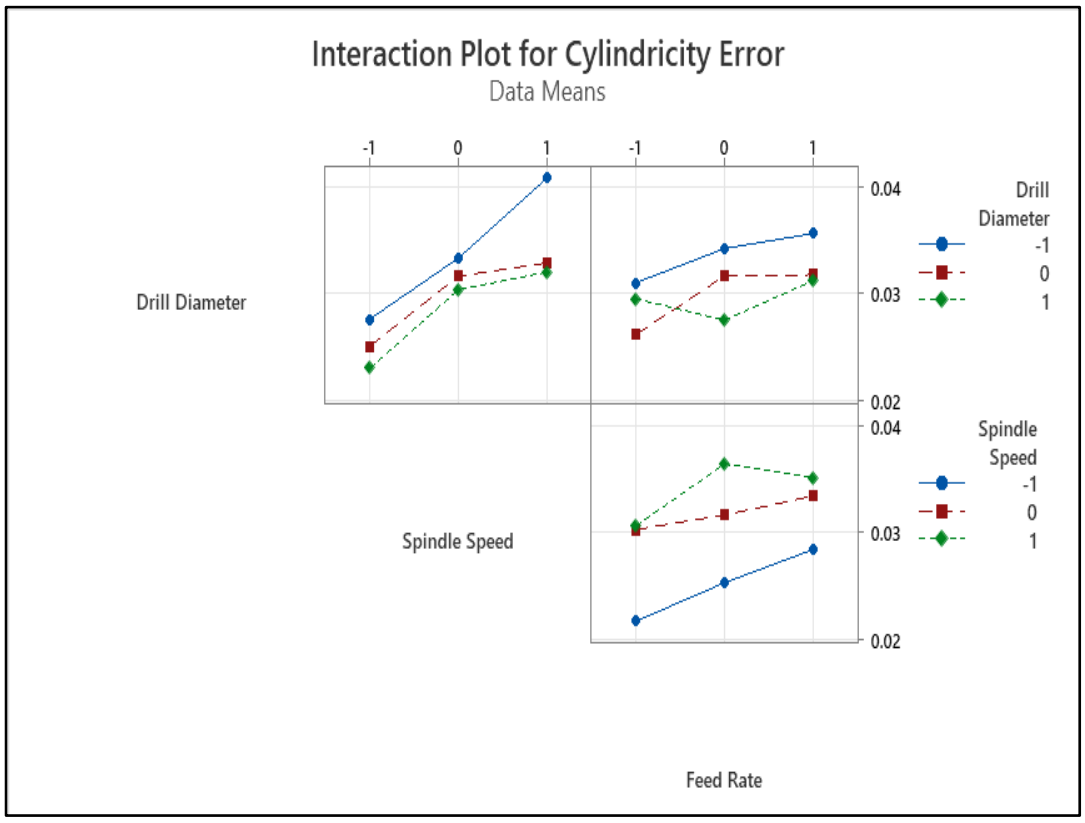

Fig. 5.32: Interaction plot for cylindricity error

Figure 5.32 gives the interaction effect of two factors on the cylindricity error of duplex stainless steel 2205 with TiAlN-coated solid carbide drill variation under hybrid MQL-LCO_2. According to the interaction plot, it can be said that the interaction between the drill diameter, spindle speed, and feed rate gives the minimum cylindricity error values.

The figure 5.33 presented the lowest value of cylindricity error and the best value of hole deviation. As per the figure, it was observed that the lowest value of cylindricity error was 0.02170 in a 4 mm drill diameter, high spindle speed of 1100 RPM, and a minimum feed rate of 0.01750 mm /rev.

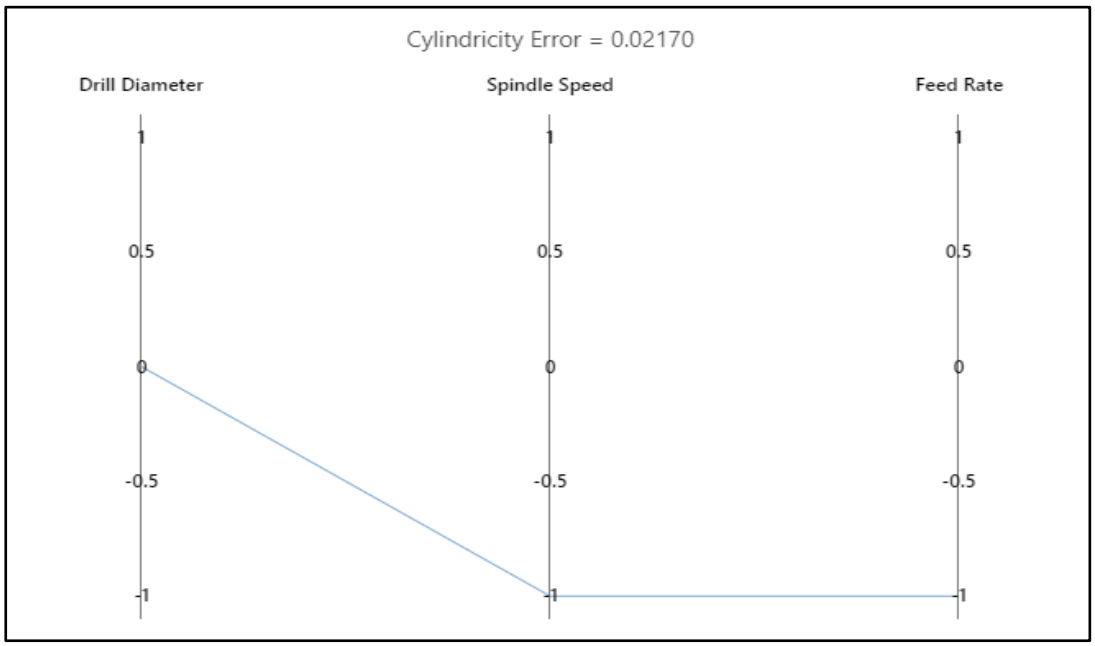

Fig. 5.33: The best value of cylindricity error

5.3.3.3 Interaction plot for circularity error

Figure 5.34 shows the interaction effect plots of cutting parameters e.g. machining environment, spindle speed, and feed rate, and their effect on circularity error as a response variable.

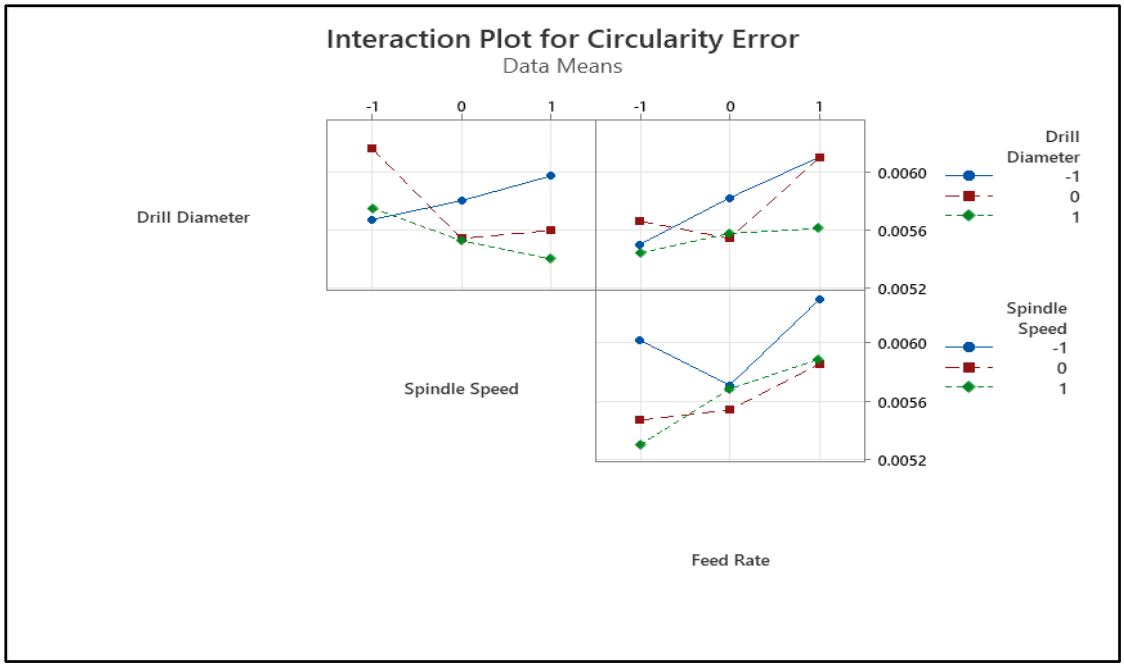

Fig. 5.34: Interaction plot for circularity error

Figure 5.34 gives the interaction effect of two factors on the circularity error of duplex stainless steel 2205 with TiAlN-coated solid carbide drill variation under hybrid MQL-LCO_2. According to the interaction plot, it can be said that the interaction between the drill diameter, spindle speed, and feed rate gives the minimum circularity error. The figure 5.35 presented the lowest value of circularity error and the best value of hole deviation. As per the figure, it was observed that the lowest value of cylindricity error was 0.00530.

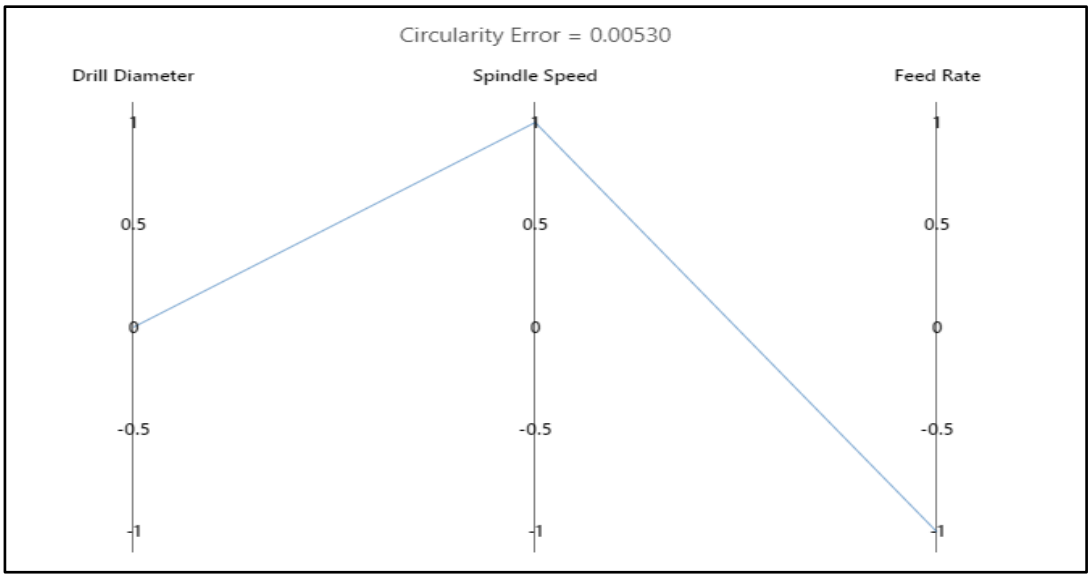

Fig. 5.35: The best value of circularity error

5.3.4 ANOVA (Analysis of Variance)

The effectiveness of the current model was tested using the ANOVA method, and the results are shown in Tables 5.14, 5.15, and 5.16 below. Using MINITAB 20 software and the regression model significance test (RMST), the significance test for each regression model coefficient (Sig Coeff), and the lack of fit (LOF) test, the analysis was performed.

5.3.4.1 ANOVA for hole deviation

ANOVA is an analysis of variance, which means mostly affects process parameters on response and their contribution. Hole deviation is largely affected by the spindle speed, feed rate, and drill diameter, respectively, according to table 5.14. Drill diameter, spindle speed, and feed rate all contribute 19.53 %, 38.90 %, and 27.74 % of the total, respectively for hole deviation. Figure 5.36 shows the graphical

representation of the % of the contribution of cutting parameters on hole deviation. It can be seen that the spindle speed, has the highest contribution on hole deviation in the drilling of DSS 2205 with TiAlN coated solid carbide drill under hybrid MQL-LCO_2 machining conditions.

Table 5.14: ANOVA for hole deviation

Source	DF	Seq of SS	Adj of SS	Adj of MS	F of Value	P of Value	Contribution
Drill Diameter	1	0.000001	0.000008	0.000004	4.56	0.048	19.53%
Spindle Speed	1	0.00000	0.000017	0.000008	9.21	0.008	38.90%
Feed Rate	1	0.00000	0.000011	0.000005	5.88	0.027	24.74%
Error	11	0.00000	0.000007	0.000001			16.83%
Lack-of-fit error	9	0.00000	0.000007	0.000001			15.57%
Pure error	2	0.00000	0.000001	0.000000			1.26%
Total	14	0.000043					100%

Model Summary- S= 0.0007152, R-Seq= 94.07%

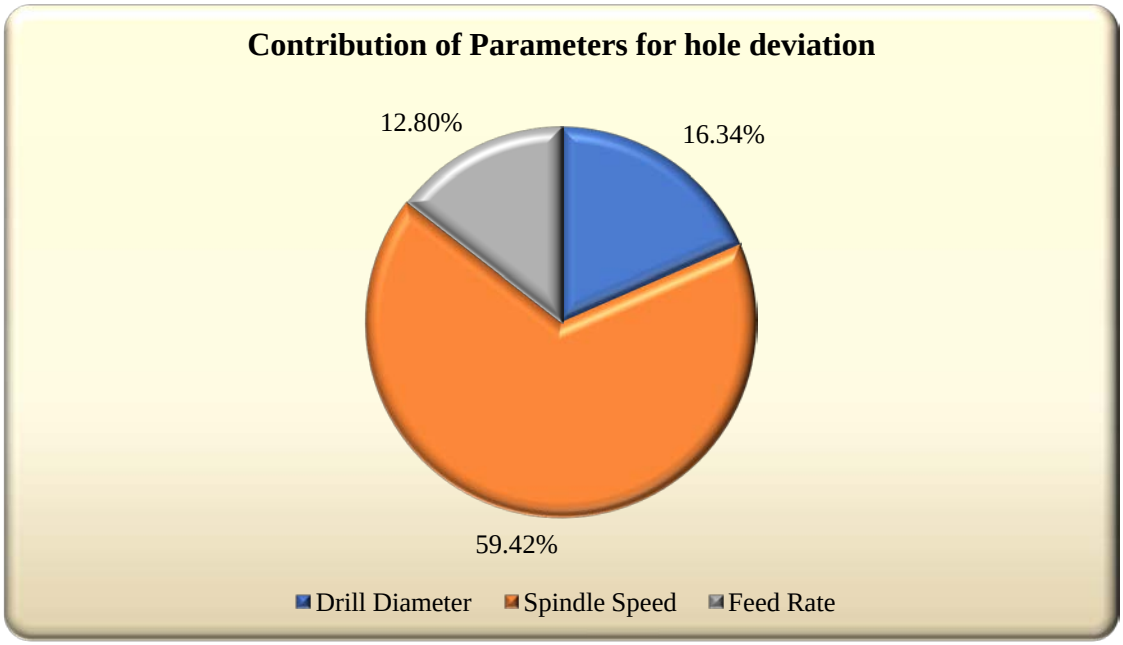

Fig. 5.36: Graphical representation of contribution of process parameter for hole deviation

5.3.4.2 ANOVA for Cylindricity Error

ANOVA is an analysis of variance, which means mostly affects process parameters on response and their contribution. Cylindricity error is largely affected by the spindle speed, drill diameter, and feed rate, respectively, according to table 5.15. Drill diameter, spindle speed, and feed rate all contribute 16.34 %, 59.42 %, and 12.80 % of the total, respectively for cylindricity error. Figure 5.37 shows the graphical representation of the % of the contribution of cutting parameters on cylindricity error. It can be seen that the spindle speed, has the highest contribution on circularity error in the drilling of DSS 2205 with TiAlN coated solid carbide drill under hybrid MQL-LCO_2 machining condition.

Table 5.15:ANOVA for cylindricity error

Source	DF	Seqof SS	Adjof SS	Adjof MS	F of Value	P of Value	Contribution
Drill Diameter	2	0.000052	0.000051	0.000025	5.53	0.031	16.34%
Spindle Speed	2	0.000190	0.000191	0.000095	20.87	0.001	59.42%
Feed Rate	2	0.000041	0.000041	0.000020	4.48	0.050	12.80%
Error	8	0.000037	0.000037	0.000005			11.43%
Lack-of-fit error	6	0.000023	0.000023	0.000004			7.25%
Pure error	2	0.000013	0.000013	0.000007			4.18%
Total	14	0.000320					100%

Model Summary- S= 0.0024027, R-Seq= 90.98%

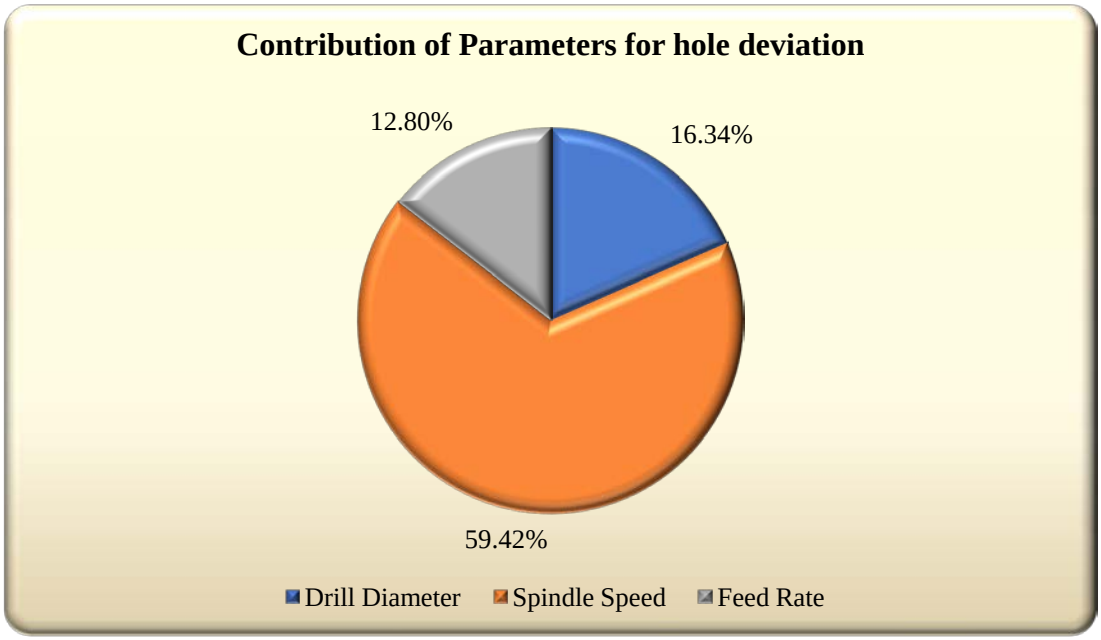

Fig. 5.37: Graphical representation of contribution of process parameter for cylindricity error

5.3.4.3 ANOVA for Circularity Error

ANOVA is an analysis of variance, which means mostly affects process parameters on response and their contribution. Circularity error is largely affected by the feed rate, spindle speed, and drill diameter, respectively, according to table 5.16. Drill diameter, spindle speed, and feed rate all contribute 10.86 %, 28.70 %, and 34.73 % of the total, respectively for circularity error. Figure 5.38 shows the graphical representation of the % of the contribution of cutting parameters on circularity error. It can be seen that the feed rate, has the highest contribution on circularity error in the drilling of DSS 2205 with TiAlN coated solid carbide drill under hybrid MQL-LCO_2 machining condition.

Table 5.16:ANOVA for Circularity Error

Source	DF	Seq SS	AdjSS	Adj MS	FValue	PValue	Contribution
Drill Diameter	2	0.00001	0.00001	0.00000	1.59	0.262	10.86%
Spindle Speed	2	0.00000	0.00000	0.00000	4.65	0.046	28.70%
Feed Rate	2	0.00000	0.00000	0.00000	5.40	0.033	34.73%
Error	8	0.00000	0.00000	0.00000			25.71%
Lack-of-fit error	6	0.00000	0.00000	0.00000	16.68	0.058	25.21%
Pure error	2	0.00000	0.000000	0.00000			0.50%
Total	14	0.00001					100%

Model Summary- S= 0.0001743, R-Seq= 86.34%

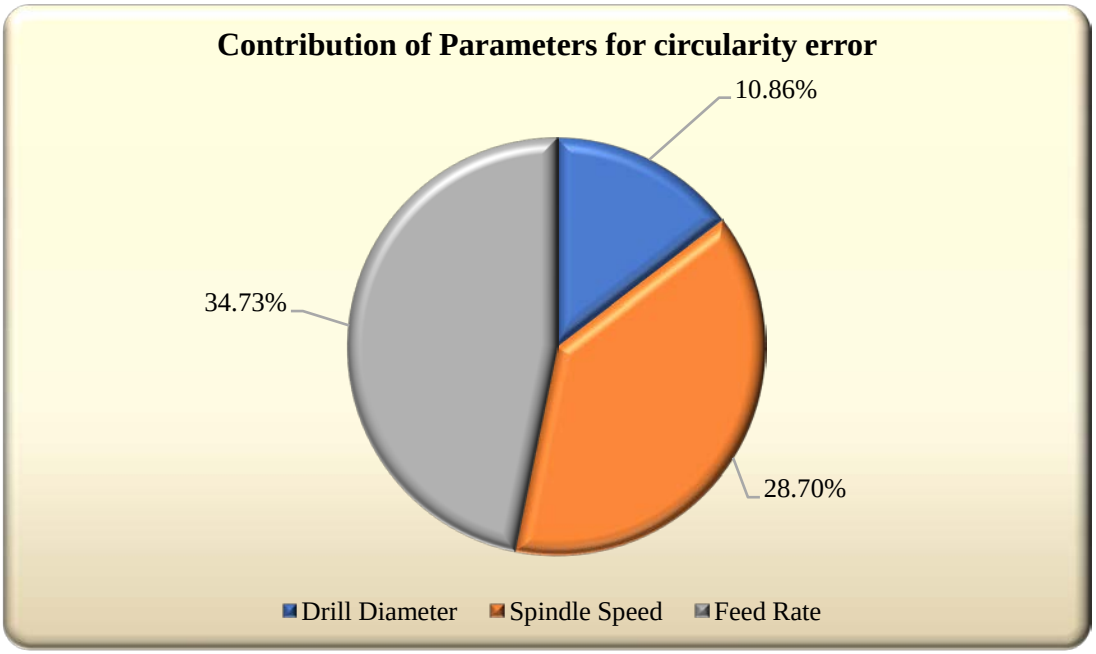

Fig. 5.38: Graphical representation of contribution of process parameter for circularity error

From Tables5.14, 5.15, and 5.16, it was observed that the 5.93 percent,9.02, 1and 3.64% percent of the total changes in hole deviation, cylindricity error, and

circularity error were indicated by the values of the determination coefficients (R^2 = 94.07 percent) for hole deviation, (R^2= 90.98 percent) for cylindricity error, and (R^2 = 86.34%) for circularity error, respectively. Since the residuals' normal distribution is a straight line, the model is significant. At a 95% confidence level, the ANOVA test identifies the significant input elements that influence the hole deviation, cylindricity error, and circularity error in CNC milling. Figures 5.39 the residual plot's normal distribution for hole deviation, cylindricity error, and circularity error respectively. The ANOVA results are shown in Tables 5.14, 5.15, and 5.16. According to the ANOVA results, spindle speed is a significant influencing factor in determining the hole deviation and cylindricity error, contributing 38.90% and 89.42%, respectively. Also, for circularity error, the most influencing factor is feed rate with 34.73% contributing.

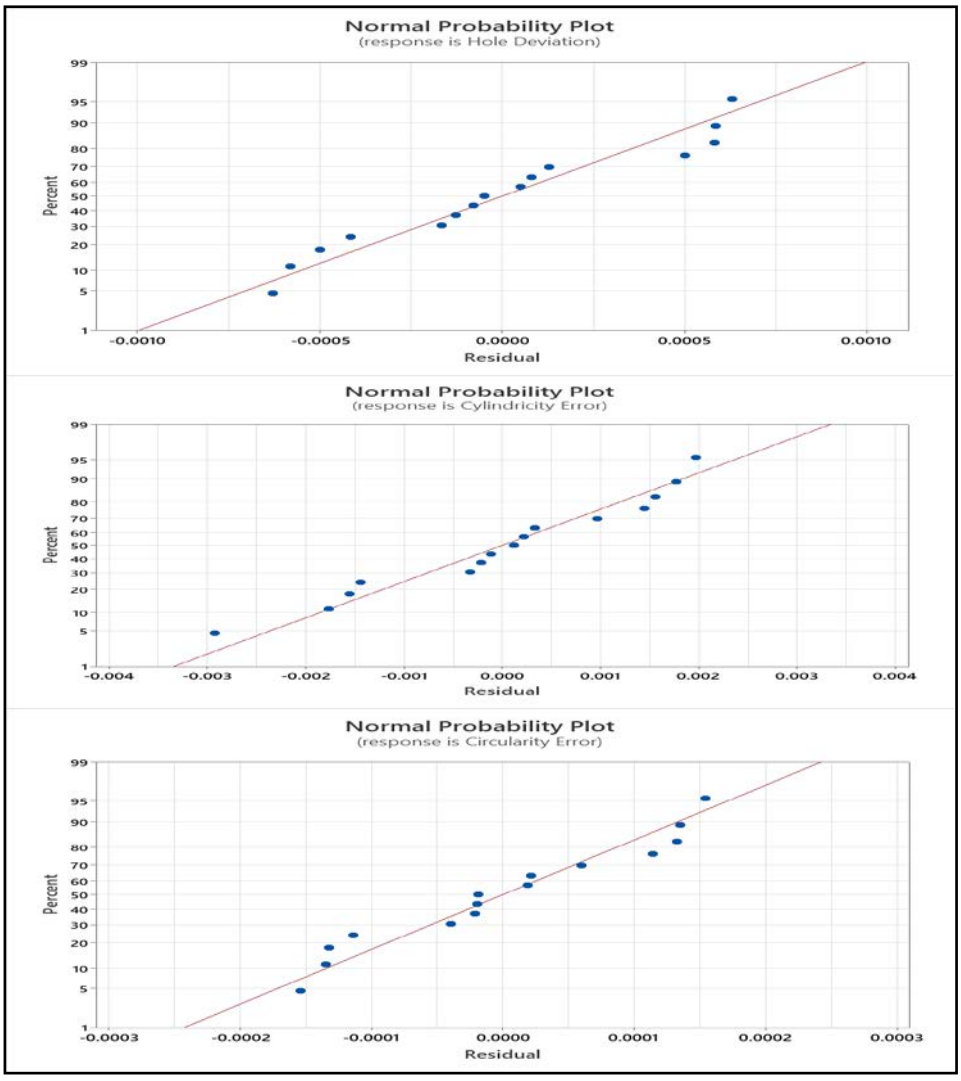

Fig. 5.39: Normal residual plot for responses

5.3.5 Contour Plot

The relationship between the response variable and two input variables is depicted in the contour plot graph. Figure 5.40 depicts the relationship between the input variable and the response variables of hole diameter error/hole deviation, cylindricity error, and circularity error. Figure 5.40 (a) shows the drill diameter and spindle speed to the hole deviation as the response variable. As per the contour plot, it can be said that the minimum hole deviation value was found at high spindle speed and 6 mm drill diameter. Similarly, Figure 5.40 (b) illustrates how a 6 mm drill and a low feed rate improve hole deviation. High spindle speed and low feed rate also result in minimal hole deviation, as seen in Figure 5.40 (c).

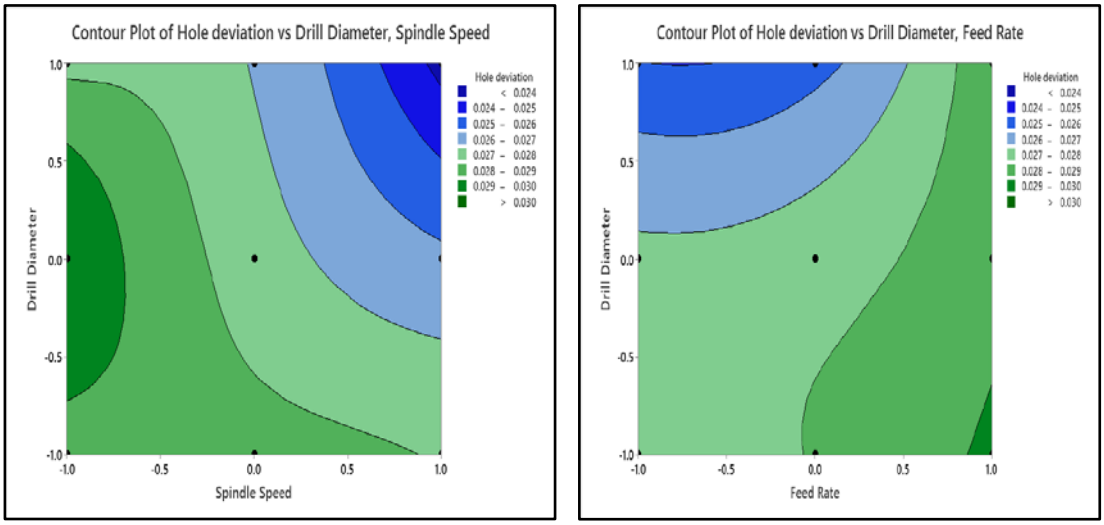

(a) (b)

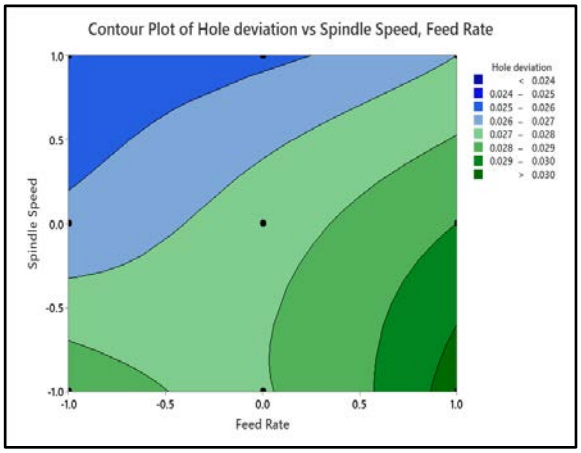

(c)

Figure 5.40 (d) plot between feed rate and spindle speed while cylindricity error as the response variable. According to plot, it can be observed that optimal cylindricity error was found low feed rate and low spindle speed. Figure 5.40 (e) shows that 6 mm drill and low feed rate improve the cylindricity error. Furthermore, as shown in figure 5.40 (f), low spindle speed and high drill diameter resulted in low cylindricity error.

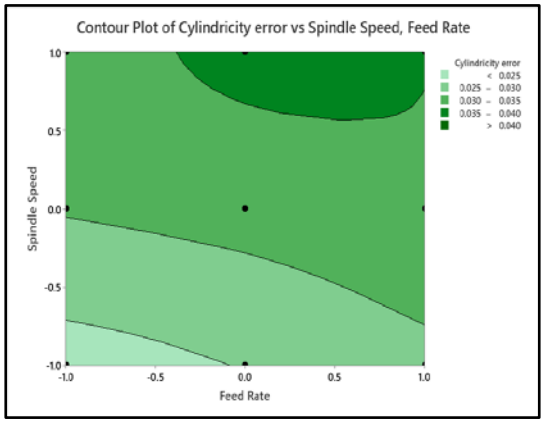

(d)

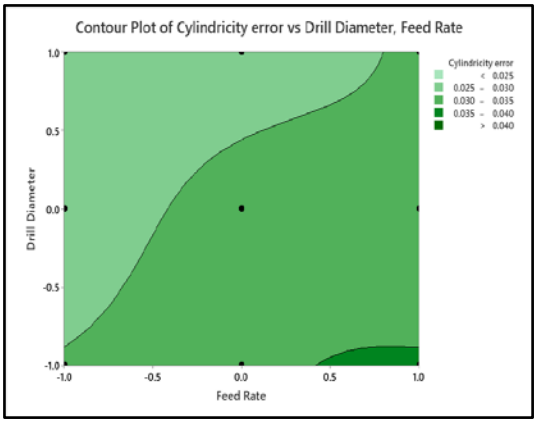

(e)

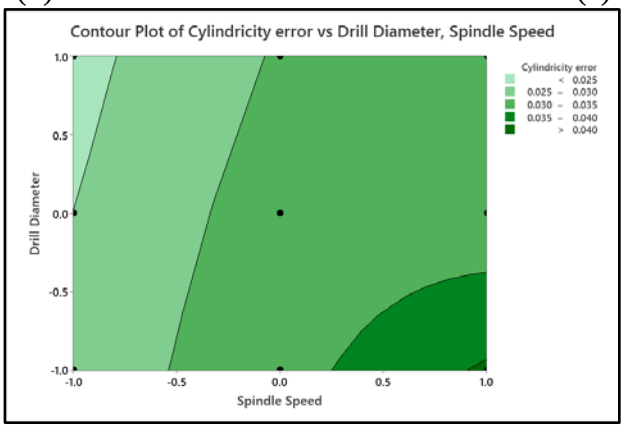

(f)

Figure 5.40 (g) plot between drill diameter and spindle speed while circularity error response variable. According to the plot, it can be observed that optimal circularity error und high drill diameter and high spindle speed. Figure 5.40 (h) shows that 6 mm drill and low feed rate improve the circularity error. Furthermore, as shown in figure 5.40 (i), high spindle speed and low feed rate resulted in low circularity error.

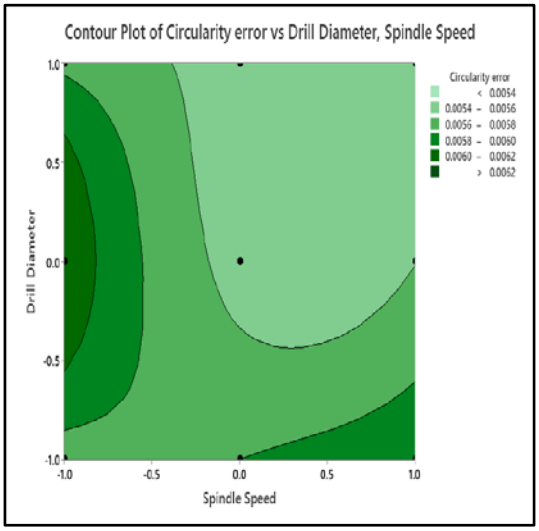

(g)

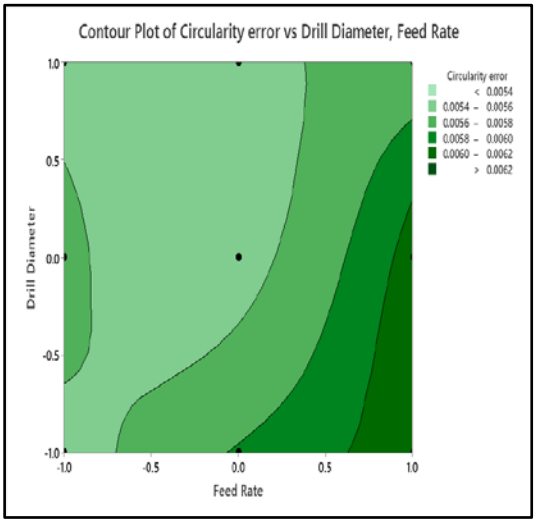

(h)

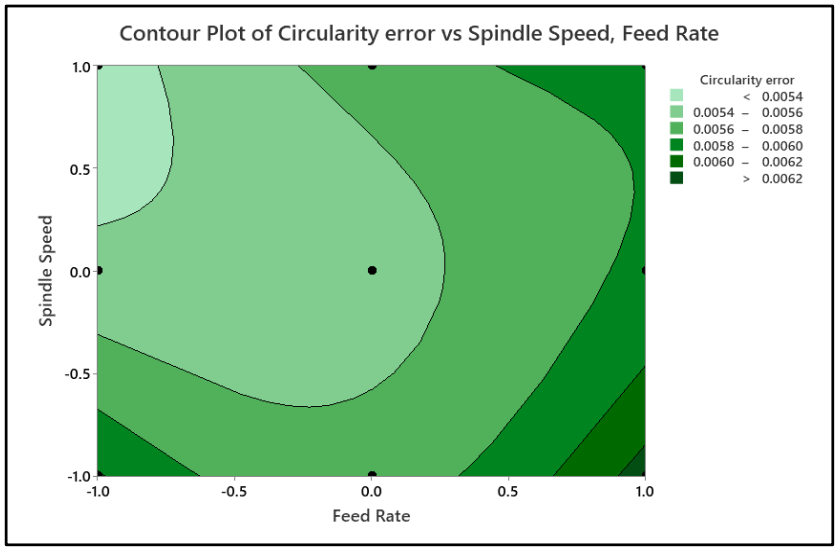

(i)

Fig. 5.40: Contour Plot for responses

5.3.6 Modeling of Process Parameters

5.3.6.1 Artificial Neural Network (ANN)

The artificial neural network is one of the most widely used computational methods for elucidating complex functions in a wide range of applications (ANN). Many different sorts of problems, including fault detection, process identification, property estimate, data smoothing, and error filtering, have been successfully addressed by ANNs. An artificial intelligence system known as a neural network uses interconnected neurons to carry out tasks. By taking advantage of the processing power of a multi-layered neural network, it has been used to model the

drilling process in order to predict the hole deviation and cylindricity error in the machining of Inconel duplex stainless steel 2205.In this investigation, the statistical impacts of drill diameter, spindle speed, and feed rate on hole deviation, cylindricity error, and circularity error in the drilling of duplex stainless steel were examined. MATLAB program created the greatest ANN architecture. Drill diameter, spindle speed, and feed rate are all represented by a corresponding neuron in the input layer. With regard to hole deviation, cylindricity error, and circularity error the output layer is appropriate. The ANN model structure may be shown in Figure 5.41. Each input neuron is fully connected to each output neuron in the hidden layer, but the reverse is true for the hidden neurons. An artificial neural network (ANN) model with 10 hidden layers, 3 inputs, and 3 outputs was developed after performing a number of tests. Levenberg-Marquardt' (LM) back propagation neural network was used to train the network. We split the data into 70% for training, 15% for testing, and 15% for each testing and validation set. Table 5.17 displays the specifics of the ANN model that was created. Figure 5.42 shows the import window for the ANN model.

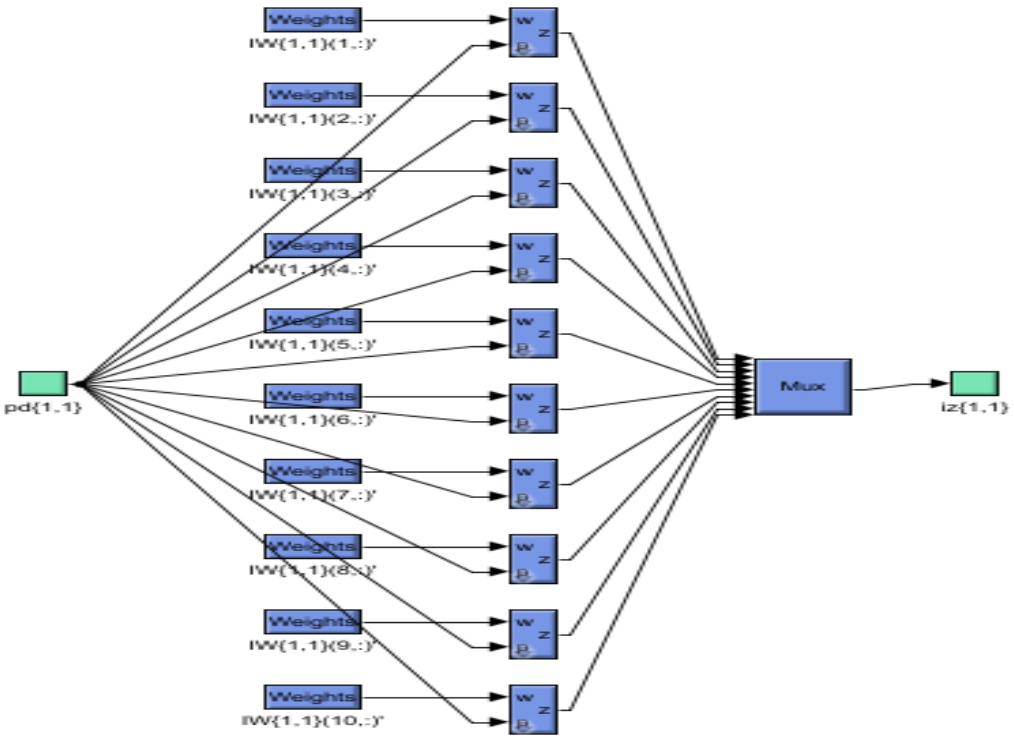

Fig. 5.41: The ANN model structure

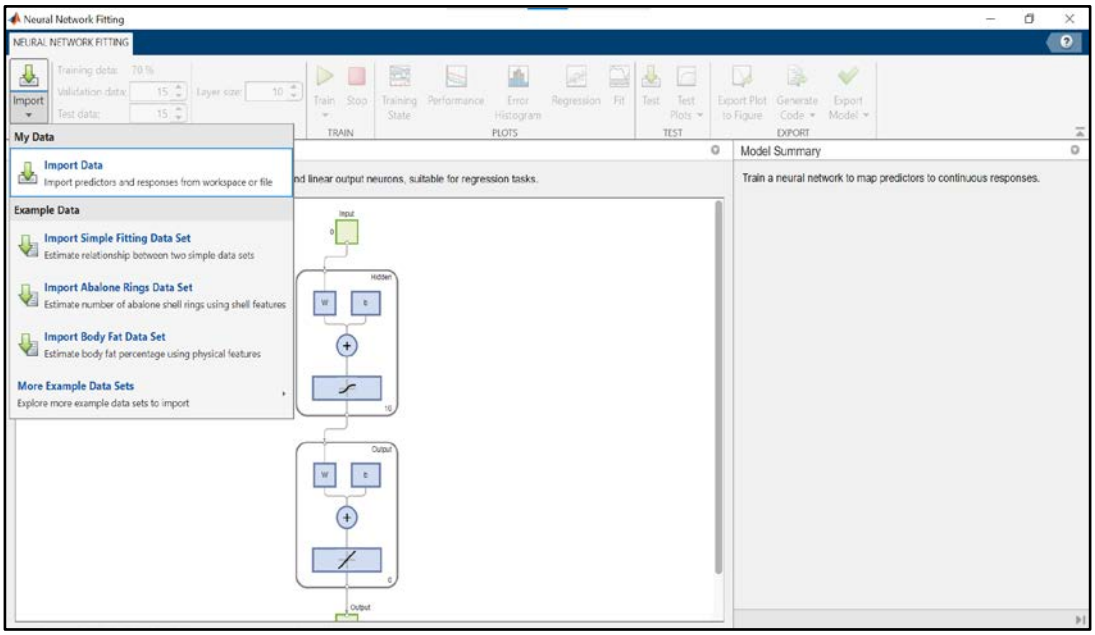

Fig. 5.42: Import window

Table 5.17: ANN Model Parameter

Learning Conditions	
Object Model	Hole Deviation, Cylindricity error, and circularity error
Input Neurons	Drill diameter, spindle speed & feed rate
Response Neurons	Hole deviation, Cylindricity error, and circularity error
Network Type	Feed-forward-back propagation
Network Technique	Levenberg–Marquardt (LM)
Pattern Vector	70 % (train), 15% (validation), and 15 % (testing)

After ANN implemented, the regression plot for the value of R-square and the value of response in each point shows in figure 5.43 (a). Figure 5.43 (b) shows the mean square error and the point of the best validation performance. It was observed that almost the value is near a straight line, so it means implemented of ANN is successful each value is close in agreement with the experimental value.

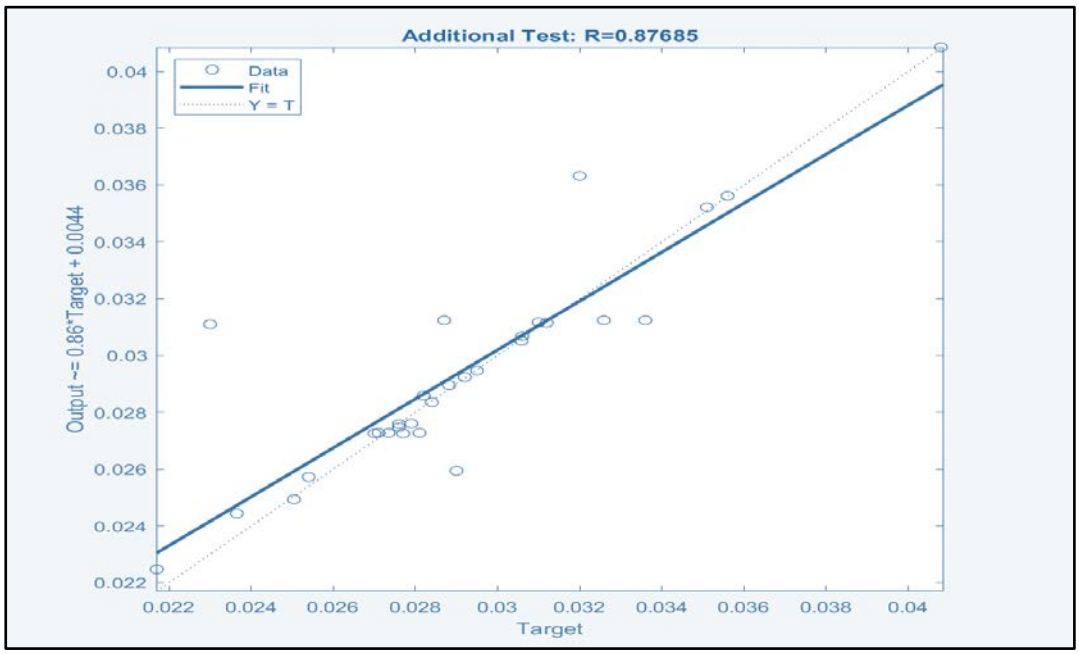

(a)

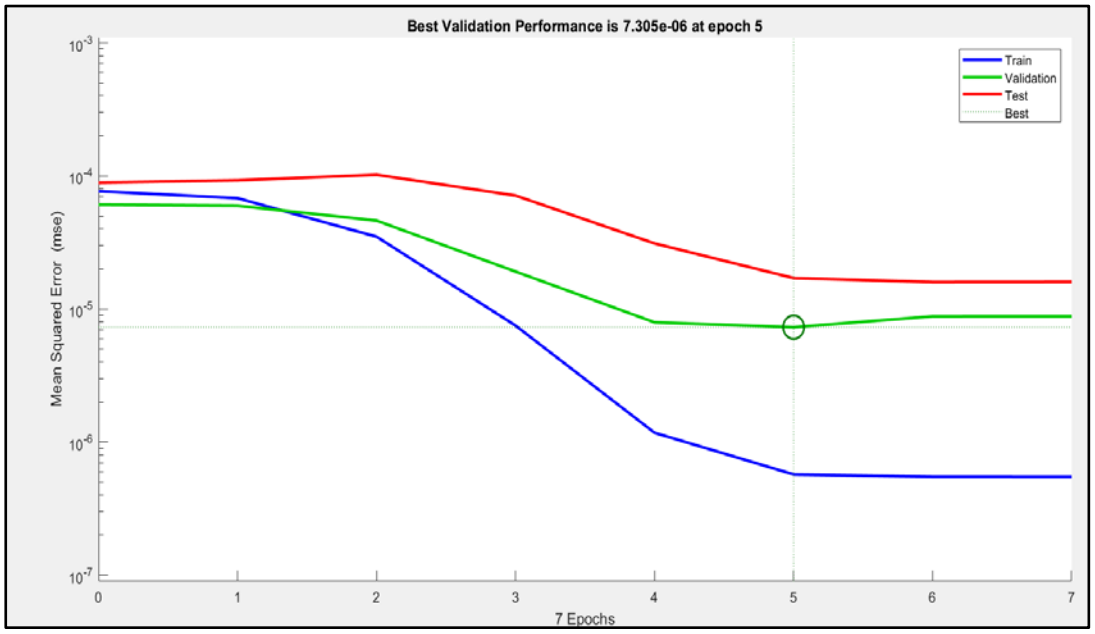

Fig. 5.43: (a) Regression Plot for responses and (b) Mean Square error for response

5.3.6.2 Response Surface Method (RSM)

RSM is primarily utilized in MINITAB 20 software to identify the relevant model terms of hole deviation, cylindricity error, and circularity error and to establish the relationship between input parameters and output parameters for fitting the full-quadratic equation to the experimental data. After 15 data measurements

from the machining circumstances, the hole deviation, cylindricity error, and circularity error in the drilling of DSS 2205 are obtained using the box-Behnken design of the matrix. The top limit and lower limit of the input parameters, respectively, were coded as +1 and -1. RSM fit full-quadratic models from the existing data in equation 5.5, equation 5.6, and equation 5.7 for hole deviation, cylindricity error, and circularity error, respectively.

Hole deviation = $0.1627-0.00054*A+ 0.000012*B – 15.41*C-0.000123A^2-0.00000B^2+410C^2-0.000002A*B+0.218A*C+0.00002B*C$ +/-€……. (5.5)

Cylindricity Error = $-0.381+0.0055*A+0.0001947*B+26.2*C+0.000262A^2-0.00000B^2-546C^2-0.000003A*B-0.290A*C-0.00220B*C$ +/-€…….. (5.6)

Circularity Error = $0.0454+ 0.001254*A-0.000014*B-3.62*C-.000007A*A+ 0.00000 B*B+97.6C*C-0.00000A*B-0.0430A*C+0.000220B*C$+/-€……...(5.7)

The experimental results were compared with the predictive model. It was observed that the predictive results and experimental are close to each other shown in Figure 5.38.

5.3.6.2.1 Surface Plot for hole deviation

Figure 5.444 is the surface plot between cutting parameters e.g. drill diameter, spindle speed, and feed rate while hole deviation is the response variable. The surface plot for hole deviation in 3-D (dimensional) by varying factor sectors at one factor is constant. As per the surface plot, it can be said, spindle speed is the most effective process parameter which affects hole deviation followed by drill diameter, and feed rate respectively.

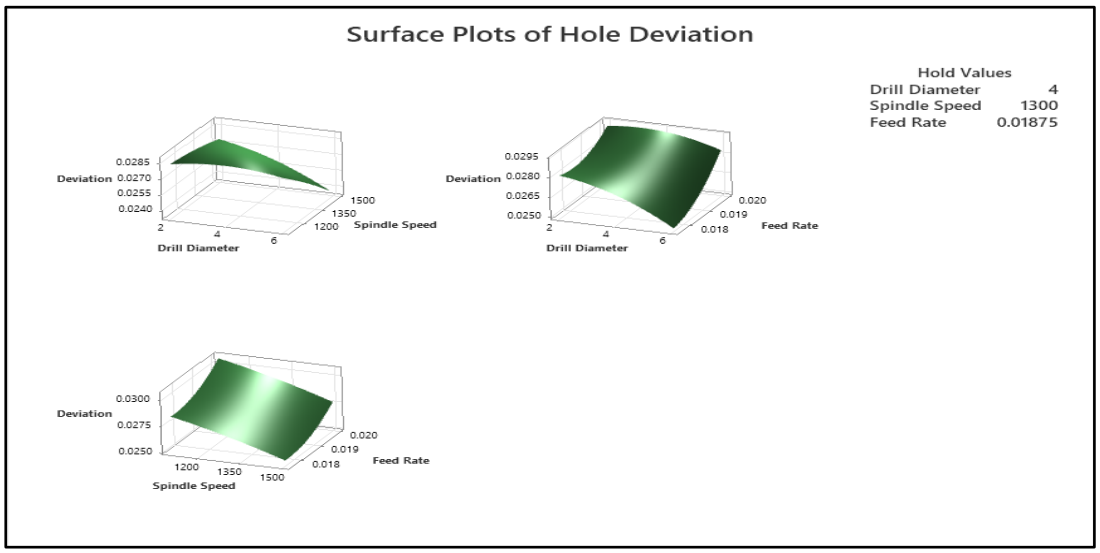

Fig. 5.44: The surface plot of the hole deviation

5.3.6.2.2 Surface Plot for Cylindricity Error

Figure 5.45 is the surface plot between cutting parameters e.g. drill diameter, spindle speed, and feed rate while cylindricity error is the response variable. The surface plot for hole deviation in 3-D (dimensional) by varying factor sectors at one factor is constant. As per the surface plot, it can be said, spindle speed is the most effective process parameter which affects cylindricity error followed by drill diameter, and feed rate respectively.

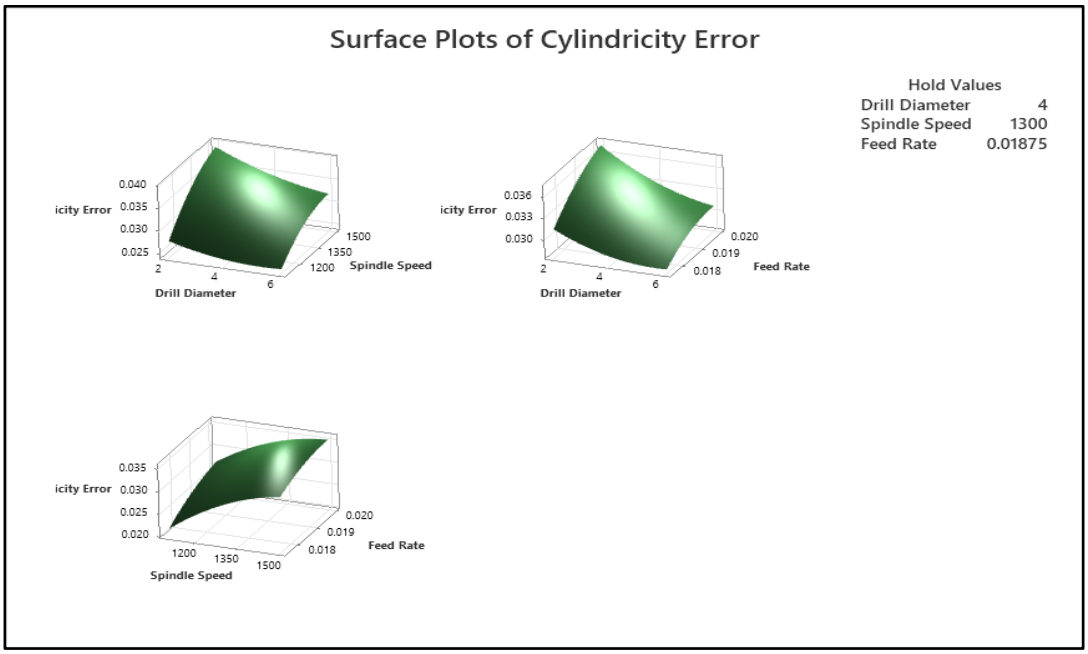

Fig. 5.45: The surface plot of the cylindricity error

5.3.6.3 .3 Surface Plot for Circularity Error

Figure 5.46 is the surface plot between cutting parameters e.g. drill diameter, spindle speed, and feed rate while circularity error is the response variable. The surface plot for hole deviation in 3-D (dimensional) by varying factor sectors at one factor is constant. As per the surface plot, it can be said, the feed rate is the most effective process parameter which affects circularity error followed by drill diameter, and feed rate respectively.

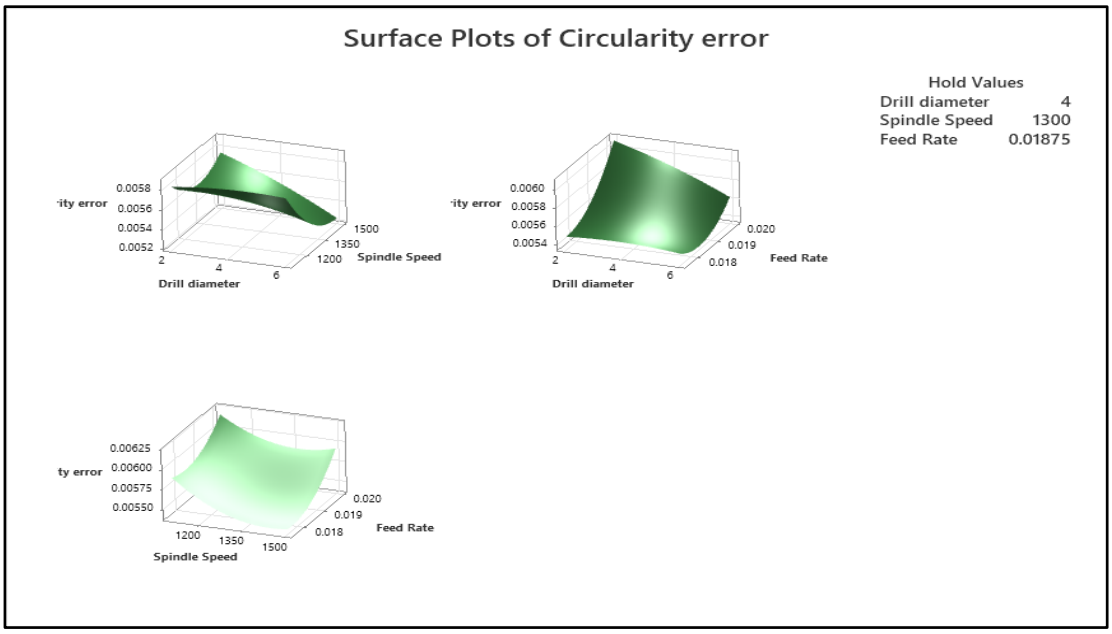

Fig. 5.46: the surface plot of the circularity Error

5.3.6.4 Fuzzy Logic System (FLS)

For the most accurate prediction of hole deviation, cylindricity error, and circularity error the fuzzy logic principle is applied. The triangle membership function is used to categorize the range of input parameters and output parameters into three groups based on experimental data shown figure. To the defuzzification model, 15 distinct rules are applied. Explaining variables and words, designing membership functions for variables, creating knowledge base rules, and obtaining fuzzy values are the basic steps in its development. The FIS editor's input and output parameters are chosen at this step. Figure 5.47 shows the FIS file. The experiment was carried out using a 5mm thick DSS 2205 sheet.

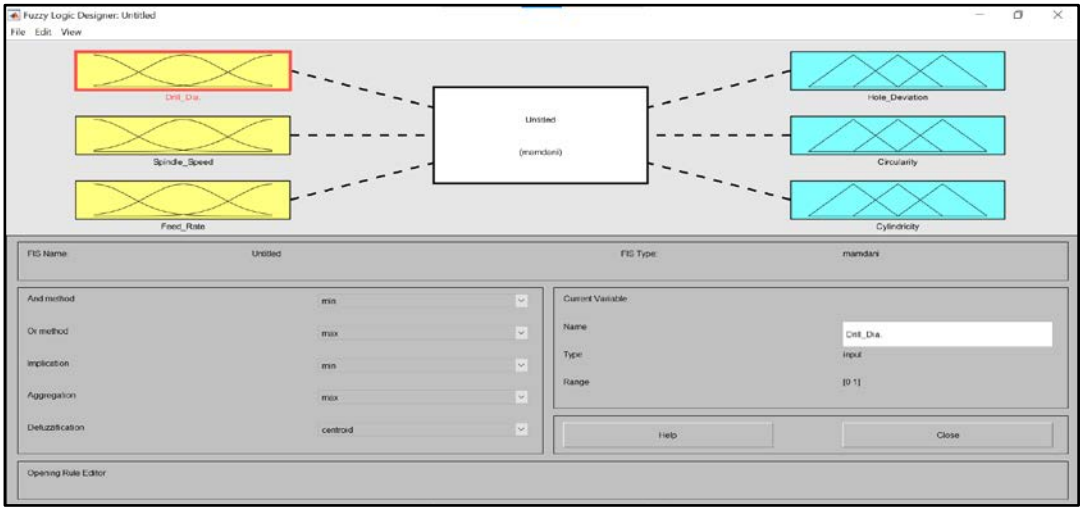

Fig. 5.47: FIS file

5.3.6.3.1 Membership Functions

Figure 5.48 shows the membership function of the drill diameter. The value of the process parameter is divided into three categories e.g. low of 2mm, medium of 4mm, and high of 6mm, which are taken from table of the level of process parameters.

Fig. 5.48: Membership function for drill diameter

Figure 5.49 shows the membership function of the spindle speed. The value of the process parameter is divided into three categories e.g. low of 1100 RPM, medium of 1300 RPM, and high of 1500 RPM, which are taken from the table of the level of process parameters.

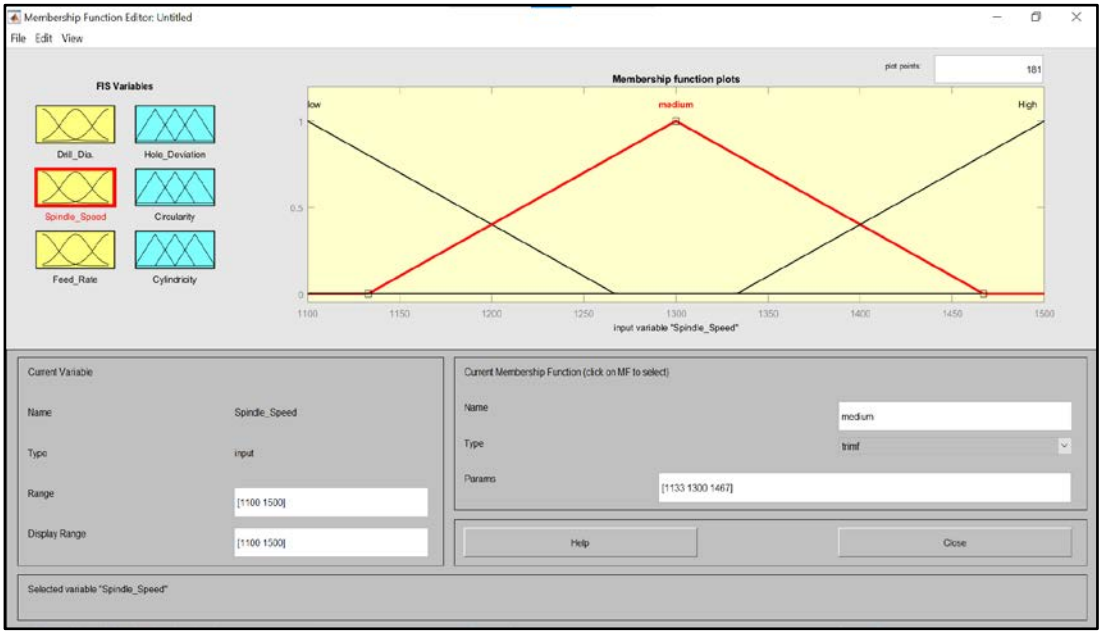

Fig. 5.49: Membership Function for Spindle Speed

Figure 5.50 shows the membership function of the feed rate. The value of the process parameter is divided into three categories e.g. low of 0.0175 mm/rev, medium of 0.01875 mm/rev, and high of 0.020 mm/rev, which are taken from the table of the level of process parameters.

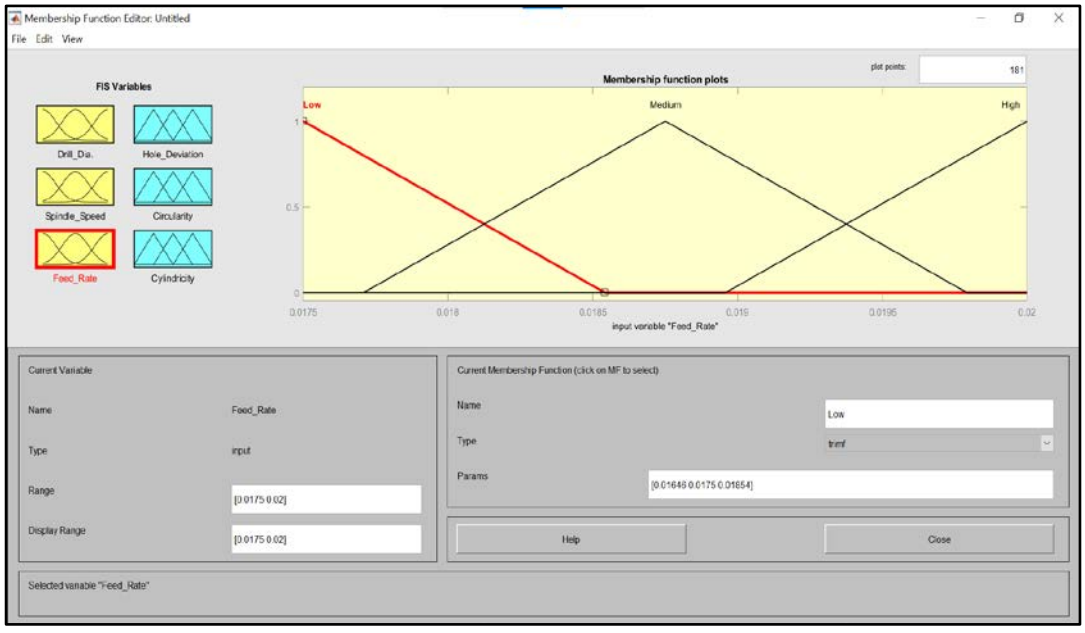

Fig. 5.50: Membership function for feed rate

Figure 5.51 shows the membership function of the hole deviation. The value of the parameter is divided into three categories e.g. low, medium, and high which are taken from the table of the experimental results.

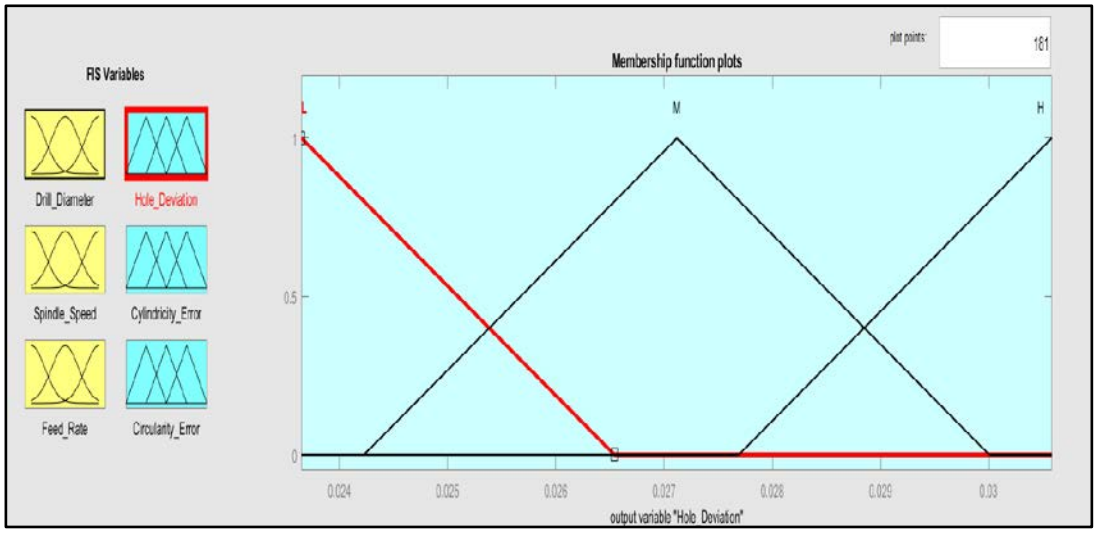

Fig. 5.51: Membership function for hole deviation

Figure 5.52 shows the membership function of the cylindricity error. The value of the parameter is divided into three categories e.g. low, medium, and high which are taken from the table of the experimental results.

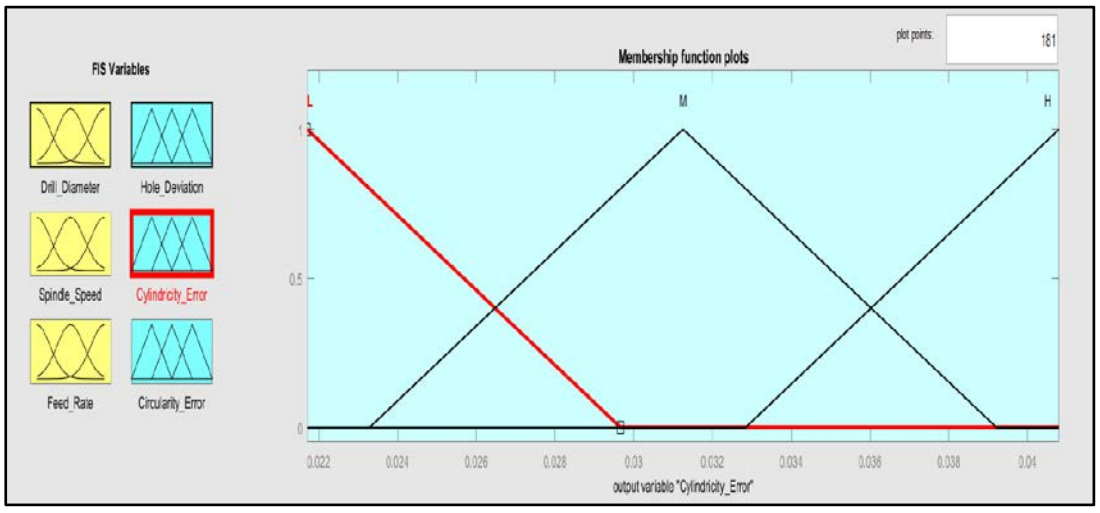

Fig. 5.52: Membership function for cylindricity error

Figure 5.53 shows the membership function of the circularity error. The value of the parameter is divided into three categories e.g. low, medium, and high which are taken from the table of the experimental results.

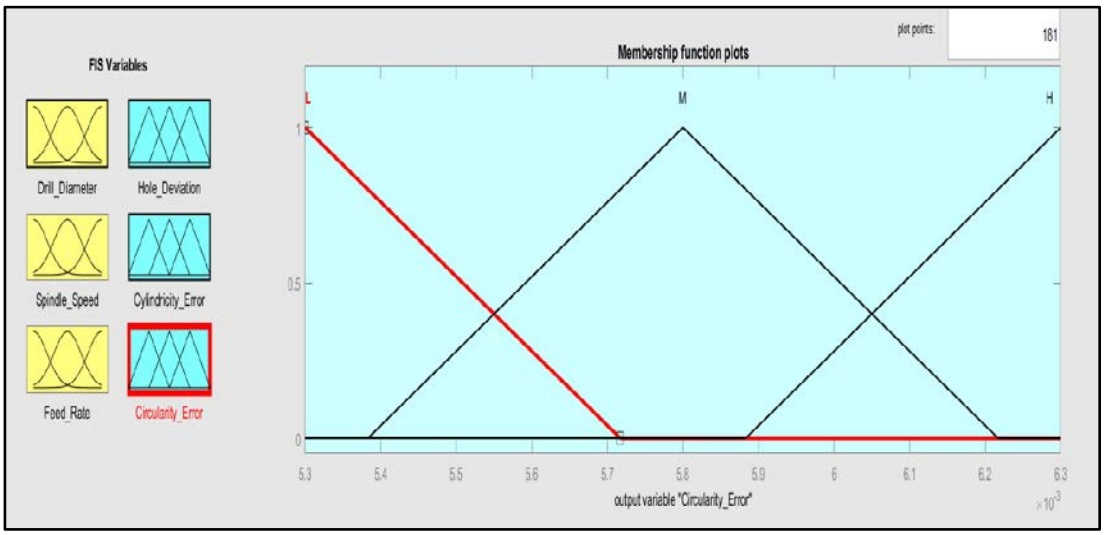

Fig. 5.53: Membership function for circularity error

5.3.6.3.2 Rules

After the membership function, the next step is making rules. Table 5.18 shows the total 15 rules, which are made by using the table of set of experiments. Also, figure 5.54 shows the rules.

Table 5.18: The rules applied for response value prediction

1	**if** (drill diameter is low) and (spindle speed is medium) and (feed rate is high) **then** (hole deviation is high) (cylindricity error is high) circularity error is high)
2	**if** (drill diameter is medium) and (spindle speed is low) and (feed rate is high) **then** (hole deviation is high) (cylindricity error is medium) circularity error is high)
3	**if** (drill diameter is high) and (spindle speed is high) and (feed rate is medium) **then** (hole deviation is low) (cylindricity error is high) circularity error is medium)
4	**if** (drill diameter is medium) and (spindle speed is medium) and (feed rate is medium) **then** (hole deviation is medium) (cylindricity error is high) circularity error is medium)
5	**if** (drill diameter is low) and (spindle speed is medium) and (feed rate is low) **then** (hole deviation is high) (cylindricity error is medium) circularity error is medium)
6	**if** (drill diameter is high) and (spindle speed is medium) and (feed rate is low) **then** (hole deviation is medium) (cylindricity error is medium) circularity error is medium)

7	**if** (drill diameter is low) and (spindle speed is low) and (feed rate is medium) **then** (hole deviation is high) (cylindricity error is medium) circularity error is medium)
8	**if** (drill diameter is medium) and (spindle speed is medium) and (feed rate is medium) **then** (hole deviation is medium) (cylindricity error is medium) (circularity error is medium)
9	**if** (drill diameter is high) and (spindle speed is low) and (feed rate is medium) **then** (hole deviation is high) (cylindricity error is low) circularity error is high)
10	**if** (drill diameter is medium) and (spindle speed is high) and (feed rate is low) **then** (hole deviation is medium) (cylindricity error is medium) circularity error is low)
11	**if** (drill diameter is medium) and (spindle speed is high) and (feed rate is high) **then** (hole deviation is medium) (cylindricity error is high) circularity error is high)
12	**if** (drill diameter is high) and (spindle speed is medium) and (feed rate is high) **then** (hole deviation is high) (cylindricity error is medium) circularity error is medium)
13	**if** (drill diameter is medium) and (spindle speed is low) and (feed rate is low) then (hole deviation is high) (cylindricity error is low) circularity error is high)
14	if (drill diameter is low) and (spindle speed is high) and (feed rate is medium) **then** (hole deviation is high) (cylindricity error is high) circularity error is high)
15	**if** (drill diameter is medium) and (spindle speed is medium) and (feed rate is medium) **then** (hole deviation is high) (cylindricity error is high) circularity error is medium)

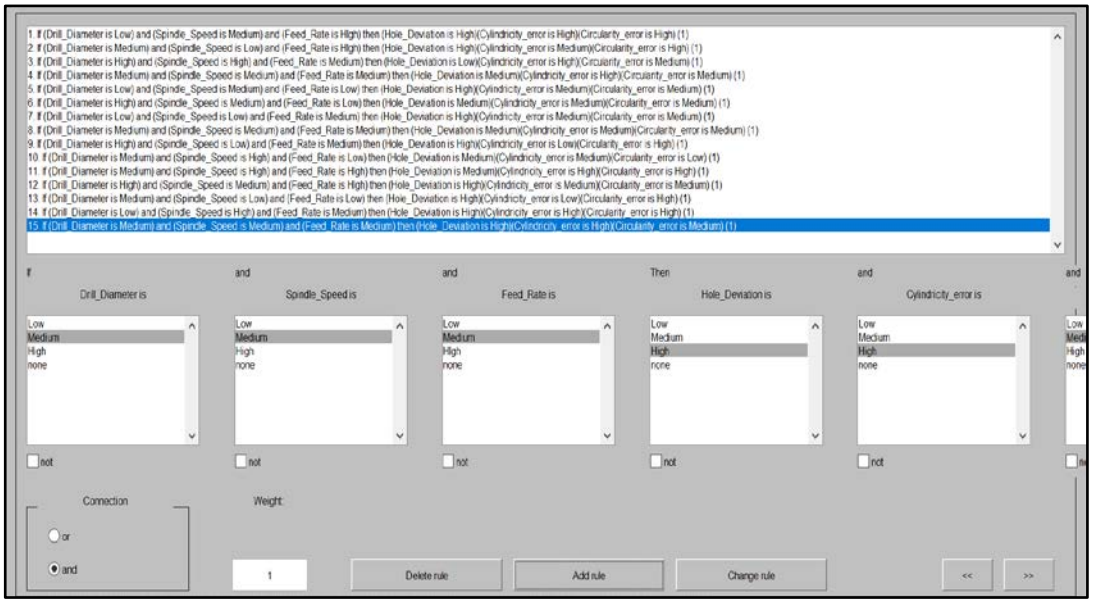

Fig. 5.54: Rules File

Figure 5.55 shows, the predicted value of responses e.g. hole deviation, cylindricity error, and circularity error by fuzzy logic interface system.

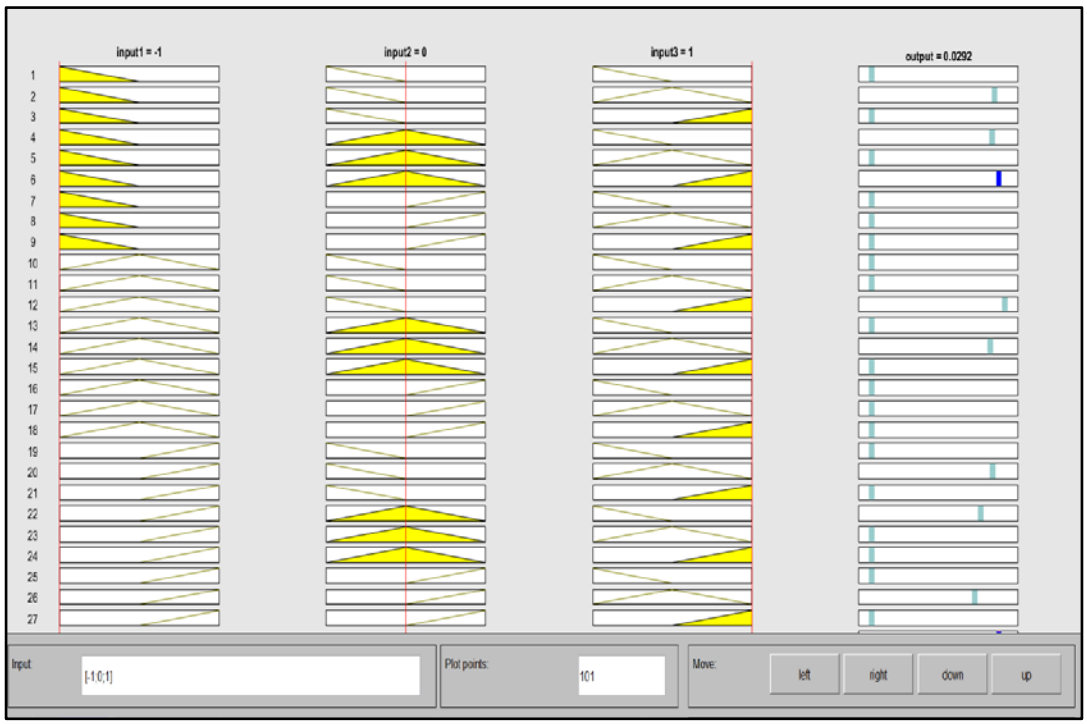

Fig. 5.55: Shows Predicated results for hole deviation

5.3.6.3 3-D surface plot

Figure 5.56 shows 3-D surface plot between process parameters to responses variable. Figure 5.56 (a), (b), (c), shows 3-D surface plot between input process parameters to hole deviation as a response variable. 3-D surface plot shows the variation of process parameters to response in way of colour.

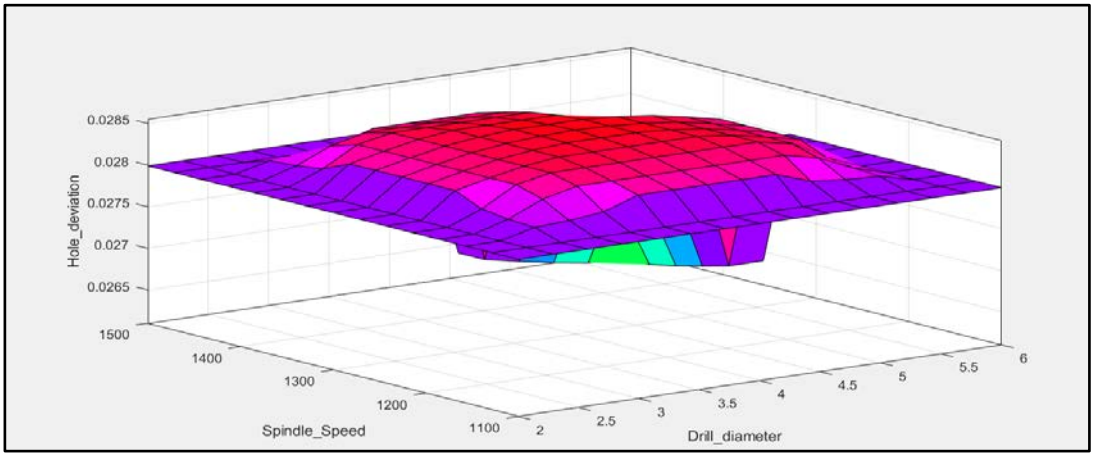
Hole_deviation
0.0285
0.028
0.0275
0.027
0.0265
Spindle_Speed
1500
1400
1300
1200
1100
Drill_diameter
2
2.5
3
3.5
4
4.5
5
5.5
6

(a)

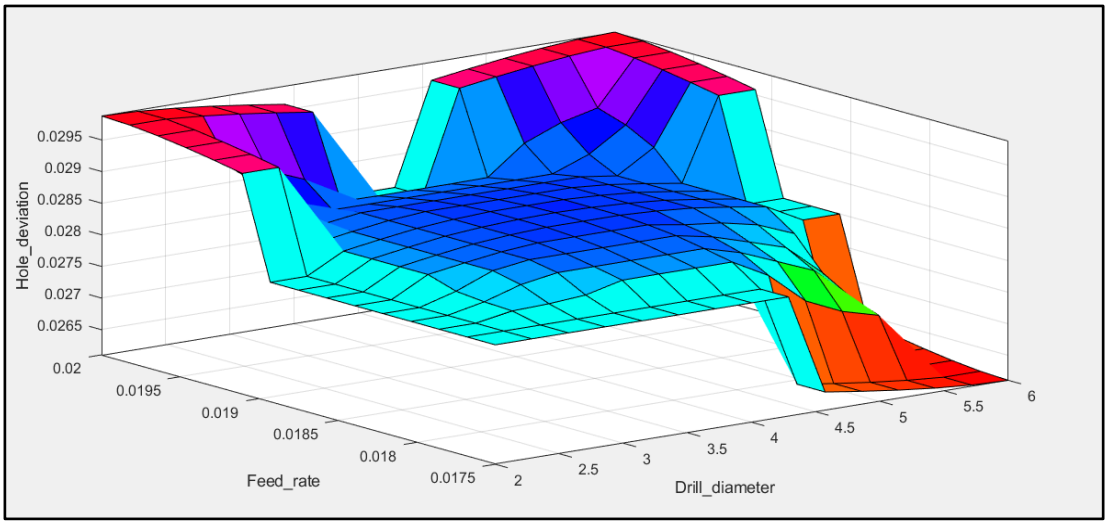
Hole_deviation
0.0295
0.029
0.0285
0.028
0.0275
0.027
0.0265
0.02
Feed_rate
0.0195
0.019
0.0185
0.018
0.0175
Drill_diameter
2
2.5
3
3.5
4
4.5
5
5.5
6

(b)

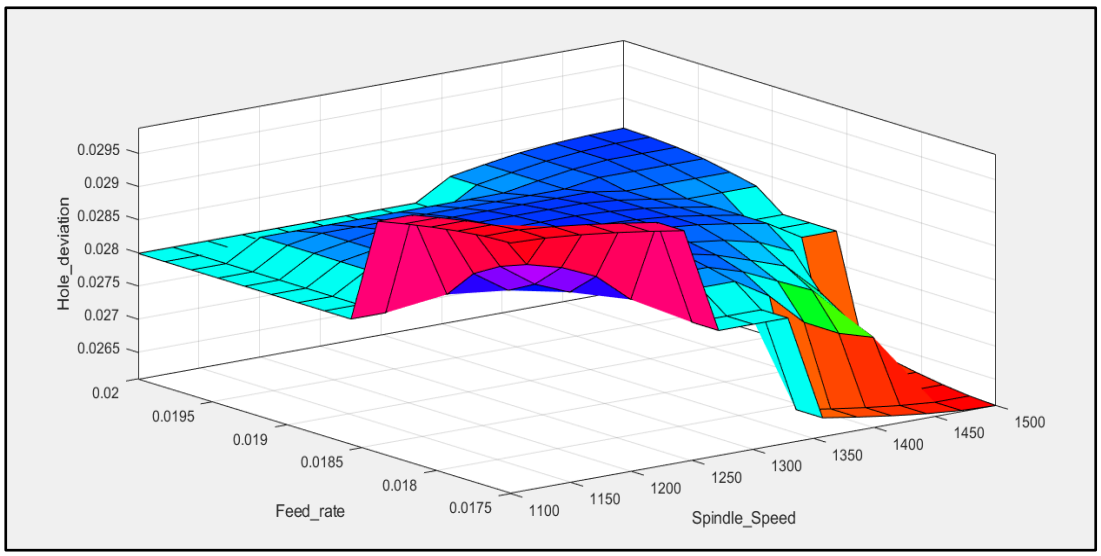
Hole_deviation
0.0295
0.029
0.0285
0.028
0.0275
0.027
0.0265
0.02
Feed_rate
0.0195
0.019
0.0185
0.018
0.0175
Spindle_Speed
1100
1150
1200
1250
1300
1350
1400
1450
1500

(c)

Figure 5.56 (d), (e), (f), shows 3-D surface plot between input process parameters to cylindricity error as a response variable. 3-D surface plot shows the variation of process parameters to response in way of colour.

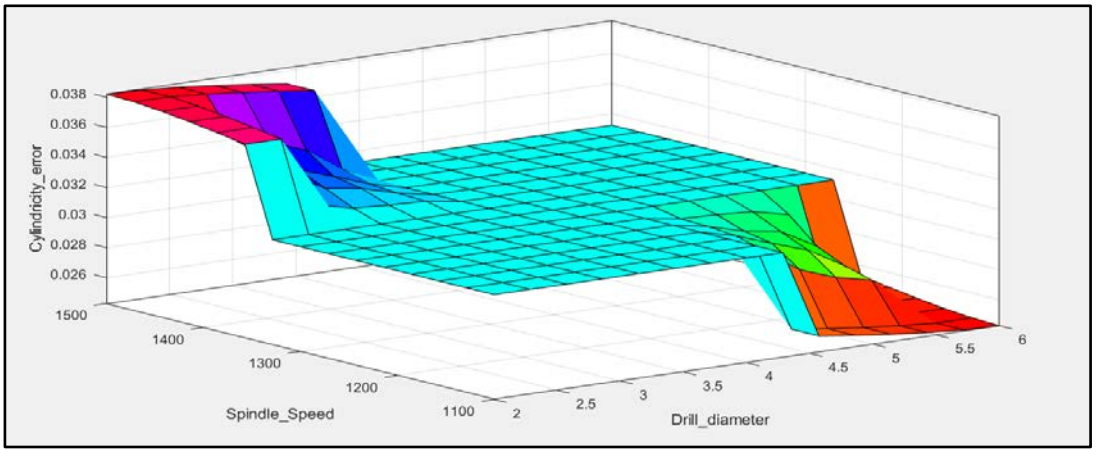

(d)

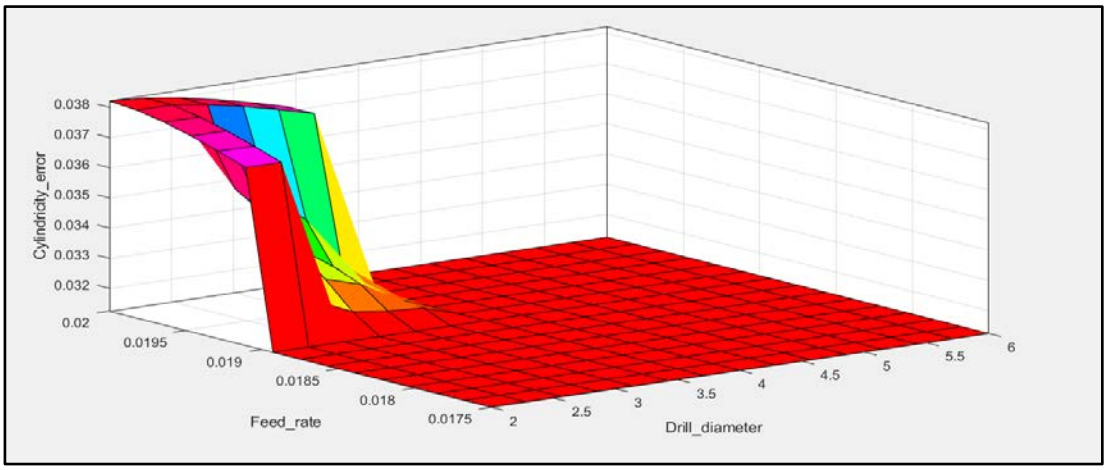

(e)

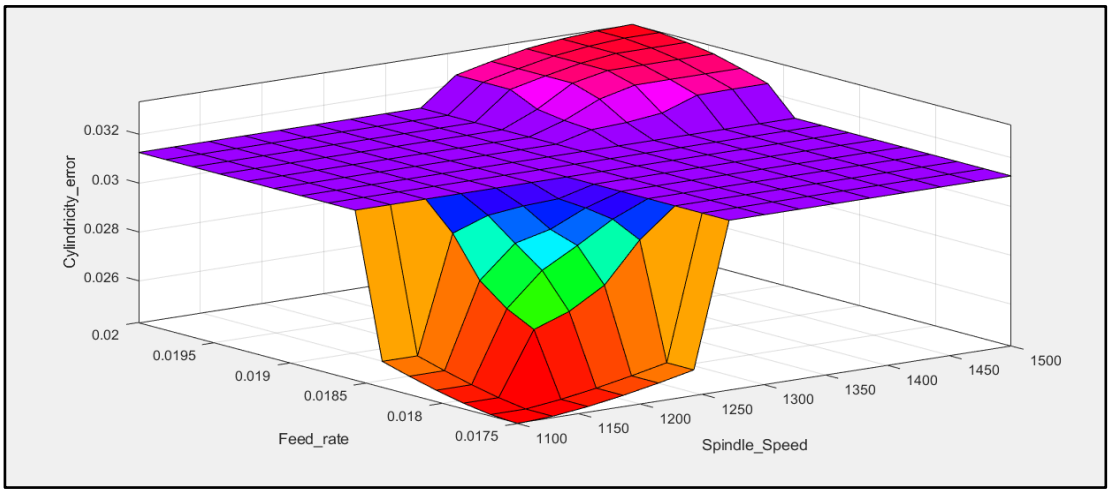

(f)

Figure 5.56 (g), (h), (i), shows 3-D surface plot between input process parameters to circularity error as a response variable. 3-D surface plot shows the variation of process parameters to response in way of colour.

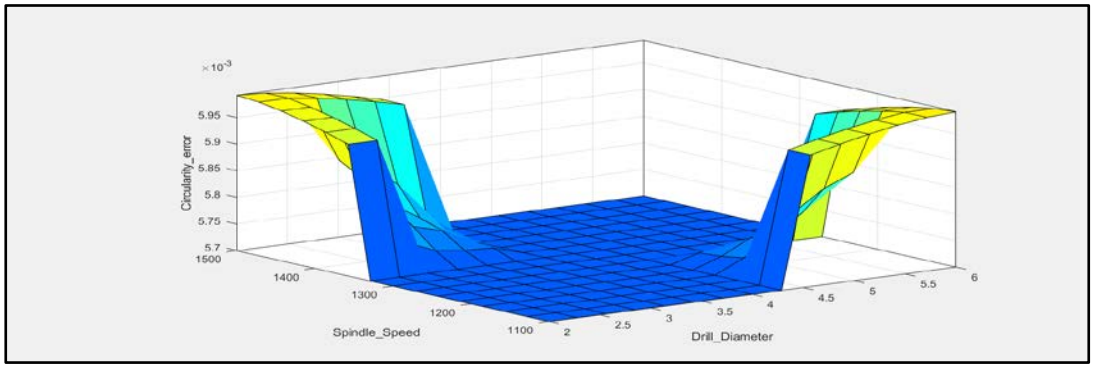

(g)

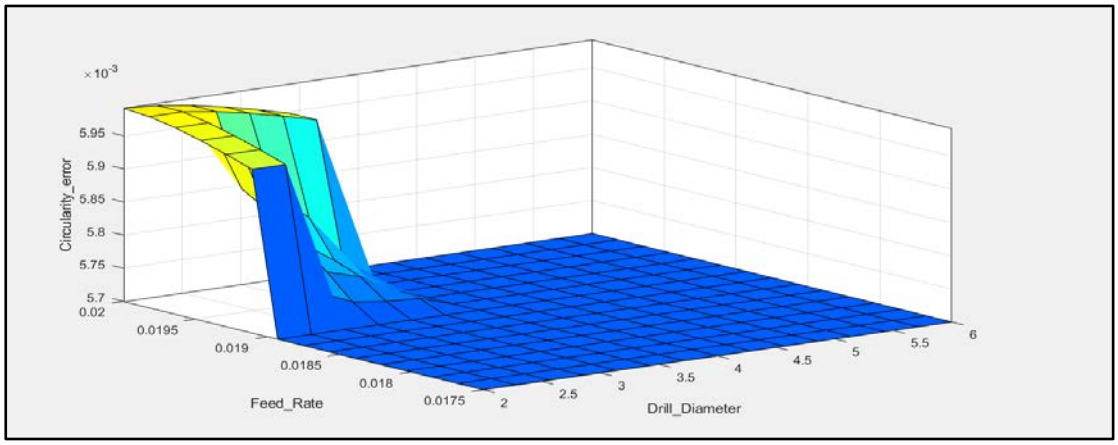

(h)

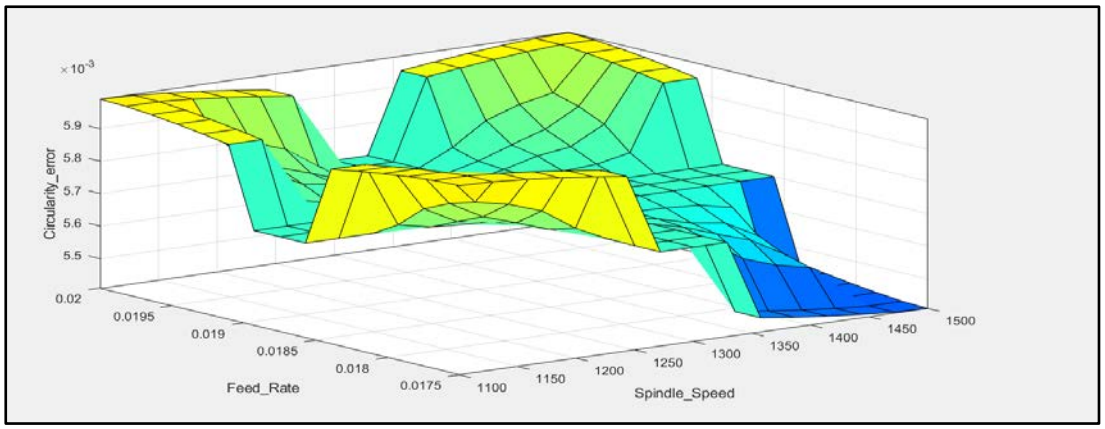

(i)

Fig. 5.56: 3-D surface plot for responses

5.3.6.4 Modeling Through ANFIS

Classification jobs, rule-based process controls, pattern recognition issues, and function approximation issues have all benefited from the application of ANFIS . The ideal distribution of membership functions is determined by the mapping relation between the input and output data in the ANFIS architecture, which combines fuzzy logic and artificial neural networks. It incorporates fuzzy logic (FL) theory and adaptive neural network (ANN) principles into adaptive network frameworks. The fuzzy interference system (FIS) application has been derived from FL theory, and by trial and error, the membership functions (MF) in FIS have been enhanced. In the ANFIS method, the ANN approach is used to create the FIS model and through it, it is possible to learn the training data for neural networks from the provided data. The factors in the Sugeno category IF-THEN rule arrangement have simultaneously mapped the results. Figure 5.57 depicts the general architecture of the ANFIS framework. This inference system is fundamentally composed of five separate layers. They are the following: layer I fuzzy, layer (ii) product, layer (iii) normalised, layer (iv) de-fuzzy, and layer (v) total output. Each layer is made up of unique nodes, where the adaptive nodes—where the variables could change—are represented by squares. The fixed nodes, however, when the factors are fixed, are represented by circles. The nodes in the preceding layers serve as the inputs for the current layers. For the sake of simplicity, it is assumed that this system has two inputs (a; b) and one output (Si) in order to demonstrate the ANFIS methods. Sugeno-type IF-THEN fuzzy rules are present in the ANFIS rule base. The import window for the ANN model is displayed in Figure 5.59.

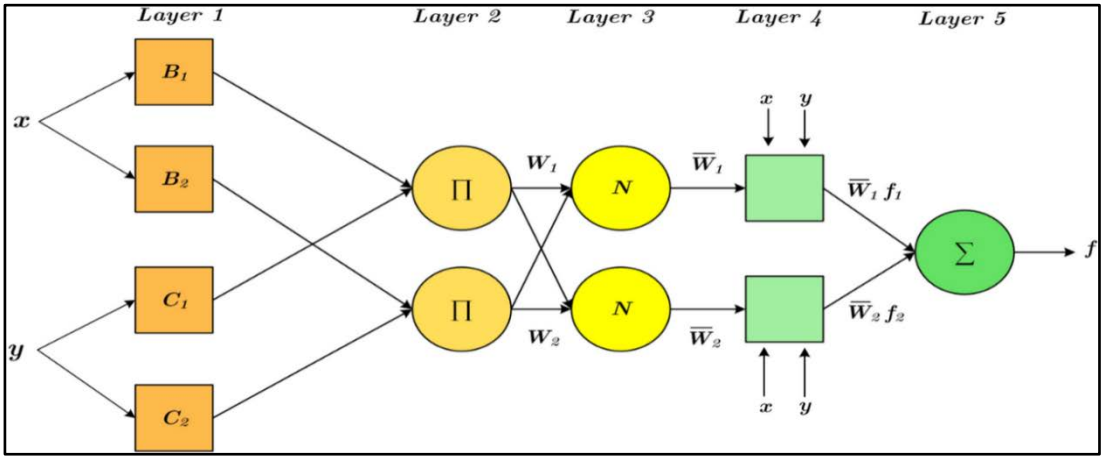

Fig. 5.57: General structure of ANFIS

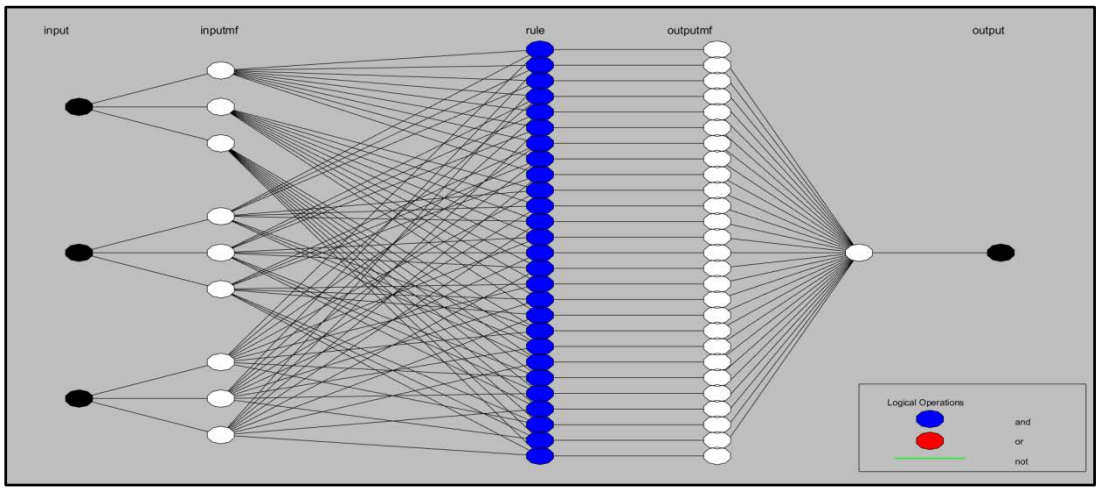

Fig.5.58: Neural Network Model for Responses

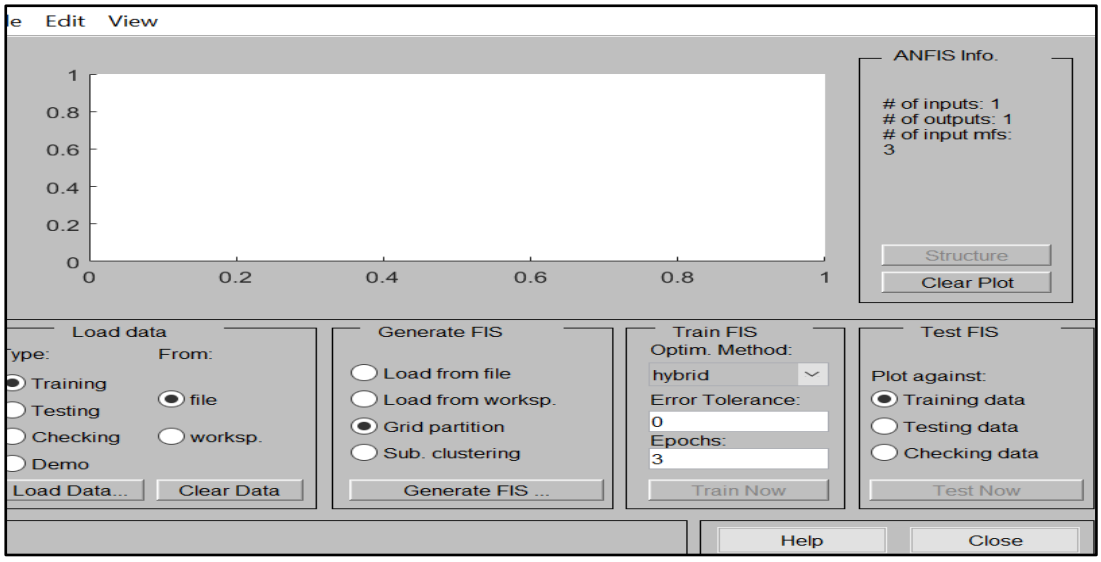

Fig. 5.59: Import Window

5.3.6.4.1 Prediction of Hole Deviation by ANFIS

The ANFIS structure and network model are used for this work to predict hole deviation of the drilled hole which is shown in Figure 5.58. It performs the systems of Sugeno-type FIS and the membership function are employed to do the training process. In this work, the FIS considers the three inputs of drilling parameters like drill diameter, spindle speed, and feed rate.

The ANFIS model performed training on the training dataset before testing the outcomes using test data. The input dataset is plotted multiple times throughout the ANFIS model's training to lower the prediction error. Epochs are the units used

to express the number of iterations necessary for mapping. In this study, the training process on 15 datasets must be completed during the course of 100 epochs (number of iterations). Figure 5.60 &5.61 shows the loading of training and testing data into the ANFIS model. RMSE for training is 0.000215333 and for testing is 0.0268731. It can result that the best optimal ANFIS structure with 3 3 3 membership function for this process. Figure 5.62 shows experimental outcomes of hole deviation under the same processing conditions as the training datasets are utilized to compare the predicted hole deviation results by the ANFIS model.

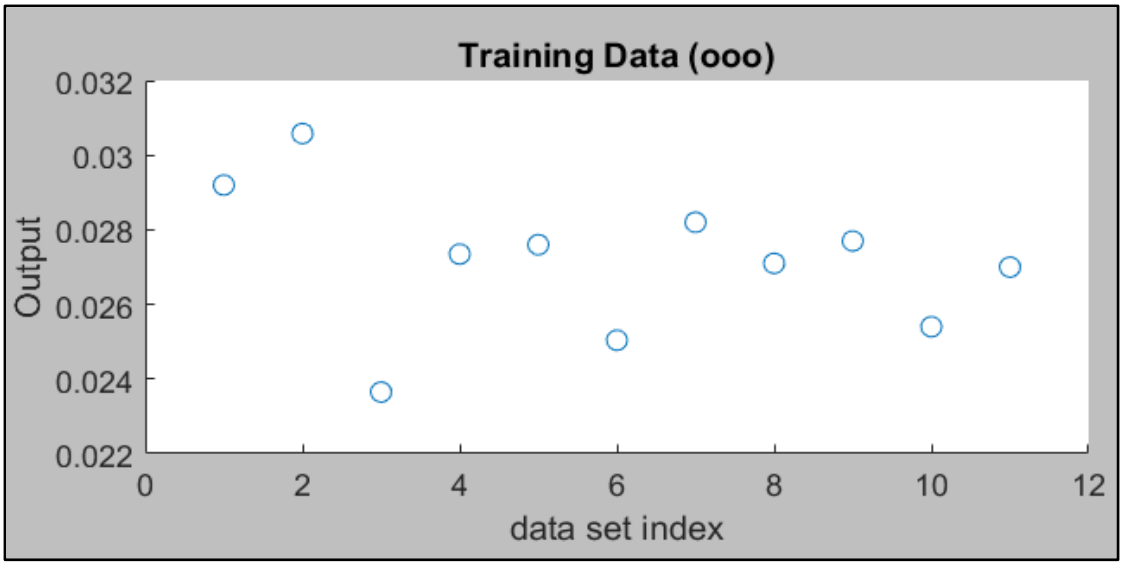

Fig. 5.60: Initial loading of training data

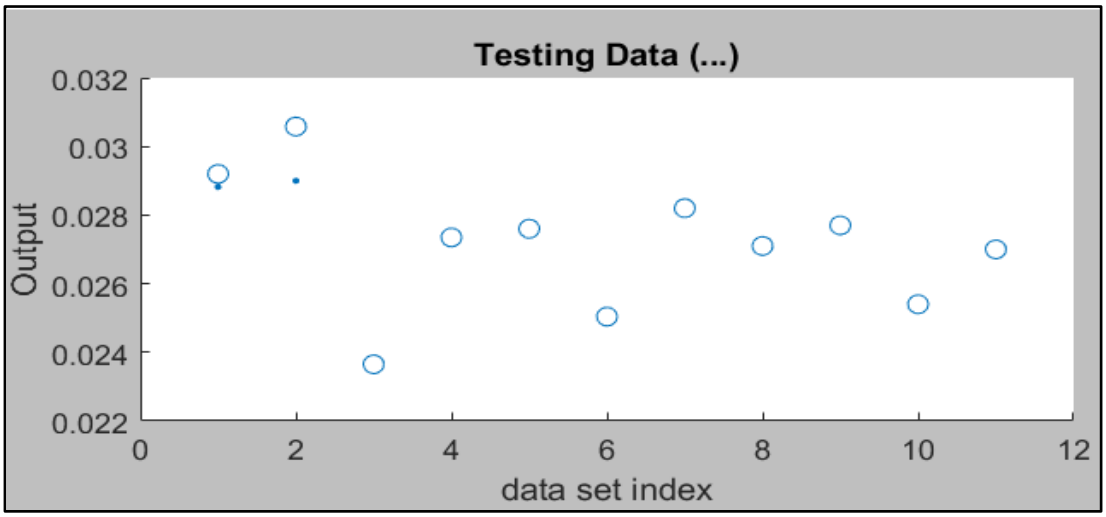

Fig. 5.61: Initial loading of testing data

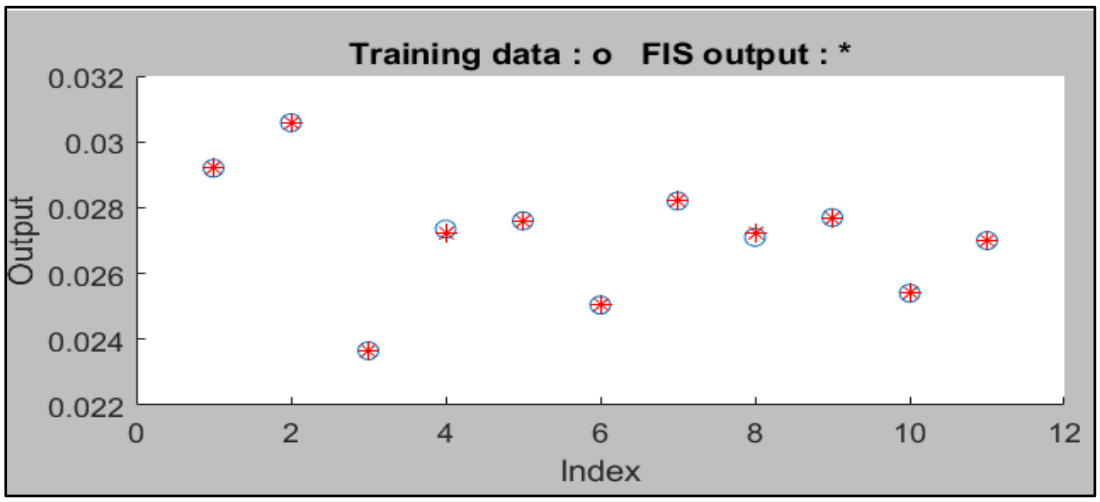

Fig. 5.62: Comparison of experimental to predicted

5.3.6.4.2 Prediction of cylindricity Error by ANFIS

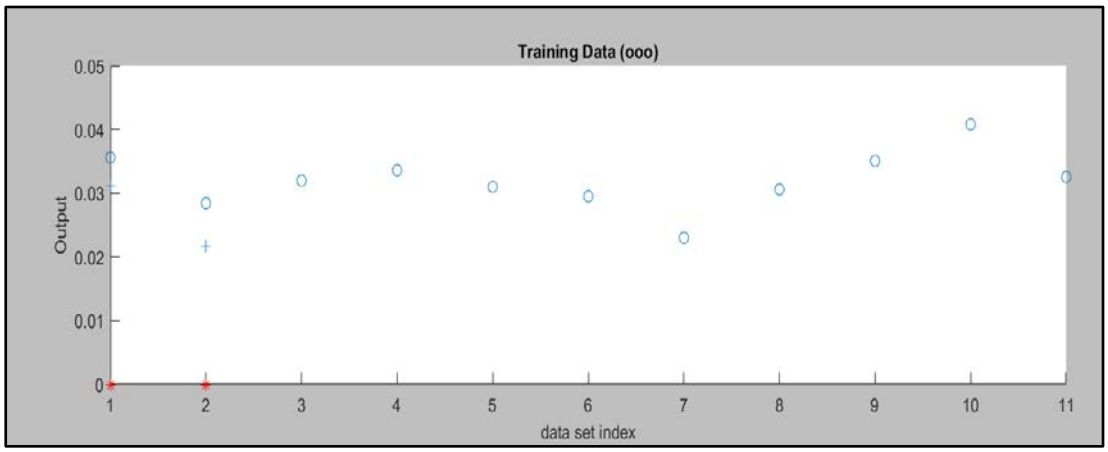

Fig. 5.63: Initial loading of training data

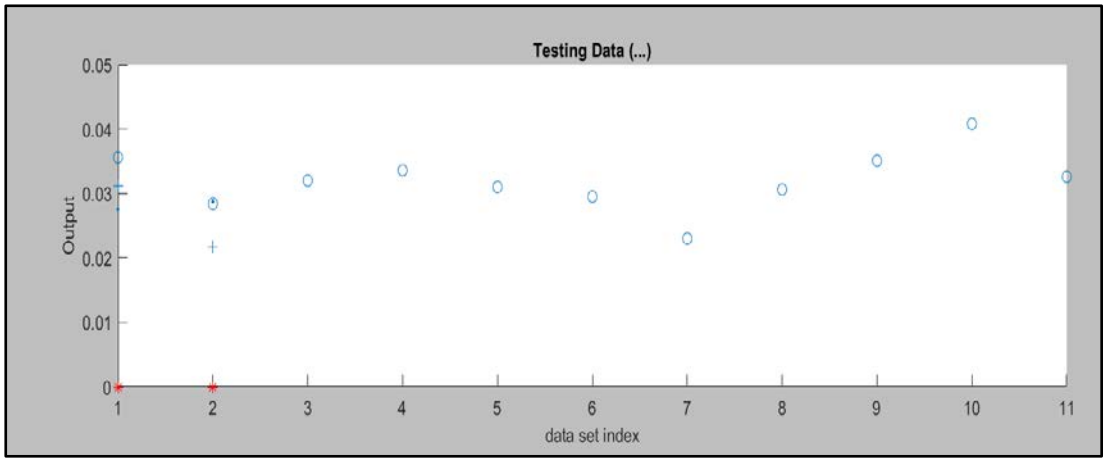

Fig. 5.64: Initial loading of testing data

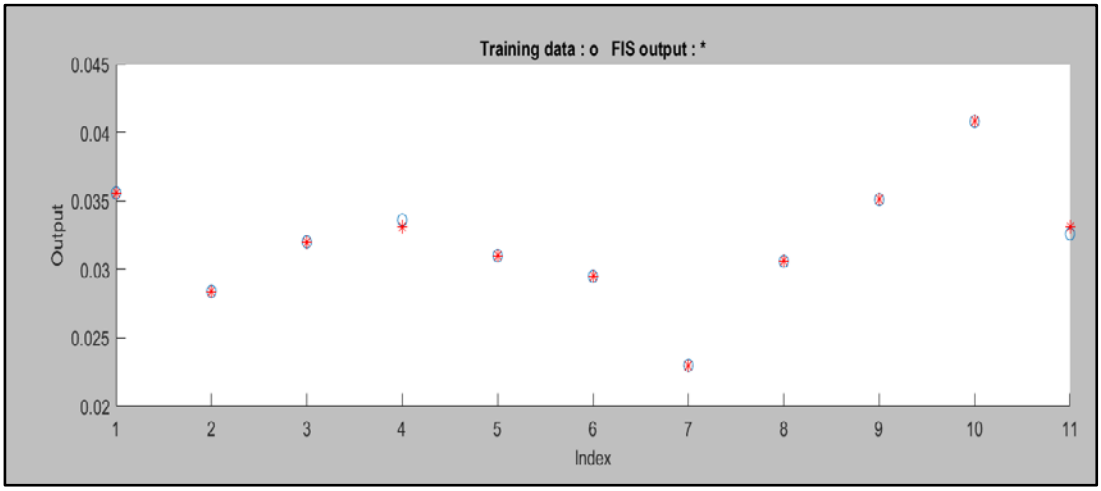

Fig. 5.65: Comparison of experimental to predicted

The ANFIS model performed training on the training dataset before testing the outcomes using test data. The input dataset is plotted multiple times throughout the ANFIS model's training to lower the prediction error. Epochs are the units used to express the number of iterations necessary for mapping. In this study, the training process on 15 datasets must be completed during the course of 100 epochs (number of iterations). Figure 5.63 &5.64 shows the loading of training and testing data into the ANFIS model. RMSE for training is 0.000215333 and for testing is 0.0268731. It can result that the best optimal ANFIS structure with 3 3 3 membership function for this process. Figure5.65 shows experimental outcomes of cylindricity error under the same processing conditions as the training datasets are utilized to compare the predicted cylindricity error results by the ANFIS model.

5.3.6.4.3 Prediction of circularity Error by ANFIS

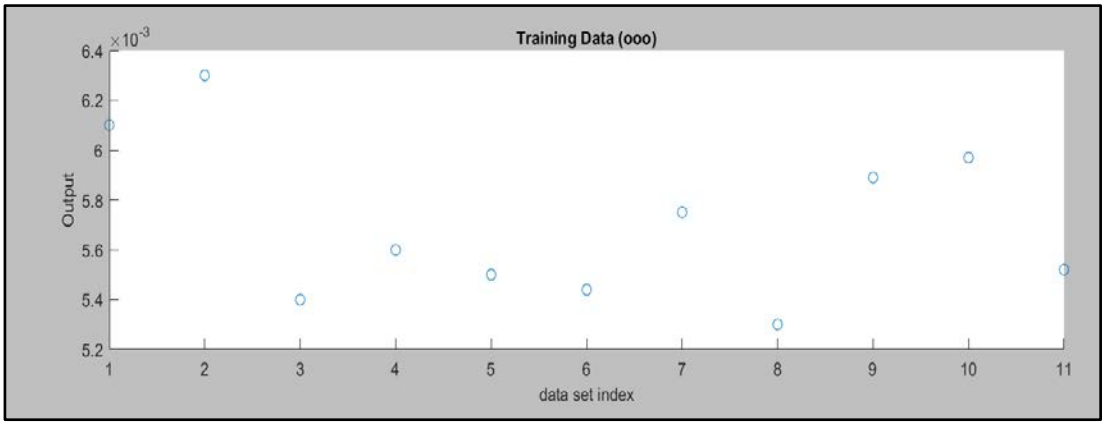

Fig. 5.66: Initial loading of training data

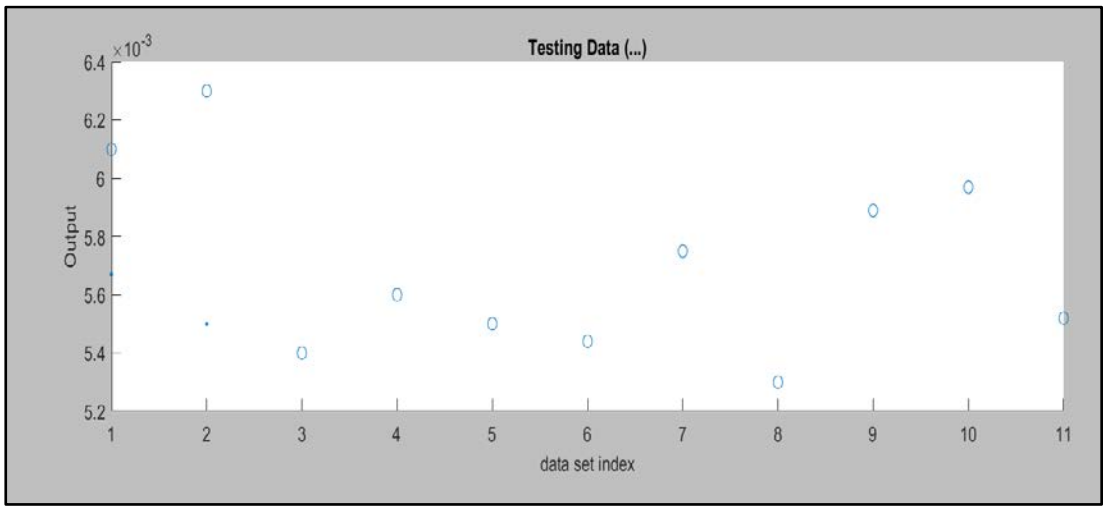

Fig. 5.67: Initial loading of testing data

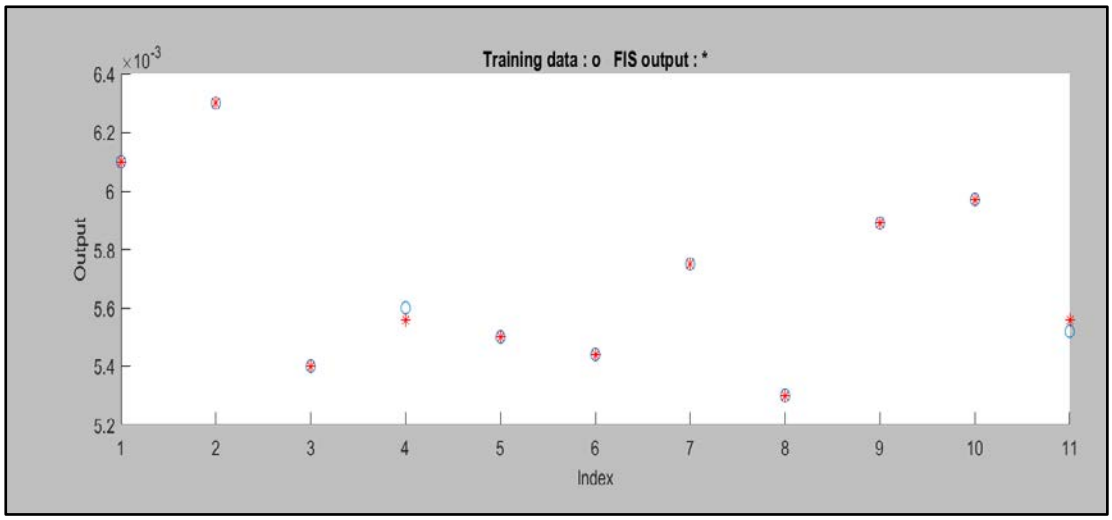

Fig.5.68: Comparison of experimental to predicted

The ANFIS model performed training on the training dataset before testing the outcomes using test data. The input dataset is plotted multiple times throughout the ANFIS model's training to lower the prediction error. Epochs are the units used to express the number of iterations necessary for mapping. In this study, the training process on 15 datasets must be completed during the course of 100 epochs (number of iterations). Figure 5.66 &5.67 shows the loading of training and testing data into the ANFIS model. RMSE for training is 1.70561e-05 and for testing is 0.005818611. It can result that the best optimal ANFIS structure with 3 3 3 membership function for this process. Figure 5.68 shows experimental outcomes of surface circularity

error under the same processing conditions as the training datasets are utilized to compare the predicted circularity error results by the ANFIS model.

5.3.7 Comparison of Experimental Value to Predicated Model Value

In the current investigation, the comparison of experimental value to predicated model value e.g. ANN, FLS, RSM, and ANFIS by using the following equations 5.8.

$$\%\ \text{Deviation}(\text{error}) = \frac{(V_e - V_p)}{V_e} \times 100 \quad \text{..... (5.8)}$$

Here,

V_e = Experimental value

V_p = Predicated value

Total absolute percentage error has been evaluated using the relationship:

After calculating the % of error individual set of experiments, then find the total absolute % of error by using the following equation 5.9.

$$\text{Total Absolute \% error} = \frac{\sum_{i=1}^{N} |(\%\ \text{error})_i|}{N} \quad \text{..... (5.9)}$$

Here,

N = Number of observations taken

5.3.7.1 Comparison of Experimental Value to Fuzzy value, RSM Model Value, ANN, and ANFIS Value for hole deviation

Table 5.19 shows experimental values and predicted values of the RSM model, FLS model, ANN model, and ANFIS. After analysis of the table, it was observed that all the predicted values of models are close to the experimental value. Figure 5.69 a comparison chart of predicated values of models to experimental value for hole deviation.

Table 5.19: Experimental value and predicted model value

Exp. No.	Experimental Value	RSM Value	FLS Value	ANN Value	ANFIS
1	0.02990	0.02980	0.0296	0.02975	0.02919
2	0.03058	0.03024	0.0295	0.02927	0.03058
3	0.02365	0.02504	0.0245	0.02560	0.02364
4	0.02735	0.02777	0.0278	0.02773	0.02722
5	0.02760	0.02766	0.0271	0.02708	0.02759
6	0.02544	0.02574	0.0243	0.02539	0.02503
7	0.02820	0.03003	0.0271	0.03215	0.02819
8	0.02790	0.02777	0.0278	0.02773	0.02722
9	0.02670	0.02821	0.0271	0.02606	0.02769
10	0.02540	0.02530	0.0245	0.02500	0.02769
11	0.02700	0.02744	0.0271	0.02607	0.02699
12	0.02882	0.02788	0.0296	0.02768	0.02799
13	0.02900	0.02810	0.0286	0.02852	0.02902
14	0.02790	0.02733	0.0271	0.02607	0.02692
15	0.02810	0.02777	0.0278	0.02776	0.02722

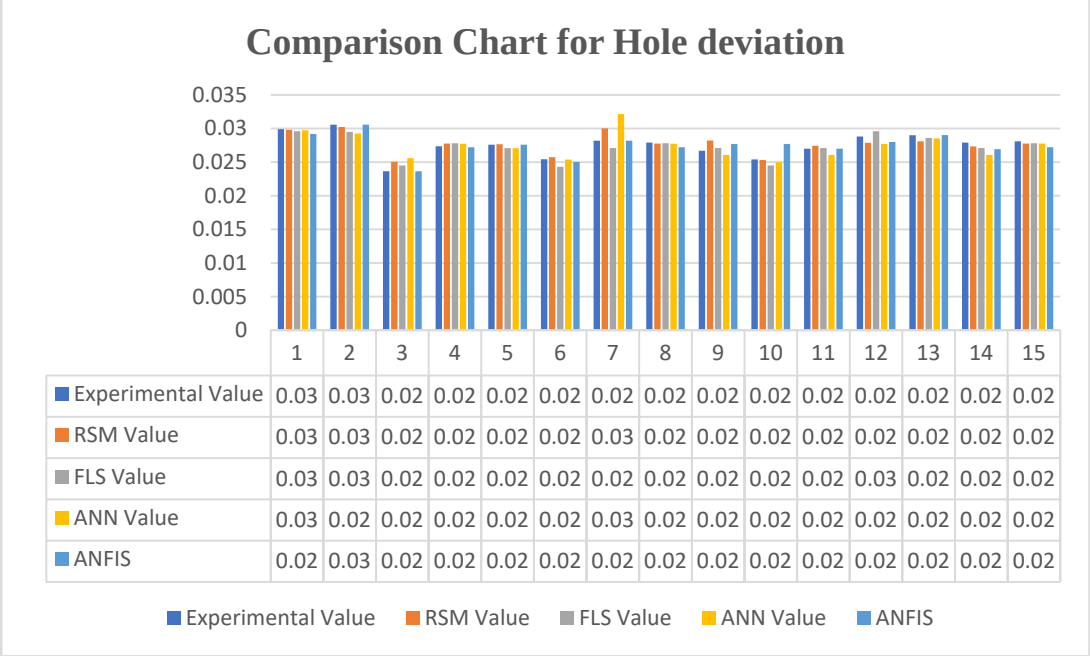

Fig. 5.69: Comparison Chart experimental value to predicted value

Table 5.20 lists the percent of error for fuzzy logic, RSM model, ANN, and ANFIS when comparing experimental value to predictive value of hole deviation. Also figure 5.70 shown graphical representation of % of error.

Table 5.20:Shows % of error for Hole deviation

S.No.	Experimental Value Vs Fuzzy Value	Experimental Value Vs RSM	Experimental Value Vs ANN	Experimental Value Vs ANFIS
1	0.3086	1.3513	0.4738	2.3973
2	1.1059	3.6627	4.4476	0.0001
3	5.5511	3.4693	7.6514	0.0001
4	1.5124	1.6187	1.3760	0.4591
5	0.2169	1.8450	1.9081	0.0001
6	1.1655	4.6913	0.1653	1.5975
7	6.0939	4.0590	12.2908	9.92909E-05
8	0.4464	0.3597	0.6072	2.4793
9	5.3661	1.4760	2.4409	3.6100
10	0.3714	3.6734	1.5784	9.84253E-05
11	1.6250	0.3690	3.5667	0.0001
12	3.3567	2.6351	4.0827	2.9315
13	3.1808	1.398	1.6648	0.0766
14	2.0557	2.9520	6.9871	3.6023
15	1.1664	1.0791	1.1921	3.2140
Total	**2.2348**	**2.3093**	**3.3622**	**1.3579**

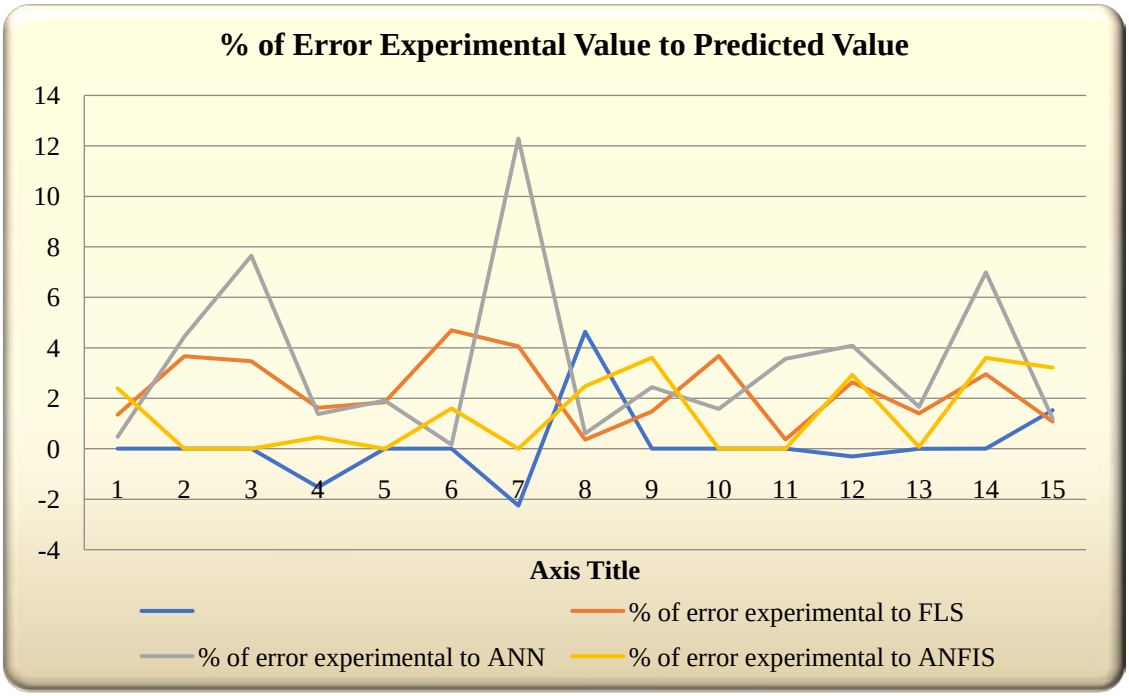

Fig. 5.70:% of error experimental value to predicted value for hole deviation

5.3.7.2 Comparison of Experimental Value to Fuzzy value, RSM Model Value, ANN, and ANFIS Value for cylindricity Error

Table 5.21 shows experimental values and predicted values of the RSM model, FLS model, ANN model, and ANFIS. After analysis of the table, it was observed that all the predicted values of models are close to the experimental value. Figure 5.71 is a comparison chart of predicated values of models to experimental values for cylindricity error.

Table 5.21: Experimental value and predicted model value

Exp. No.	Experimental Value	RSM Value	FLS Value	ANN Value	ANFIS
1	0.0356	0.03588	0.0382	0.03388	0.03559
2	0.0284	0.02867	0.0312	0.02674	0.02839
3	0.0320	0.03367	0.0312	0.03492	0.03309
4	0.0336	0.03128	0.0330	0.03156	0.03309
5	0.0310	0.03151	0.0312	0.03099	0.03099
6	0.0295	0.02778	0.0312	0.02949	0.02949
7	0.0276	0.02800	0.0243	0.02756	0.02699
8	0.0287	0.03128	0.030	0.03011	0.03009
9	0.0230	0.02407	0.0243	0.02301	0.02299
10	0.0306	0.03390	0.0312	0.03062	0.03059
11	0.0351	0.03827	0.0382	0.03521	0.03509
12	0.0312	0.03106	0.0312	0.03118	0.02169
13	0.0217	0.02430	0.0312	0.02158	0.02169
14	0.0408	0.03800	0.0382	0.04078	0.04079
15	0.0325	0.03128	0.033	0.03111	0.03309

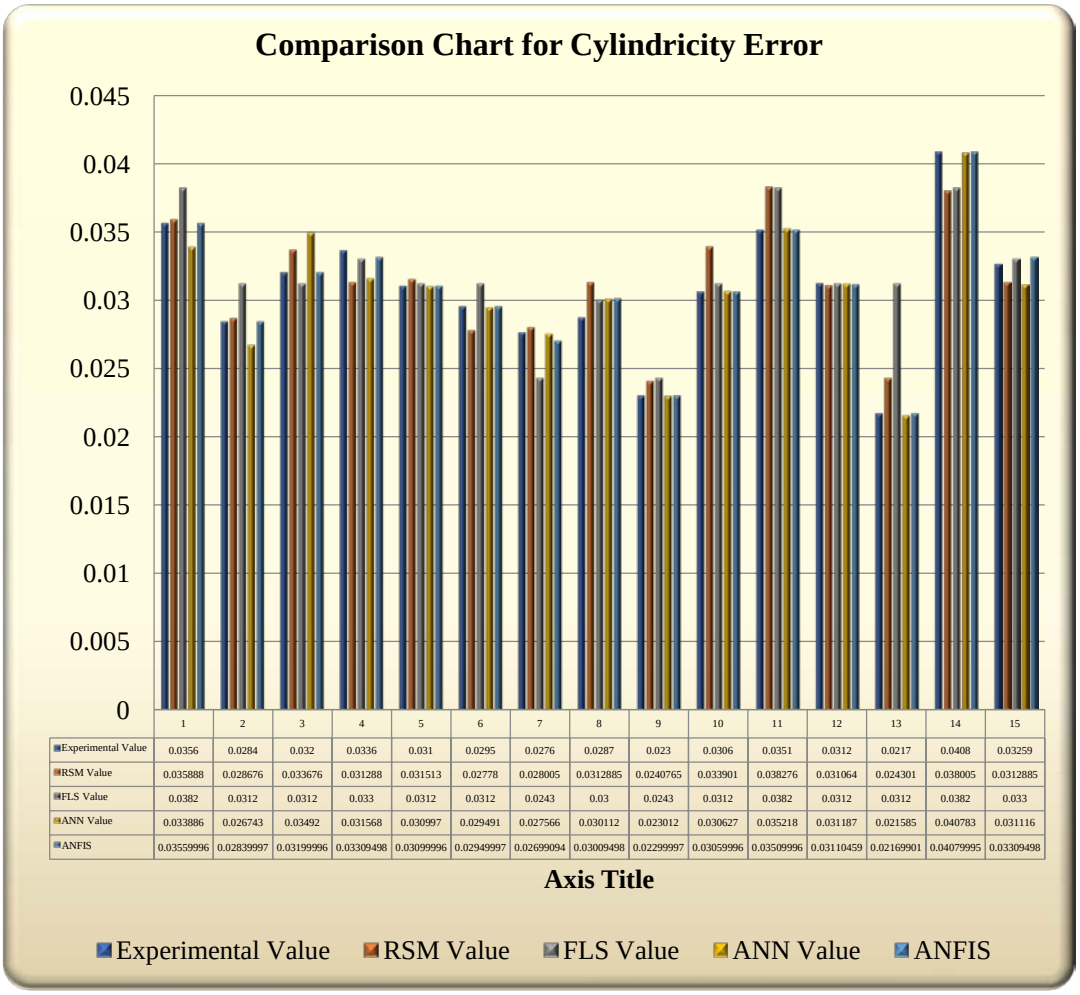

	1	2	3	4	5	6	7	8	9	10	11	12	13	14	15
Experimental Value	0.0356	0.0284	0.032	0.0336	0.031	0.0295	0.0276	0.0287	0.023	0.0306	0.0351	0.0312	0.0217	0.0408	0.03259
RSM Value	0.035888	0.028676	0.033676	0.031288	0.031513	0.02778	0.028005	0.0312885	0.0240765	0.033901	0.038276	0.031064	0.024301	0.038005	0.0312885
FLS Value	0.0382	0.0312	0.0312	0.033	0.0312	0.0312	0.0243	0.03	0.0243	0.0312	0.0382	0.0312	0.0312	0.0382	0.033
ANN Value	0.033886	0.026743	0.03492	0.031568	0.030997	0.029491	0.027566	0.030112	0.023012	0.030627	0.035218	0.031187	0.021585	0.040783	0.031116
ANFIS	0.03559996	0.02839997	0.03199996	0.03309498	0.03099996	0.02949997	0.02699094	0.03009498	0.02299997	0.03059996	0.03509996	0.03110459	0.02169901	0.04079995	0.03309498

Fig. 5.71: Comparison Chart experimental value to predicted value

Table 5.22 lists the percent of error for fuzzy logic, RSM model, ANN, and ANFIS when comparing experimental value to the predictive value of cylindricity error. Also, figure 5.72 shows a graphical representation of % of error.

Table 5.22: shows % of error for cylindricity Error

S.No.	Experimental Value Vs Fuzzy Value	Experimental Value Vs RSM	Experimental Value Vs ANN	Experimental Value Vs ANFIS
1	0.7803	6.8062	5.0581	0.0001
2	0.9624	8.9743	6.1960	0.0001
3	4.9768	2.5641	8.3619	0.0001
4	7.3894	1.8181	6.4369	1.5259
5	1.6279	0.6410	0.0096	0.0001
6	6.1915	5.4487	0.0305	2.2565
7	1.4461	13.5802	0.1233	4.6352
8	8.2730	4.3333	4.6891	0.0001
9	4.4711	5.3497	0.0521	0.0001
10	9.7371	1.9230	0.0881	0.0001
11	8.2976	8.1151	0.3350	0.3067
12	0.4378	0	0.0416	0.0045
13	10.7032	30.4487	0.5327	0.0045
14	7.3543	6.8062	0.0416	0.0001
15	4.1596	1.2424	4.7371	1.5258
Total	**5.1205**	**6.5367**	**2.4489**	**0.6840**

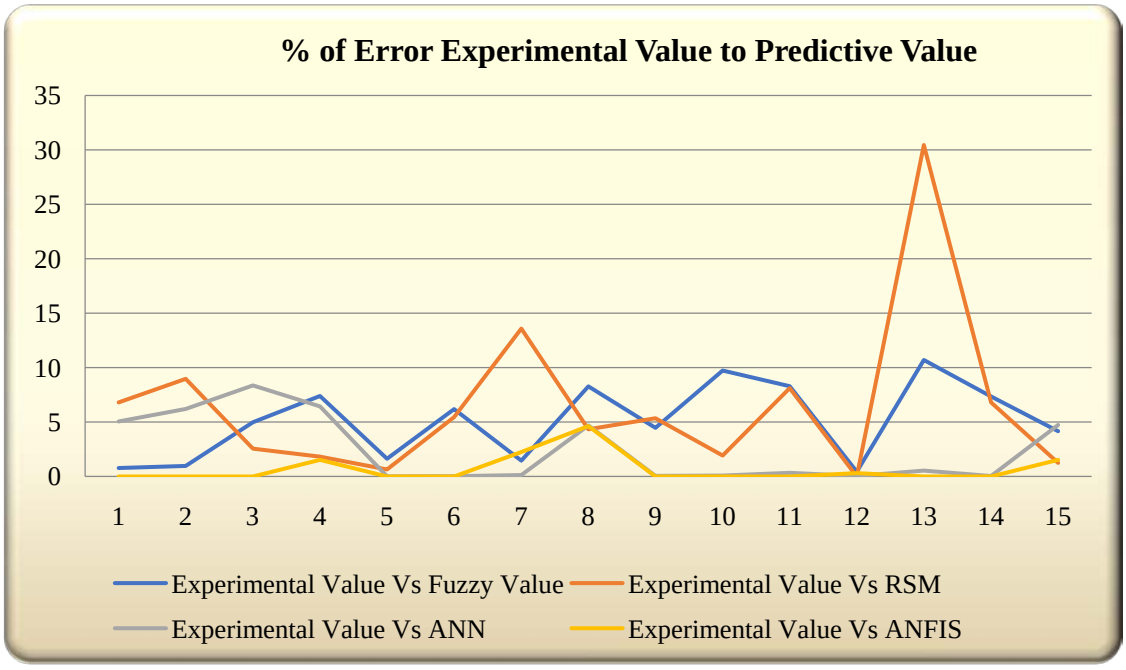

Fig. 5.72: % of error experimental value to predicted value for cylindricity Error

5.3.7.3 Comparison of Experimental Value to Fuzzy value, RSM Model Value, ANN, and ANFIS Value for circularity Error

Table 5.23 shows experimental values and predicted values of the RSM model, FLS model, ANN model, and ANFIS. After analysis of the table, it was observed that all the predicted values of models are close to the experimental value. Figure 5.73 shows a comparison chart of predicated values of models to experimental value for circularity error.

Table 5.23: Experimental value and predicted model value

Exp. No.	Experimental Value	RSM Value	FLS Value	ANN Value	ANFIS
1	0.0061	0.00591	0.00616	0.00597	0.00609
2	0.0063	0.00599	0.00616	0.0063	0.00629
3	0.0054	0.00548	0.00544	0.00536	0.00539
4	0.0056	0.00567	0.00569	0.00556	0.00555
5	0.00550	0.00552	0.00544	0.00548	0.00549
6	0.00544	0.00548	0.00544	0.00540	0.00543
7	0.00567	0.00581	0.0058	0.0058	0.00559
8	0.0055	0.0055	0.00569	0.00556	0.00555
9	0.00575	0.00558	0.0058	0.00570	0.00574
10	0.0053	0.00510	0.0054	0.00529	0.00529
11	0.00589	0.00549	0.0058	0.00583	0.00588
12	0.00561	0.00557	0.0058	0.00557	0.05609
13	0.00602	0.00590	0.00616	0.00600	0.00601
14	0.00597	0.00571	0.00616	0.00590	0.00596
15	0.00552	0.00551	0.00569	0.00556	0.00555

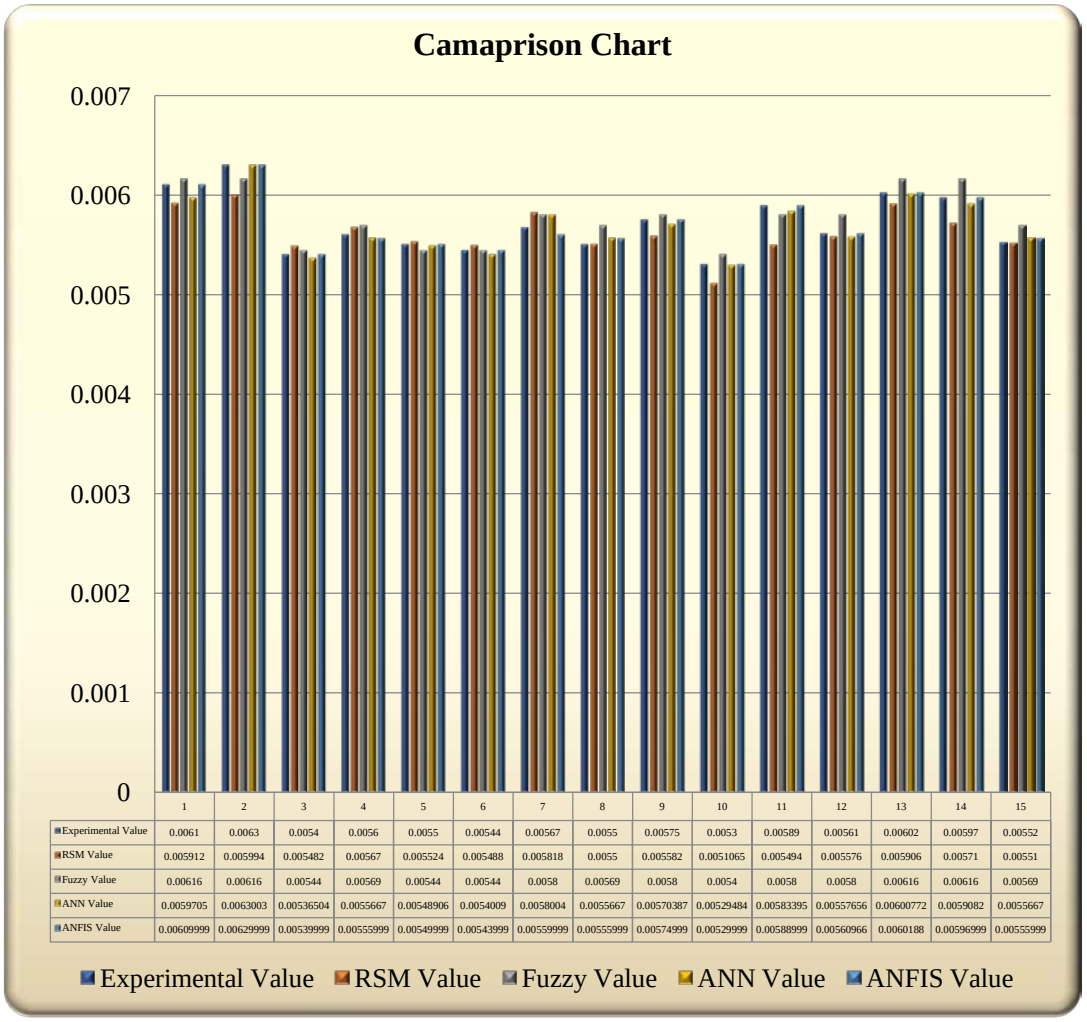

	1	2	3	4	5	6	7	8	9	10	11	12	13	14	15
Experimental Value	0.0061	0.0063	0.0054	0.0056	0.0055	0.00544	0.00567	0.0055	0.00575	0.0053	0.00589	0.00561	0.00602	0.00597	0.00552
RSM Value	0.005912	0.005994	0.005482	0.00567	0.005524	0.005488	0.005818	0.0055	0.005582	0.0051065	0.005494	0.005576	0.005906	0.00571	0.00551
Fuzzy Value	0.00616	0.00616	0.00544	0.00569	0.00544	0.00544	0.0058	0.00569	0.0058	0.0054	0.0058	0.0058	0.00616	0.00616	0.00569
ANN Value	0.0059705	0.0063003	0.00536504	0.0055667	0.00548906	0.0054009	0.0058004	0.0055667	0.00570387	0.00529484	0.00583395	0.00557656	0.00600772	0.0059082	0.0055667
ANFIS Value	0.00609999	0.00629999	0.00539999	0.00555999	0.00549999	0.00543999	0.00559999	0.00555999	0.00574999	0.00529999	0.00588999	0.00560966	0.0060188	0.00596999	0.00555999

Fig. 5.73: Comparison Chart experimental value to predicted value

Table 5.24 lists the percent of error for fuzzy logic, RSM model, ANN, and ANFIS when comparing experimental value to the predictive value of circularity error. Also, figure 5.74 shows a graphical representation of % of error.

Table 5.24: Shows % of error for circularity Error

S.No.	Experimental Value Vs Fuzzy Value	Experimental Value Vs RSM	Experimental Value Vs ANN	Experimental Value Vs ANFIS
1	0.97402	3.17997	2.169	0.00010
2	2.27273	5.10511	0.00476	0.00010
3	0.73529	1.49580	0.65163	0.00010
4	1.58172	1.23456	0.5982	0.71947
5	1.10294	0.43446	0.19931	0.00010
6	0	0.87463	0.72395	0.00010
7	2.24137	2.54382	2.24812	1.25016
8	3.33919	0	1.19819	1.07908
9	0.86206	3.00967	0.80875	0.00010
10	1.85185	3.78929	0.09745	0.00010
11	1.55172	7.20786	0.96076	0.00010
12	3.27586	0.60976	0.59965	0.00593
13	2.27272	1.93024	0.2044	0.01993
14	3.08441	4.55342	1.046	0.00010
15	2.98769	0.18149	0.83891	0.71937
Total	**1.87557**	**2.41000**	**0.82327**	**0.25992**

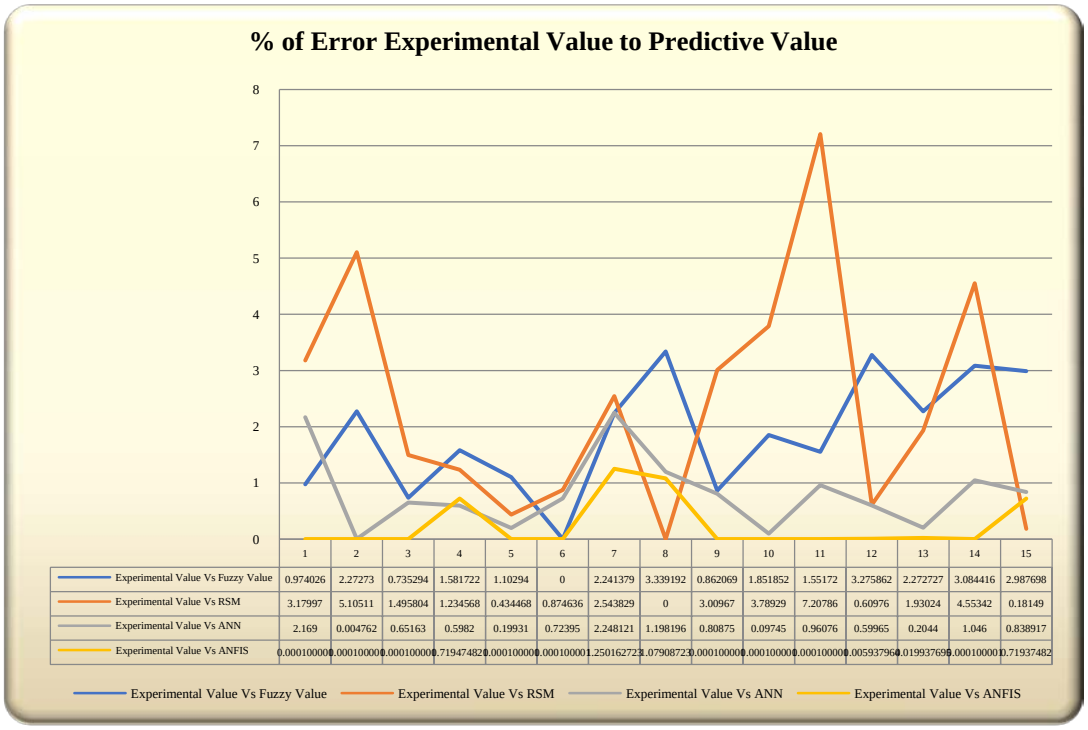

	1	2	3	4	5	6	7	8	9	10	11	12	13	14	15
Experimental Value Vs Fuzzy Value	0.974026	2.27273	0.735294	1.581722	1.10294	0	2.241379	3.339192	0.862069	1.851852	1.55172	3.275862	2.272727	3.084416	2.987698
Experimental Value Vs RSM	3.17997	5.10511	1.495804	1.234568	0.434468	0.874636	2.543829	0	3.00967	3.78929	7.20786	0.60976	1.93024	4.55342	0.18149
Experimental Value Vs ANN	2.169	0.004762	0.65163	0.5982	0.19931	0.72395	2.248121	1.198196	0.80875	0.09745	0.96076	0.59965	0.2044	1.046	0.838917
Experimental Value Vs ANFIS	0.000100000	0.000100000	0.000100000	0.719474820	0.000100000	0.000100000	1.250162723	1.079087210	0.000100000	0.000100000	0.000100000	0.005937964	0.019937694	0.000100000	0.719374820

Fig. 5.74: % of error experimental value to predicted value for cylindricity Error

Total % of Error

Table 5.25 shows the total % of error experimental value to predicated model value e.g. fuzzy logic system (FLS), artificial neural network (ANN), response surface method (RSM), and Adaptive neural fuzzy interface system (ANFIS) for responses e.g. hole deviation, cylindricity error, and circularity error.

Table 5.25: Total % of error

Total % of error				
Comparison model	**Exp. Vs fuzzy**	**Exp. Vs RSM**	**Exp. Vs ANN**	**Exp. Vs ANFIS**
Hole deviation	2.2348	2.3093	3.3622	**1.3579**
Cylindricity error	5.1205	6.5367	2.4489	**0.6840**
Circularity error	1.8755	2.4100	0.8232	**0.2599**

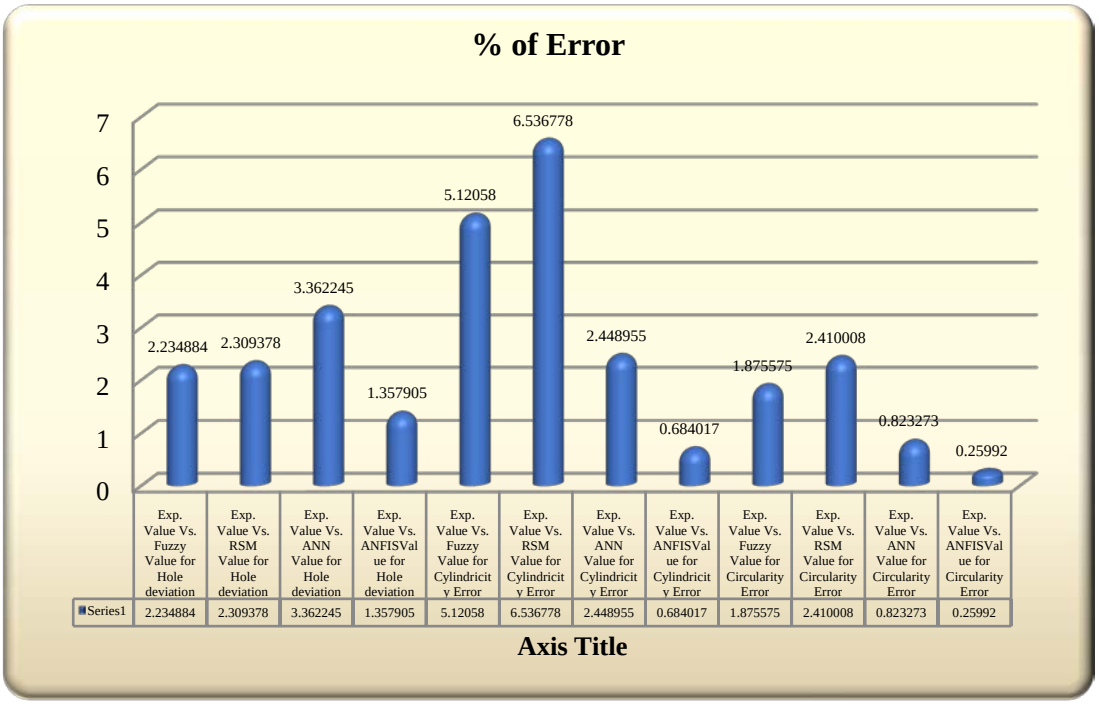

Fig. 5.75: Total % of error

After analysis figure 5.75, it was observed that minimum % of error 1.3579%, 0.6840%, and 0.2599%, respectively for hole deviation, cylindricity error, and circularity error, obtained by using ANFIS mode.

5.3.8 TOPSIS

To select solutions from a limited number of possibilities, a unique and multi-criteria decision-making method known as TOPSIS (Technique for Order Preference by Similarity to Ideal Solution) is utilized. In 1981, Hwang and Yoon developed one of the MCDM approaches, which was later enhanced by (Wang, 2007). This method's central principle is the idea that the selected alternative is farthest from the negative ideal solution and closer to the positive ideal solution. The positive ideal solution optimizes benefit criteria and minimizes cost criteria or qualities, in contrast to the negative ideal solution, which maximizes cost criteria and minimizes benefit criteria. The positive ideal solution, thus, consists of all conceivable best values, and the negative ideal solution, of all possible worst values. The minimum hole deviation, cylindricity error, and circularity error are the objectives of the investigation. The following are the steps taken in the TOPSIS approach.

Step 1

The TOPSIS method facilitates choosing a normalized value through the elimination of units of selected parameters. Table 5.26 shows the normalized performance matrix (r_{ij}) obtained using Eq. (1). In the present work, experiments were designed using the Response surface method which involves three input parameters and each with three levels. The order of run and experimental design matrix is shown in Table 5.13. The output responses (hole deviation, cylindricity error, & circularity error) have different units, however, got normalized in TOPSIS through multiplication with Eq. (5.10).

$$r_{ij} = \frac{X_{ij}}{\sqrt{\sum_{i=1}^{m} X_{ij}^2}} \quad i = 1,2,\ldots 8; \quad j = 1,2. \qquad \ldots\ldots\ldots\ldots\ldots\ldots\ldots\ldots\ldots\ldots\ldots\ldots\ldots\ldots\ldots\ldots\ldots\ldots\ldots\ldots\ldots\ldots (5.10)$$

Table 5.26: Normalized Matrix

Exp. No.	Drill Dia.	Spindle Speed	Feed Rate	Normalized Matrix		
				Hole deviation	Cylindricity Error	Circularity Error
1	-1	0	1	0.0707	0.0771	0.0712
2	0	-1	1	0.0741	0.0615	0.0736
3	1	1	0	0.0573	0.0693	0.0631
4	0	0	0	0.0662	0.0728	0.0654
5	-1	0	-1	0.0668	0.0671	0.0642
6	1	0	-1	0.0606	0.0639	0.0635
7	-1	-1	0	0.0683	0.0598	0.0662
8	0	0	0	0.0656	0.0622	0.0642
9	1	-1	0	0.0671	0.0498	0.0671
10	0	1	-1	0.0615	0.0663	0.0619
11	0	1	1	0.0654	0.0760	0.0688
12	1	0	1	0.0698	0.0676	0.0655
13	0	-1	-1	0.0702	0.0470	0.0703
14	-1	1	0	0.0676	0.0884	0.0697
15	0	0	0	0.0680	0.0706	0.0645

Step 2

The weighted normalized matrix (r_{ij}) was obtained which is the product of the normalized value and the weighted values. The responses were weighted using procedure and constructed based on relative importance (Responses have equal importance, 33.33% each). The responses were ordered from least to most important and the weighted normalized matrix table 5.27 was computed using Eq. (5.11).

$$\vartheta_{ij} = w_j * r_{ij} \quad i = 1, 2, \ldots 8; \quad j = 1, 2. \qquad \text{.....5.11}$$

Table 5.27: Normalized Weighted Matrix

Exp. No.	Drill Dia.	Spindle Speed	Feed Rate	Weighted Matrix		
				Hole deviation	Cylindricity Error	Circularity error
1	-1	0	1	0.0235	0.0257	0.0237
2	0	-1	1	0.0247	0.0205	0.0245
3	1	1	0	0.0191	0.0231	0.0210
4	0	0	0	0.0220	0.0242	0.0218
5	-1	0	-1	0.0222	0.0223	0.0214
6	1	0	-1	0.0202	0.0213	0.0211
7	-1	-1	0	0.0227	0.0199	0.0220
8	0	0	0	0.0218	0.0207	0.0214
9	1	-1	0	0.0223	0.0166	0.0223
10	0	1	-1	0.0205	0.0221	0.0206
11	0	1	1	0.0218	0.0253	0.0229
12	1	0	1	0.0232	0.0225	0.0218
13	0	-1	-1	0.0234	0.0156	0.0234
14	-1	1	0	0.0225	0.0294	0.0232
15	0	0	0	0.0226	0.0235	0.0215
S^+ (Ideal best)				0.0191	0.0156	0.0206
S^-(Ideal worst)				0.024701	0.029473	0.024539

Step 3

Every response considered as an ideal alternative to the best alternative performance (S^+) and the worst alternative performance (S^-) is identified. These values shown in table 5.26.

$$S^+ = \{[\max(S_{ij})|j \in J] \text{ or } [\min(S_{ij})|j \in J'], \quad i = 1, 2, \ldots 8\} \quad \text{.....5.12}$$

Step 4

In this step, the performance criterion has been measured as the best alternative distance (D+ ij) from the S+ values, and the worst alternative distance (D^- ij) from the S^- values. The D^+ij and D^- ij values are determined using Eqs. (5.13) and (5.14). The performance characteristics of selected alternative is shown in Table 5.27.

$$D_{ij}^+ = \sqrt{\sum_{i=1}^{27} (\vartheta_{ij} - S_j^+)^2}$$

$$D_{ij}^+ = \sqrt{\sum_{i=1}^{27} (\vartheta_{ij} - S_j^+)^2} \quad \text{..... 5.13 \& 5.14}$$

Step 5

Using Eq. (5.15), the closeness coefficient (Ci) was computed for all alternatives

$$CC_i = \frac{D_i^-}{D_i^- + D_i^+} \quad i = 1, 2, \ldots 8; 0 \leqslant C_i \leqslant 1 \quad \text{.....5.15}$$

The selection of the best alternative is on the basis of the preference rank as per the CC_i order and close to the ideal solution. The closeness coefficient values (CC_i) of all alternatives using the L15 set of experiments are shown in Table 5.28. The CC_i are ranked in ascending order. The maximum closeness coefficient value was found in experimental run 9 among all other experiments. The ideal alternative was selected which corresponds to maximum CC_i. Hence the process parameters of an experiment run 9 give the optimal. Figure 5.76 shows the closeness coefficients of corresponding experimental runs.

Table 5.28: Closeness coefficients and ranking of alternatives.

Exp. No.	D_i^+	D_i^-	CC_i	Rank
1	0.0114	0.0039	0.2590	14
2	0.0083	0.0089	0.5171	9
3	0.0074	0.0091	0.5516	7
4	0.0091	0.0064	0.4118	12
5	0.0074	0.0081	0.5199	8
6	0.0057	0.0098	0.6315	4
7	0.005809	0.0100	0.6332	3
8	0.005826	0.0096	0.6246	5
9	0.0038	0.0132	0.7757	1
10	0.0065	0.0093	0.5862	6
11	0.0103	0.0052	0.3386	13
12	0.0081	0.0075	0.4824	10
13	0.0051	0.0138	0.7295	2
14	0.0144	0.0025	0.1483	15
15	0.0086	0.0069	0.4446	11

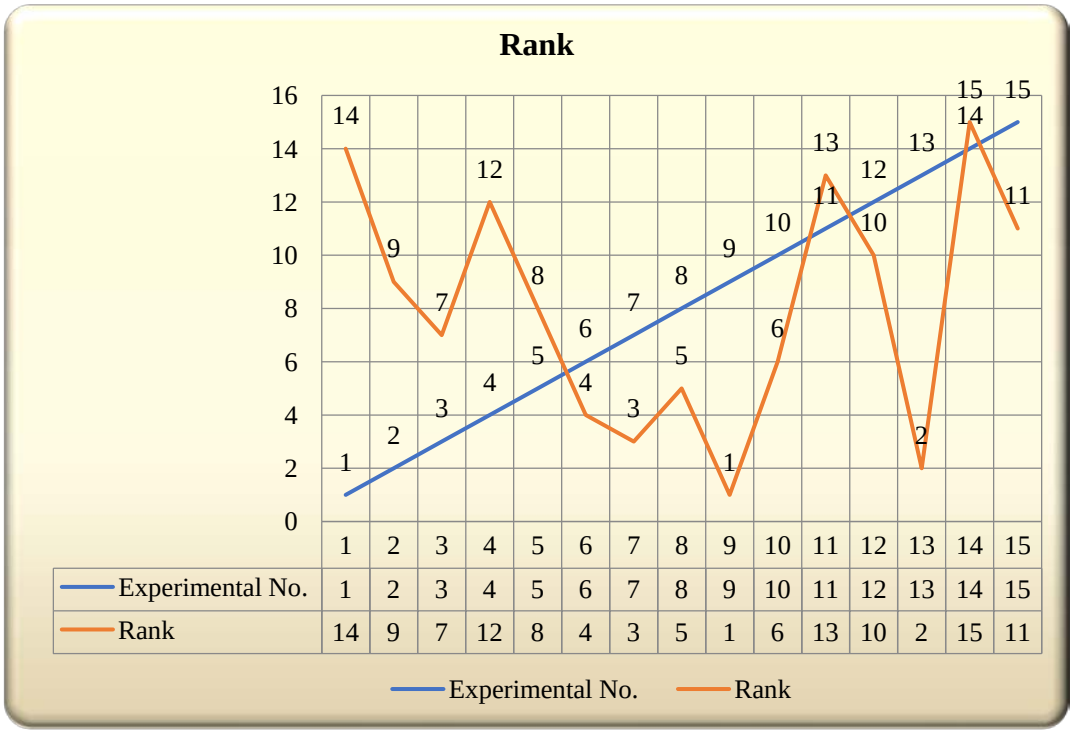

Fig. 5.76: Closeness coefficients of the experimental run

TOPSIS (techniques for order performance by similarity to ideal solution) is a useful technique in dealing with multi attribute or multi criteria decision making (MCDM) in problem in the real word. TOPSIS is based on the fundamental premise that the best solution has the shortest distance from the positive ideal solution, and the longest distance from the negative ideal one. Alternatives are ranked with the use of an overall index calculated based on the distances from the ideal solutions.

In present investigation TOPSIS is implemented for multi-objectives e.g. hole deviation, cylindricity error, circularity error for find the best optimal process parameters for minimizing the value of responses. After table 5.27, it was observed that 9 number of set of experiment have ranked 1, so easily observed that 9 number of set of experiment provide minimum value or optimal process parameters in multi-objectives problems.